Self-organizing Coordination of Multi-Agent Microgrid Networks

by

Samantha Janko

A Dissertation Presented in Partial Fulfillment
of the Requirements for the Degree
Doctor of Philosophy

Approved October 2019 by the
Graduate Supervisory Committee:

Nathan Johnson, Chair
Wenlong Zhang
Wesley Herche

ARIZONA STATE UNIVERSITY

December 2019

ABSTRACT

This work introduces self-organizing techniques to reduce the complexity and burden of coordinating distributed energy resources (DERs) and microgrids that are rapidly increasing in scale globally. Technical and financial evaluations completed for power customers and for utilities identify how disruptions are occurring in conventional energy business models. Analyses completed for Chicago, Seattle, and Phoenix demonstrate site-specific and generalizable findings. Results indicate that net metering had a significant effect on the optimal amount of solar photovoltaics (PV) for households to install and how utilities could recover lost revenue through increasing energy rates or monthly fees. System-wide ramp rate requirements also increased as solar PV penetration increased. These issues are resolved using a generalizable, scalable transactive energy framework for microgrids to enable coordination and automation of DERs and microgrids to ensure cost effective use of energy for all stakeholders. This technique is demonstrated on a 3-node and 9-node network of microgrid nodes with various amounts of load, solar, and storage. Results found that enabling trading could achieve cost savings for all individual nodes and for the network up to 5.4%. Trading behaviors are expressed using an exponential valuation curve that quantifies the reputation of trading partners using historical interactions between nodes for compatibility, familiarity, and acceptance of trades. The same 9-node network configuration is used with varying levels of connectivity, resulting in up to 71% cost savings for individual nodes and up to 13% cost savings for the network as a whole. The effect of a trading fee is also explored to understand how electricity utilities may gain revenue from electricity traded directly between customers. If a utility imposed a trading fee to recoup lost revenue then trading is financially infeasible for agents, but could be

feasible if only trying to recoup cost of distribution charges. These scientific findings conclude with a brief discussion of physical deployment opportunities.

DEDICATION

For my parents, my brother, my husband, my best friend, my team, and all the kids out there who have a curiosity that can't be satisfied with a one-word answer.

ACKNOWLEDGMENTS

I want to thank first and foremost my parents for raising me to never let me think I couldn't. I learned everything I know, including how to learn, from you. Your unconditional support and inspiration made me who I am, and I want the world for you.

Also thank you to my brother who is the only one who knows what it was like to be raised like I did, can give me advice when I think I can't ask anyone, and can always fall back in step with me no matter how long it has been since we talked.

Thank you to my husband who has watched this journey from the beginning and provided never-ending love and care. This man has an answer for everything, a bottomless amount of optimism, and always has my happiness in mind. Not to mention, he can design and build a super computer in a weekend. Thank you for always trying to make me laugh and for loving me with all you have.

Thanks to my best friend that despite everything she has on her plate is always down for a working day or a destresser when it's needed most. Thank you for being there for me since forever.

Thank you to all of my friends that lent me their time, their ears, and their spare computers. Your kindness aided in the completion of this work.

A huge thank you to my research lab of determined, insanely intelligent individuals who are not just a sounding board for ideas, but a support network for everything from daily frustrations to a ride home when you need it. Also, they may be one of the only groups of people who understand the importance of the number 8760.

Thank you to all of those that offered me internship opportunities and a chance to grow. Every internship I had taught me something that went into this dissertation. I truly couldn't have finished it without you and your support.

Thank you to my committee members for their valuable insight and for lending me their Halloween to hear me defend.

And finally, a deep thank you from the bottom of my heart to my mentor who was with me every step of the way from undergrad. I am honored to be a part of our team and cannot express enough the gratitude I have for the opportunities and support you have given me. Thank you for helping me grow as a writer, a professional, and a person. I hold you in the highest regard and respect. Thanks for always leaving your door open whether it's work or chat.

TABLE OF CONTENTS

Page

CHAPTER Page

LIST OF TABLES

Table Page

Table Page

LIST OF FIGURES

Figure Page

Figure Page

Figure Page

Figure Page

CHAPTER 1

INTRODUCTION

1.1. Motivation of Work

The cost of distributed energy resources (DER) have been rapidly decreasing, including solar photovoltaics (PV), energy storage, combined heat and power, fuel cells, demand response, and other technologies. This has facilitated an increase in the number of installed assets each year, with the expected global capacity expected to approach 530 GW by 2026 (Navigant 2017). Individual assets and groups of assets can be configured to form small-scale power systems called microgrids that can operate independently (islanded) from a larger electric grid. Islanding allows microgrid owners to maintain reliable and resilient power in the event of a grid outage. Microgrids may also generate excess power to support nearby loads or the main grid. The latter is a new use-case for microgrids. Though they have existed for decades in the form of fossil-fuel generators supporting remote off-grid locations with prime power or on-grid critical loads with back-up power, they have only recently been used to export power back to the grid.

Microgrids are currently being researched as a viable option to decrease power cost, reduce emissions, utilize energy resources more efficiently, and increase grid reliability (U.S. DOE Office of Energy n.d.; Parhizi et al. 2015; NREL 2016). Accomplishing these goals requires technical sophistication in microgrid controllers that provide control automation, consumer-side engagement, and communication between microgrid assets. Innovation is needed in advanced control algorithms that enable high-level coordination between multiple networked microgrid controllers to manage information transfer between microgrids and create a framework for a modernized grid with plug-and-play operability

of microgrids and DERs. Distributed control between microgrids enabled by the ecological principles of self-organization can improve coordination, facilitate expansion, and provide seamless integration to realize the full financial and technical benefits of microgrids for individual sites and the larger grid.

1.2. Value Proposition for Microgrids and DERs

The driving factors behind DER growth have been a combination of technological improvements, decreasing cost of components, increasing efficiency as the market grows in scale, and policies encouraging adoption of renewables (Baker et al. 2014). Increasing attention has also been placed on the reduction of soft costs of DER installation such as labor, supply chain, permitting, financing, and various transaction costs which account for more than half of total installation cost (Friedman et al. 2013). Tax incentives, subsidies, and rebates offered by governments and utilities provide additional price reductions that further increase the value proposition of DERs for end-users (Baker et al. 2014). Improvements in financing of DERs including leasing models, better financing tools, and customer targeting will drive future growth by opening new customer segments and enabling better management of upfront costs.

The growth in DER has disrupted traditional electricity business models. Local electricity generation and storage provides customers with a means of obtaining power another way and at a cheaper expense. However, the grid must continue to deliver functionality with a fixed cost even as the amount of energy sold to consumers decreases (Baker et al. 2014; Wood et al. 2016). This challenges conventional electricity markets as many small-scale competitors reduce load or push power back onto the grid. In an attempt to recover costs, utilities may raise rates and consequently more consumers may adopt

DERs, creating a “death spiral” that leads to the financial fall of the utility (Lacey 2014). Part of the challenge is that present utility regulation and business models are structured on capital-intensive purchases that require cost recovery through energy sales, rather than being financially rewarded using performance mechanisms that facilitate the adoption of DERs and grid stability with high amounts of DERs (Whited, Woolf, and Napoleon 2015).

Some consumers install microgrids to achieve increased autonomy and reliability of critical loads in case of a grid outage (Hirsch, Parag, and Guerrero 2018). Utilities and other energy stakeholders must alter their strategy to align with these changes by modernizing grid infrastructure to more easily integrate DERs and microgrids, offering additional services to accommodate consumer expectations, and altering their market and regulation models to have more flexibility (Baker et al. 2016). Further, development of advanced control techniques for DERs and microgrids can help enable these new strategies by providing ancillary services to the grid, improving customer satisfaction by involving their preferences and increasing accessibility, and decreasing operational cost through coordination and participation in an energy market. This creates value propositions for several energy stakeholders:

- **Energy Utilities:** Automated coordination of DERs and microgrids can reduce management responsibilities of the utility and allow for simpler integration of future assets. Additionally, advanced control can improve system reliability by providing seamless transition to alternate generation sources in the event of a contingency. It can also increase return-on-investment through reduced operation and maintenance costs. Improvements to customer satisfaction also occur through improved power quality and may result in cost savings passed to ratepayers.

- **Energy System Developers:** Integration of advanced controls in new and existing energy system technologies provides operational improvement and cost savings through better utilization of intermittent resources and increased system configuration flexibility. This allows developers to provide additional value to their customers and expand their portfolio by more easily scaling systems to include more DERs.
- **Energy System Owners and Operators:** Advanced controls enabling participation of DERs and microgrids in energy markets or ancillary service markets create economic benefit for system owners.
- **Independent System Operators (ISO) and Regional Transmission Organizations (RTO):** Advanced controls enabling participation of DERs and microgrids in energy markets or ancillary service markets provide reliability and resiliency support to the grid.

1.3. Microgrid Control Concepts

Existing power system and microgrid control strategies can be categorized as hierarchical controls, centralized and decentralized architectures, and internal microgrid asset coordination and microgrid network coordination. The following sections differentiate between these categorizations, specify the focus of this work, and analyze existing literature.

1.3.1. Primary, Secondary, and Tertiary Control Levels

Large-scale grid networks traditionally utilize a hierarchical frequency control structure consisting of primary, secondary, and tertiary control levels (see Figure 1.1). These control levels together at different response times to maintain stability in the power

grid following disturbances (NERC 2011). Primary control maintains balance between generation and load and stabilizes frequency after a disturbance, but may not return frequency to the nominal value for large disturbances. Governor control actions and load reduction methods are then utilized and respond within a few seconds. This control is often implemented autonomously using governor actions and load reduction (NERC 2011; Undrill 2018). Secondary control actions follow primary control and restore frequency to a nominal value through alteration of spinning reserve and non-spinning reserve operating set points. This occurs between 30 seconds and 15 minutes following a disturbance. This control can be automatic or manual and involves altering operating points of generating units (NERC 2011). Tertiary control is any action taken to get resources online and dispatched to handling present and future contingencies including changing operating set points, rescheduling or altering interchange, and load control. This occurs 10 or more minutes following a disturbance. This control is centralized and involves changing operating set points, rescheduling/altering interchange, and controlling load (NERC 2011).

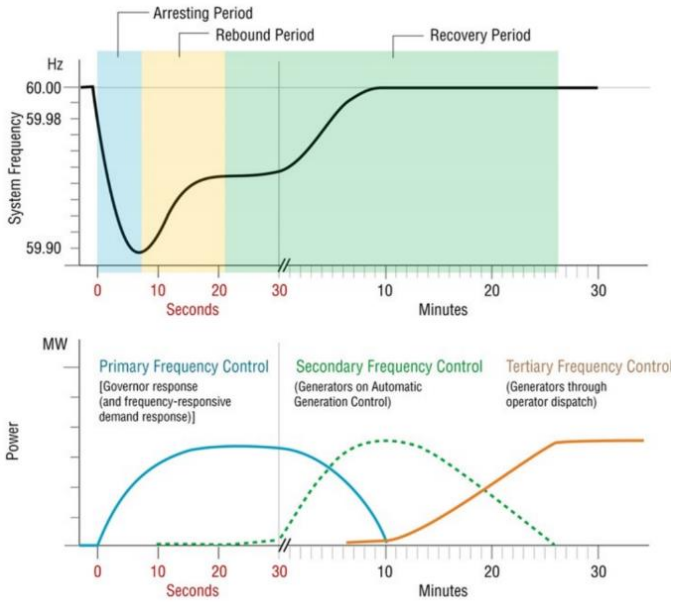

Figure 1.1: Hierarchical frequency control structure. Figure from (Eto et al. 2018).

These traditional hierarchical control structures have parallels to microgrid controls. However, microgrids often have additional functionalities such as islanding capability, coordinating distributed energy resource (DER), optimizing operation based on economics, resynchronization with the main grid, and controlling power exchange with the main grid (Bidram and Davoudi 2012). In microgrid controls, primary control stabilizes voltage and frequency, but also enables DER connection through power sharing and mitigates circulating currents. Additionally, in a small-scale microgrid, power quality can be an issue due to the small amount of available inertia to damper frequency changes, and therefore voltage-source inverters can be used to regulate frequency by simulating inertia characteristics (Olivares et al. 2018). Extensive technical literature can be found addressing primary microgrid control (Wang, Wu, and Zhang 2018; Xiang et al. 2016; Bendib et al. 2017; Li, J. et al. 2016; Quesada et al. 2014; Mongkoltanatas, Riu, and Lepivert 2013; Raghami, Ameli, and Hamzeh 2013; Li et al. 2017; Wang et al. 2019; Vandoorn et al. 2013; Horhoianu 2018; He et al. 2017; Kahrobaeian and Mohamed 2015). Communication-based techniques such as concentrated control, master/slave control, and distributed control are used to achieve voltage regulation and power sharing (Han et al. 2016; Rokrok, Shafie-khah; and Catalão 2018). Another primary control technique is droop control, which regulates frequency by adjusting active power and therefore does not require inter-unit communication. This allows for power sharing with less complexity (Han et al. 2016; Rokrok, Shafie-khah; and Catalão 2018). Secondary microgrid control typically occurs through an energy management system (EMS) within the microgrid. The EMS monitors voltage deviations to dispatch assets, and thereby maintains balance between supply and

loads to stabilize voltage levels within nominal ranges (Bidram and Davoudi 2012; Olivares et al. 2018). Control strategies such as real-time optimization and expert systems control enable the EMS to find optimal dispatch and unit commitment of distributed energy resources (Bui et al. 2017; Abass, Al-Awami, and Jamal 2016; Fossati et al. 2015). Tertiary control focuses on power exchange with the main grid during grid-tied operation as well as determining long-term, optimized set points for economic dispatch (Bidram and Davoudi 2012). Tertiary control coordinates internal assets and can schedule power sharing externally with other microgrids or the main grid (Caldognetto and Tenti 2014; Pashajavid et al. 2017a). Control strategies in this space such as gossiping algorithms, multi-agent control, and more recently value-based transactive energy have been utilized to create additional value through improved reliability, reduced cost, and more efficient use of renewables.

1.3.2. Internal Microgrid Control and Microgrid Network Control

Control schemes for a single microgrid and control of multiple microgrids can be difficult to distinguish because, at its core, a microgrid is simply a collection of DER assets and loads that can act as a single controllable entity and can isolate from the grid (Ton and Smith 2012). These single controllable entities can have common goals of supplying reliable power to loads in the event of a contingency, offering power at the lowest cost, and utilizing renewables efficiently, but each microgrid site has different critical loads, spinning and non-spinning reserve capacity, storage, and operational capabilities that make them unique.

The uniqueness of each microgrid requires that design engineers and controls vendors consider the composition and architecture of the microgrid as well as specific

priorities of the microgrid owner and beneficiaries. Secondary and tertiary controls of the microgrid can be customized and adapted to address local needs and coordinate asset setpoints used in primary control (Bidram and Davoudi 2012). Techniques for coordinating assets internal to a microgrid has been a well-researched topic with key strategies including optimal dispatch, bidding, model predictive control, game theory, and AI-based techniques such as particle swarm optimization, artificial neural networks, fuzzy logic, and agent-based control (Olivares et al. 2014; Bouzid et al. 2015; Lewis et al. 2013; Maknouninejad et al. 2012; Zhang et al. 2014; Ghanbarian et al. 2017; Jang and Kim 2017; Li et al. 2015; Lagorse, Simoes, and Miraoui 2009; Fossati et al. 2015; Al-Saedi et al. 2013). This research has made foundational steps in microgrid control but has only just begun to consider how to also coordinate the import and export of power from the main grid or other external sources. If other microgrids are within close proximity, it is a natural next question to consider how they might interact and coordinate towards common operational and environmental goals. Recent literature has described this as multi-microgrid coordination or microgrid network control. Microgrid networks can either be on-grid, where microgrids have a method (such as a transfer switch) to connect and disconnect from the main grid, or off-grid, where microgrids are isolated. There is far less literature available on multi-microgrid networks than on internal microgrid control, with the minimal available research suggesting methods such as game theory, hierarchical optimization, and self-organization can improve financial and technical metrics for all members of the network (Pashajavid et al. 2017a; Rivera, Farid, and Youcef-Toumi 2014; Chakraborty, Nakamura, and Okabe 2014; Mei et al. 2019; Du et al. 2018; Nikmehr, Najafi-Ravadanegh, and Khodaei 2017;

Kumrai et al. 2017, Zhang and Xu 2019; Lahon, Gupta, and Fernandez 2019; Jadhav, Patne, and Guerrero 2019).

1.3.3. Centralized and Decentralized Architectures

EMS and network-level microgrid controllers can be designed in centralized and decentralized architectures to provide tertiary control.

In a centralized control scheme, one dedicated controller makes control action decisions and delegates those actions across nodes within the microgrid. A generic depiction of this control strategy is shown in Figure 1.2a. Nodes implement the issued control actions at the local level. Nodes also provide feedback to the central controller such as measurements, status, and local setpoints. The central controller therefore has complete knowledge of asset states and the entire system state to include in decision making and action delegation. All computational processing occurs inside of this dedicated controller node, and the control action commands are absolute (must be implemented). It has the advantage of being simple in comparison to more modern methods, but also one major disadvantage in that changes require a complete reconfiguration of the central control process (Dressler 2008). There is only one major point of failure in a centralized system, which makes maintenance simple. However, the entire system will be compromised if this point is faulted (Baran 1962). Centralized architectures are difficult to scale, but simple to develop. This makes them ideal for applications that do not require changes or evolution of architecture.

A decentralized system architecture (see Figure 1.2b) uses controllers at each node to perform computational processing locally (Prabaharan et al. 2018; Olivares et al. 2014). No single node has complete information about the overall system state, though

communication between neighboring nodes is possible. Local control action decisions are made based on local data and information collected from neighboring nodes (Olivares et al. 2014). A central bus node may be used to establish network communication and messaging between nodes. These features of decentralized control allow microgrids to be easily extendable, scalable, and have the unique ability to adapt in the event of a failure. If one node is faulted, the majority of the system can remain functional (Prabaharan et al. 2018). Coordination is essential so a single asset doesn't accidently cause disruptions in the network due to limited awareness of the node, but the system is more tolerant against individual control process failures.

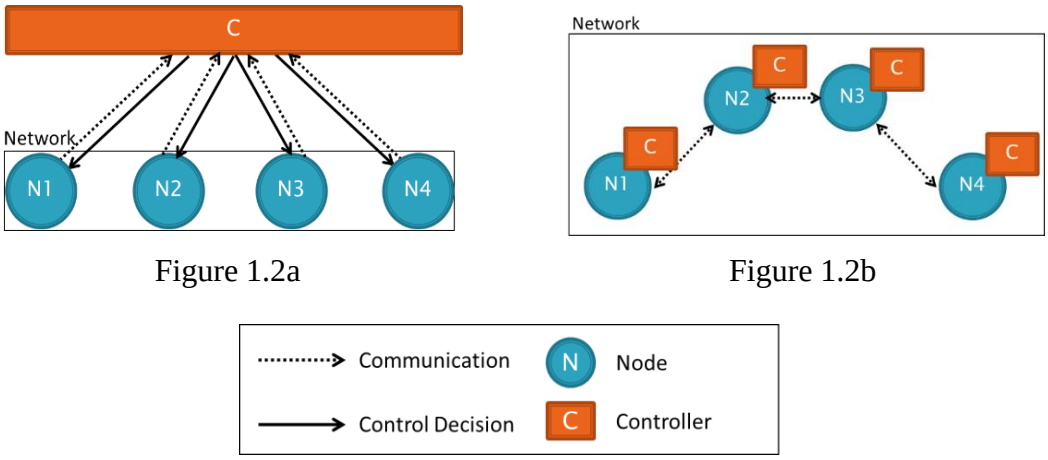

Figure 1.2a

Figure 1.2b

Figure 1.2: Centralized and decentralized control architectures.

Centralized architectures encompass much of microgrid controls literature (Olivares, Canizares, and Kazerani 2014; Al-Mulla and Elsherbini 2014; Tsikalakis and Hatziargyriou 2008; Jaiswal and Ghose 2017; Ambia, Al-Durra, and Muyeen 2011; Hajimiragha and Zadeh 2013; Li, Liu, and Zhang 2016), but decentralized architectures have gained attention in recent years for their scalability and adaptability (Harmouch, Krami, Hmina 2018; He et al. 2017; Sonnenschein et al. 2015; Liu, Y. et al. 2018; Divshali, Choi, and Liang 2017). In a microgrid using a centralized control paradigm, each DER

asset in the system sends information about its status to a central microgrid controller. The central microgrid controller gathers information from all parts of the system, then makes asset dispatch and setpoint control decisions that it sends back to the assets. Microgrids with decentralized control mechanisms have smaller-scale asset controllers on each DER asset that utilize a communication network to share information with one another. The assets make control decisions based on the information they receive from other assets. To preserve privacy and reduce points of vulnerability, the amount of information shared between neighboring assets is usually limited (He and Wei 2016; Wang, Yang, and Wang 2012).

The previously described examples of centralized control in power systems literature have been utilized to both coordinate assets within a single microgrid (usually through an EMS) (Olivares, Canizares, and Kazerani 2014; Yang et al. 2016; Rezaei and Kalantar 2014) and coordinate power exchange between multiple microgrids (Zenginis et al. 2017; Daneshvar, Pesaran, and Mohammadi-ivatloo 2018; Esfahani et al. 2019; Mei et al. 2019). Decentralized control is also used for both internal microgrid control (Yu et al. 2016; Mahmoud and Hussain 2015; Lou et al. 2017) and inter-microgrid network control (Du et al. 2018; Harmouch, Krami, and Hmina 2018; Wang et al. 2018; Mohamed et al. 2017). These methodologies can be combined in several ways, as summarized in Figure 1.3, with varying levels of implementation complexity for communication and hardware. These combined strategies are defined by the place in which control decisions are made and where information is shared. When centralized control is implemented within a microgrid, all microgrid assets send information to a central microgrid controller which then provides asset-level control decisions and setpoints back to the assets (Figures 1.3a

and 1.3b). When centralized control is implemented at the network level, the microgrid network controller handles communication and control decisions between the microgrids and the main grid system (Figures 1.3a and 1.3c). In decentralized internal microgrid control, microgrid assets can communicate directly with one another to coordinate their control actions and make decisions locally (Figures 1.3c and 1.3d). Decentralized control at the network level requires microgrids or microgrid assets to communicate and coordinate their control actions between microgrids and the main grid direction (Figures 1.3b and 1.3d). Inclusion of decentralized control at both the network level and internal microgrid level is the most complex case. More communication pathways, a larger number of controllers, and advanced control algorithms are required to make this configuration possible, but this approach allows for the most flexibility using the plug-and-play capability of hardware and controls.

Centralized Microgrid Network Control Decentralized Microgrid Network Control

Centralized Internal Microgrid Control

Decentralized Internal Microgrid Control

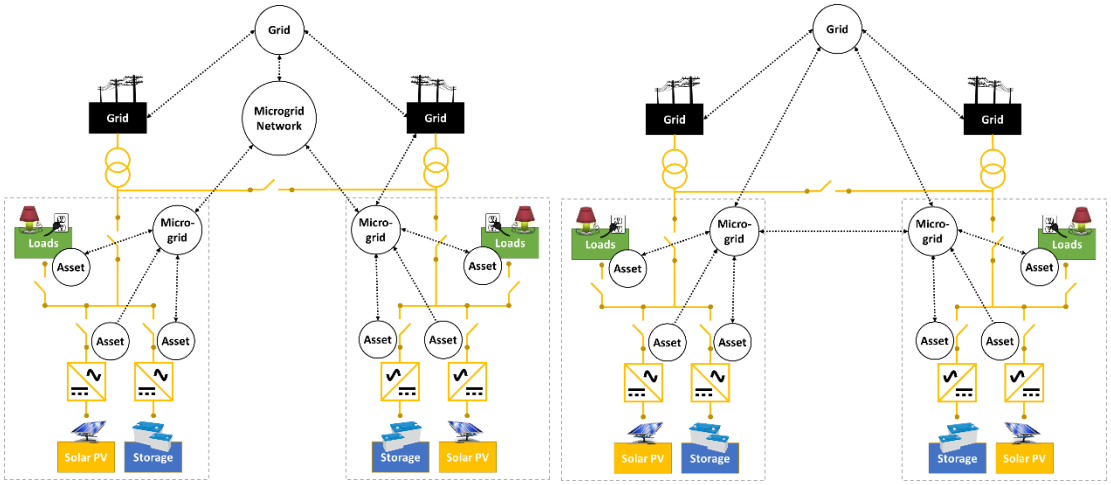

Figure 1.3a

Figure 1.3b

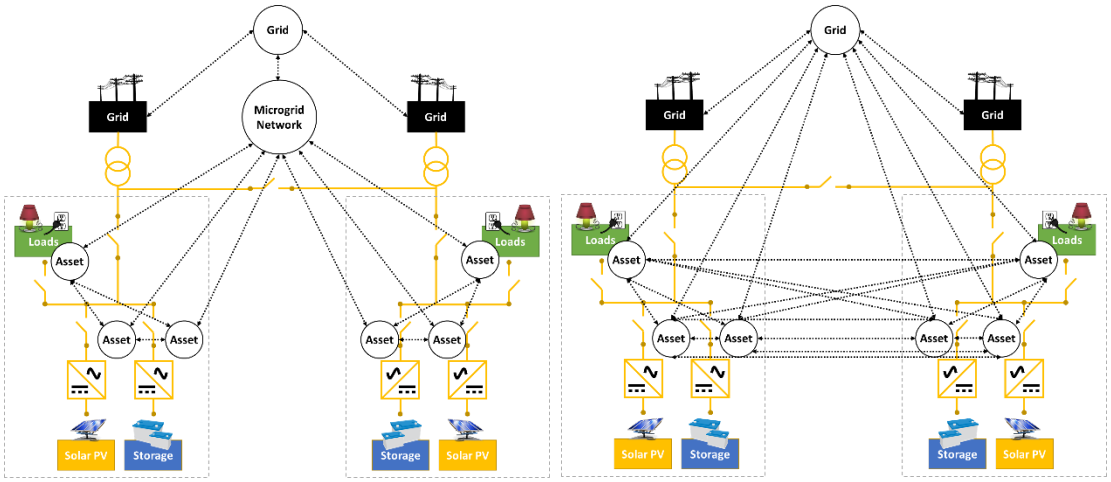

Figure 1.3c

Figure 1.3d

Key:

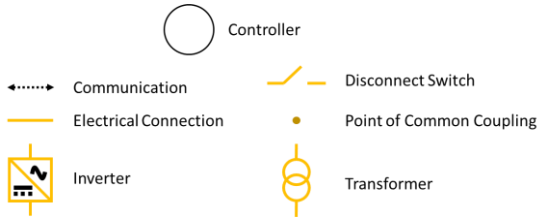

Figure 1.3: Control strategies combining centralized and decentralized control at the microgrid and microgrid network level.

1.4. Transactive Energy

Recent studies have identified transactive energy as a potential technique for managing dynamic balancing between supply and demand at the tertiary control level (The GridWise Architecture Council 2015). Transactive energy markets can prioritize both individual and global objectives to seek optimal results for the system. Energy, power, and ancillary services are traded within the network and value is assigned based on interaction between nodes. Transactive energy techniques have many applications (Holmberg et al. 2016) including energy trading across neighboring microgrids (Chen and Hu 2016; Divshali, Choi, and Liang 2017; Marzband, et al. 2018), mitigating voltage fluctuations caused by high penetration renewables (Chassin et al. 2017), and managing motor start-up currents (e.g., air conditioning) (Behboodi et al. 2018). Coordination between multiple microgrids and their control actions has shown promise to reduce cost by improving DERs utilization through improved dispatching (Wu and Guan 2013; Khodaei 2015; Zenginis et al. 2017). This benefit is especially enticing for off-grid applications where operation costs can be high and fossil fuel reserves have limited availability (Daneshvar, Pesaran, and Mohammadi-ivatloo 2018; Prinsloo, Mammoli, and Dobson 2017).

Physical demonstrations of transactive energy systems have been implemented across the world (Kok and Widergren 2016). Within the United States, a well-known example is the Olympic Peninsula Demonstration, which provided a transactive energy proof-of-concept between the years 2006-2007. Sponsored by the US Department of Energy, the network consisted of several controllable assets including demand response from 112 homes, five water pumps, and two diesel generators. A double-auction market technique was implemented on a five-minute timescale to coordinate real-time energy

purchasing through energy market clearing prices. Generators and pumps would bid into the market based on operational costs and water-reservoir levels, respectively, while the residents of the households could specify price-response preferences through their personal demand-response interface. The project demonstrated how a transactive energy system could achieve multiple objectives including system peak load management and energy cost savings for all market participants (Hammerstorm 2007). Though this project included demand response and some distributed generation, it did not incorporate home-based solar PV and energy storage that could be used for additional grid services and a finer degree of control at individual nodes across the electrical network. Additionally, power trading between home systems was not permitted. The Pacific Northwest Smart Grid Demonstration was an additional project in the United States that involved collaboration between multiple rural electric co-ops, investor-owned utilities, municipal utilities, and public utilities (Battelle Memorial Institute 2015). The transactive system introduced in this project consisted of 27 nodes exchanging information on delivered cost of electricity and predicted energy to be exchanged on the next time horizon with neighboring nodes. The system demonstrated how distributed assets can coordinate and respond dynamically across large regions. A transactive energy instrument called PowerMatcher has been implemented on over 1000 households and industrial sites across the Netherlands and Denmark (Kok 2013; PowerMatchSuite Transactive Smart Energy 2017). PowerMatcher allows consumers to sell the operational flexibility of their owned devices (e.g., appliances, electric vehicles) to interested parties. The only data exchanged consisted of aggregated information on power levels and prices, which protects the privacy of the customer from sharing local-specific data. Multi-objective optimization has been demonstrated with

respect to two different subsystems: market operations and active distribution network management. Field implementations have shown results including scalability beyond 1 million customers, distribution-level peak-load-reductions of 30-35%, and wind imbalance reduction of 80%.

Though these transactive energy projects have successfully demonstrated techniques such as pricing-based control, distributed asset coordination, scalability, and multi-objective optimization, further scientific development and physical demonstration is needed of direct power exchange between nodes using decentralized control architectures. Sometimes called peer-to-peer trading, a few projects exist including Piclo (Piclo 2018) and Vandebron (Vandebron n.d.) that provide energy consumers the ability to choose exactly where their electricity comes from, community-based projects such as SonnenCommunity (SonnenCommunity 2018) that focus on a central pool of energy shared by all members, and blockchain-based project such as the Brooklyn Microgrid that has a functional peer-to-peer transaction mechanism secured through blockchain (Brooklyn Microgrid 2018). Figure 1.4 shows an example of these peer-to-peer transactions on a single neighborhood street in Brooklyn. However, these existing projects utilize a centralized virtual marketplace or controlling entity to ensure a balanced market within the system. These efforts provide evidence for more research needed in development and physical demonstration of decentralized control techniques for microgrid networks.

Figure 1.4: Peer-to-peer energy trading on the Brooklyn Microgrid. Figure from (Lilic 2015).

1.5. Self-organizing Control Techniques for Microgrids and DERs

Self-organization is the process by which complex behaviors of a system can emerge from the collective interactions of distributed agents in a network (see Figure 1.5). Common examples of self-organization come from nature and biology where organisms act independently, but their actions and interactions with fellow organisms create global coordination (Lakhtakia and Martin-Palma 2013). This can be seen in group navigation of a flock of birds or the construction of an ant nest. Replicating this type of behavior has proven useful in many fields including computer science (Yang, Cui, and Xiao 2013), robotics (Floreano et al. 2010), and material science (Diesendruck 2015). Electrical grid controls can similarly incorporate self-organizing principles to coordinate DER or microgrid nodes that make control action decisions for both the benefit of the individual node and the entire network.

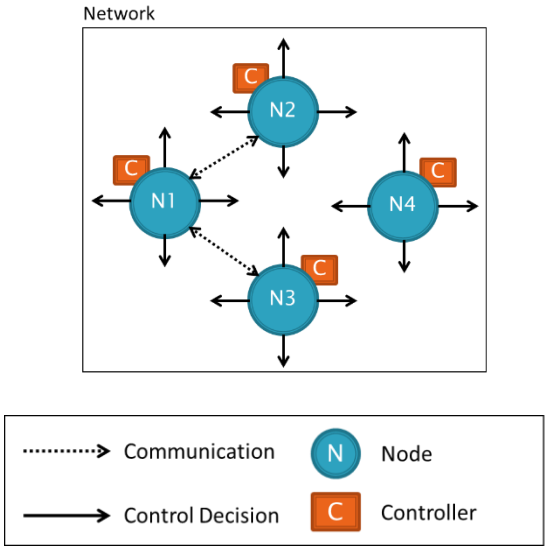

Figure 1.5: Self-organizing coordination between subsystems.

Several self-organizing control algorithm techniques for microgrid networks have been developed such as artificial neural networks for adaptive learning and forecasting (Chaouachi et al. 2013; Li et al. 2015), fuzzy-based logic for addressing forecasting uncertainties (Chaouachi et al. 2013), and multi-agent systems for distributing computations (Jiang 2006; Cossentino and Lodato 2011; Leng and Polmai n.d.; Dimeas and Hatziargyriou 2005; Oyarzabal et al. 2005; Zheng and Cai 2010; Logenthiran et al. 2010; Olivares et al. 2014). Multi-agent systems are particularly useful frameworks that can increase system scalability, flexibility, autonomy, and resiliency. They can be implemented in a centralized or decentralized control architecture, with significant advantages such as lower computation time and increased robustness when decentralized (Sharma, Srinivasan, and Kumar 2016). Agents can aggregate with other agents and there is essentially no limit on the number of agents that can join a group. This degree of expandability is desirable for larger networks and integration of other self-organizing techniques such as machine learning, cluster analysis, and fuzzy logic. In addition, agents

can self-heal and recover from loss of resources and dynamically coordinate to respond to faults in the system (Rivera, Farid, and Youcef-Toumi 2014). Multi-agent systems have emerged as a prominent technique for implementing transactive energy systems (Prinsloo, Mammoli, and Dobson 2017; Liu, Y. et al. 2018; Madkour 2016; Rosa de Jesus 2018).

Multi-agent frameworks are common in literature for implementing communication and interaction between microgrids. Each entity in the network can be represented by an agent or set of agents that interact to accomplish tasks (Pashajavid, Shahnia, and Ghosh 2017b; Prinsloo, Mammoli, and Dobson 2017; Li, Q. et al. 2016; Liu, Y. et al. 2018; Liu, W. et al. 2018; Wang et al. 2018; Harmouch, Krami, and Hmina 2018; Rivera, Farid, and Youcef-Toumi 2014). Agents interact in a competitive or cooperative environment that has parallels to game theory. Competitive games involve agents with opposing interests, while cooperative games involve strategic collaboration between agents with aligned interests (Colman 2014). The information shared between agents provides awareness to the agent on the state of the network and contributes to the decisions and strategies it makes locally. The amount and order in which information is received may change actions taken by the agent and therefore affect the outcome of the game. Agents are also capable of modifying their decision-making strategies and forming opinions about one another based on trends of past engagements.

1.6. Present Literature on State-of-Art Controls

This dissertation advances best-in-practice microgrid control algorithms by incorporating self-organizing techniques to achieve automated coordination and decreased operational cost for microgrid assets. Literature review identified specific areas in need of future research including multi-microgrid networks, markets for inter-microgrid trading,

and how to formulate local control actions within the individual microgrids to also achieve global-level benefits. The work summarized in Chapters 3 and 4 of this dissertation suggest use of the architecture shown in Figure 1.3b, where internal asset coordination is handled by a centralized microgrid controller while coordination between microgrids remains completely decentralized. In this hierarchy, control decisions within a single microgrid are optimized using state information of all assets within that microgrid and the available power and price of power to be purchased from or sold to neighboring microgrids. Primary control at each asset maintains stability, secondary control manages assets within a microgrid as suggested by past work (Olivares et al. 2014; Hatziargyriou 2013), and tertiary control manages inter-microgrid trading across the network. As such, this work will remain focused on the tertiary level of control.

A selection of 26 representative studies on tertiary-level methods for multi-microgrid network coordination controls are displayed in Appendix A. Definitions for each category used to characterize the literature can be found in Tables 1.1 and 1.2. The works were limited to those published in the past 10 years (2009 – 2019). Some of the literature refers to microgrid networks in different terms such as microgrid communities or single controllable buildings within one microgrid, but they were selected based on their organization of DER assets into single controllable entities with points of common coupling to each other and/or the main grid. Some literature also studies the entire control structure containing elements of primary, secondary, and tertiary control. They were included in the list for the portion of their research that covers tertiary control.

Table 1.1: Characteristics of Study Methods

Characteristic	Definition	Options
Objective	Goals of the work and benefits they are seeking to implement in the network.	Various
Control Techniques	Major control techniques used to achieve objective.	Various
Internal Microgrid Control Modeled	Whether or not the method included asset scheduling, physical asset modeling, and/or asset-level controllers inside the microgrid.	Yes
		No
Internal Microgrid Control Topology	The control architecture used for internal microgrid control modeling.	Centralized
		Decentralized
Microgrid Network Control Topology	The control architecture used for microgrid network modeling.	Centralized
		Decentralized

Table 1.2: Characteristics of Case Studies

Characteristic	Definition	Options
Network Architecture	How nodes are connected in the case study.	Abstract (Graph theory-based)
		Arbitrary
		Modified or Exact Existing Systems
		Modified or Exact IEEE Test Cases
		Modified or Exact Benchmarking Test Cases (Other)
		Synthetically Generated
Time Scale	Smallest time increment simulated in case study.	Various
Grid	Whether or not the case study included a connection to the main grid.	Yes
		No
Voltage Level	Voltage level at which case study system is operating.	Low
		Low/med
		Med
Asset Types	Types of assets included in the case study system.	Electrical
		Electrical/thermal
Max Node #	Maximum number of nodes simulated in case study	Various

The majority of studies implement decentralized techniques for microgrid network control and centralized control for internal asset control (see Figures 1.6 and 1.7). Agent-based control techniques are common. This correlates with the architecture described in Figure 1.3b and often involves well-defined hierarchical control levels between assets and the larger network. Hybrid approaches with techniques from both centralized and decentralized paradigms were also present in several studies.

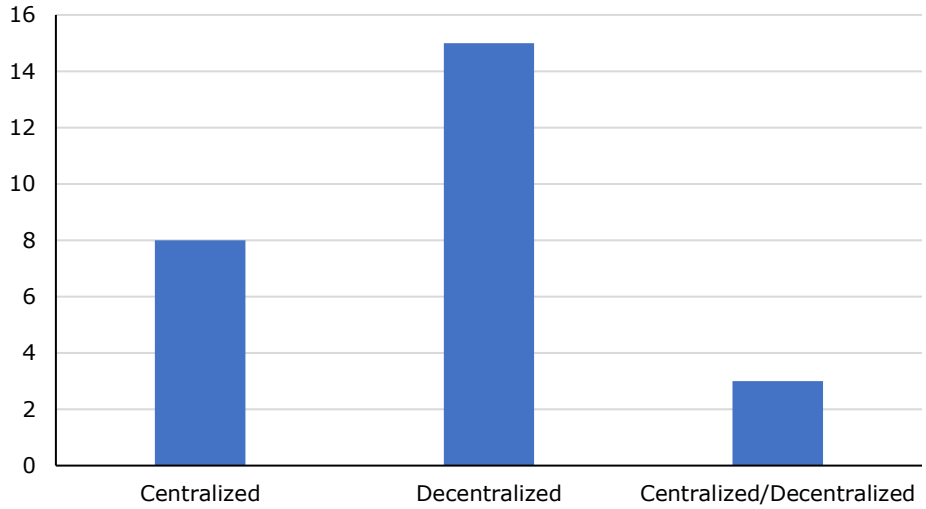

Figure 1.6: Microgrid network control topologies utilized in selected literature.

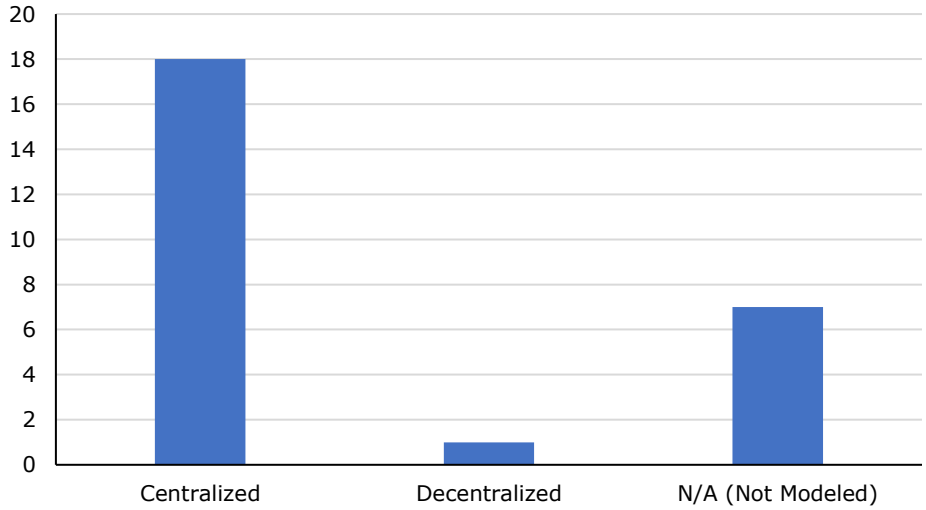

Figure 1.7: Internal microgrid control topologies utilized in selected literature.

Existing literature included minimal study and discussion of how network architecture and levels of connectivity effect simulated results. The network architecture types utilized in literature can be categorized in the following ways:

- **Abstract (Graph theory-based)**: Nodes are connected according to a classical, graph-theory based network configuration. These are generalizable and well-understood. Example: Linear networks; fully-connected network.
- **Arbitrary**: Nodes are connected in an arbitrary configuration with no reference to any synthetic, standardized, or existing configuration. Example: A figure and/or description provided with no reference.
- **Existing Systems**: Nodes are modeled and connected based on the configuration of existing or future physical systems. Example: University campus electrical network; city electrical network.
- **Modified or Exact Benchmarking Test Cases (Other)** – Nodes are connected according to a standardized benchmarking test case network developed by a group of energy industry professionals or energy authority. Pre-defined data sets are often available for these cases, though some literature modifies the test case to include different types of assets and data. Example: European Union Benchmark LV Microgrid Network.
- **Modified or Exact IEEE Test Cases** – Nodes are connected according to a standardized test case network developed by industry professionals within the IEEE Distribution System Analysis Subcommittee to evaluate and benchmark power-flow algorithms. Pre-defined data sets are often available for these test

cases, though some literature modifies the test case to include different types of assets and data. Example: IEEE 13-bus Feeder; IEEE 123-bus Feeder.

- **Synthetically Generated (AI)** – Nodes are connected in a configuration defined by a synthetically generated network. These synthetically generated networks are often created with artificial intelligence algorithms trained on existing or standardized network configurations. Example: Network created by AI algorithms trained on IEEE test cases.
- **Synthetically Generated (Random)** – Nodes are connected in a randomly generated configuration. Example: Randomly selected distances and connections between nodes.

IEEE and other benchmarking test cases have well-understood behavior given the use of measurements from real systems and repeated study by researchers. This makes it easier to compare to other network architecture types and algorithms, with findings that are easily generalizable to other applications within power/energy such as high-voltage transmission-level networks. Existing systems are comparable to other network architecture types and generalizable within the power/energy field since they are based on realistic, functioning systems. They have well-understood behavior since data often comes from measurement of a physical system but cannot be easily generalized to other applications. Since synthetically generated network configurations are a newly formed, unstudied systems, they have less well-understood behavior. Abstract (or graph theory-based) networks also tend to have very well understood behavior due to the vast amount of study in graph theory over several decades (Chen 1971; Golumbic 1980; Leeuwen 1990; Ito 2008). They can be compared to networks in any field of application and to the other

network architecture types discussed here. Arbitrary architectures are usually designed in a generalizable network with a shared distribution feeder or complete-graph configuration, which can be comparable to other networks in the power/energy field but do not have the connectivity justified in any other way.

A summary of the network architectures used in the selected literature set are shown in Figure 1.8. The majority (38%) used case studies with arbitrary architectures, while 15% used existing systems and 15% used either IEEE test cases or other benchmarking test cases. Synthetically generated networks based on machine learning of other networks were not found in any of the selected literature, but 15% used randomly generated synthetic networks. Only one piece of literature (Gregoratti and Matamoros 2015) used graph-theory based networks and considered several different topologies including ring, line, and fully-connected networks.

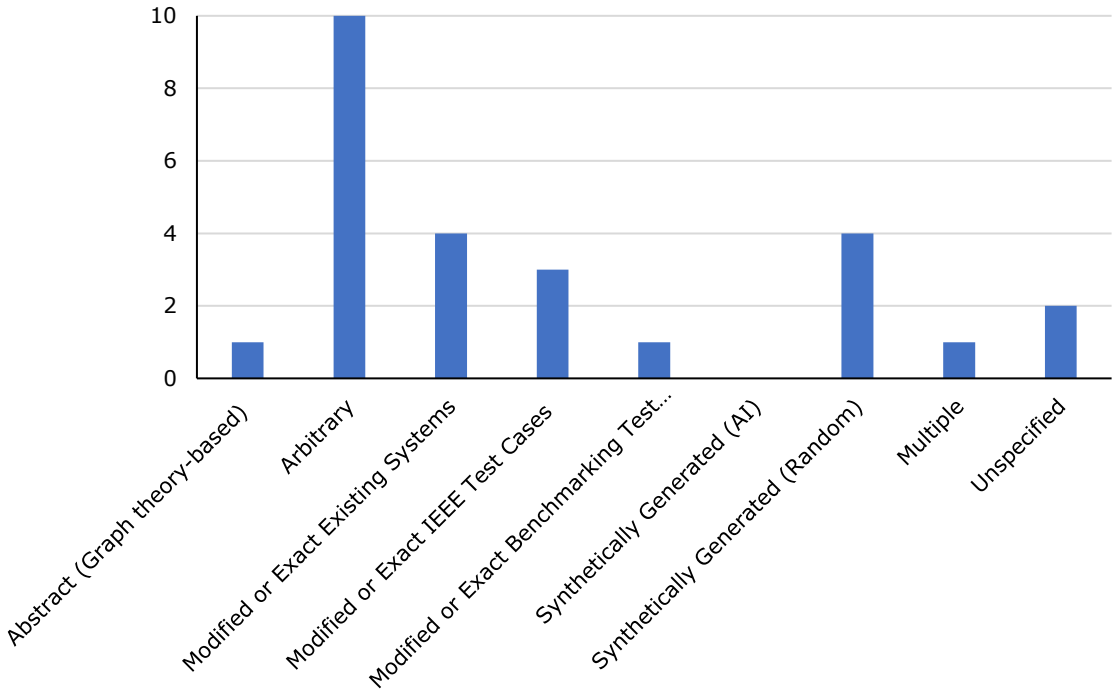

Figure 1.8: Microgrid network architectures utilized in selected literature.

The maximum number of nodes utilized in case studies is shown in Figure 1.9. Most case studies analyzed 10 nodes or less, though several did have more than 100 nodes (Wu and Guan 2013; Chakraborty, Nakamura, and Okabe 2014; Hammad, Farraj, and Kundur 2015a; Mei et al. 2019; Sadd, Han, and Poor 2011). Of the surveyed literature that analyzed a network larger than 10 nodes, 80% used synthetically generated network architectures and all used synthetically or randomly generated load data. It should be noted that due to the nature of randomization, some of these network configurations may have been unrealistic. This is especially true for those that randomly generated power demand in a wide range (i.e. 0-100 MW across five minutes), as it could create load profiles with large peaks and unrealistic or unmanageable transients if translated to a physical network.

Figure 1.10 shows the minimum increment used for time steps within the case studies. The most common time step used was hourly, which is common for day-ahead energy asset scheduling. These results provide satisfactory high-level metrics on the benefits of the proposed approaches, however for them to be utilized in real-time operations they would require primary, secondary, and additional tertiary control mechanisms. It should also be noted that many of the surveyed literature did not specify the time step of their data in the text and could not be determined by the graphs provided. All literature was at the distribution network level and below (low or medium voltage).

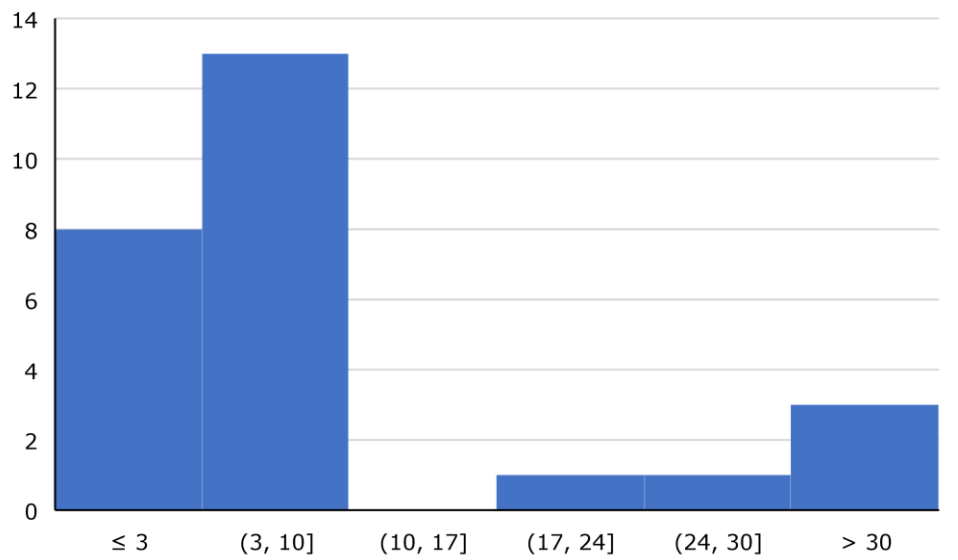

Figure 1.9: Maximum number of nodes used in case studies of selected literature.

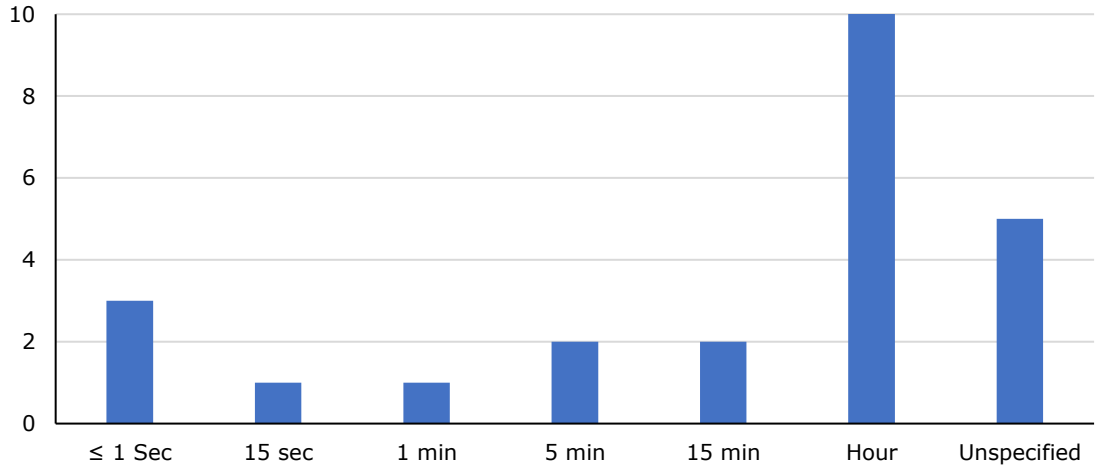

Figure 1.10: Minimum time step used in case studies of selected literature.

1.7. Objectives of Dissertation Research

This dissertation provides background information on existing microgrid and microgrid network control strategies in Chapter 1 and supporting evidence for the need of advanced controls strategies with the growth of distributed energy resources in Chapter 2. Chapter 3 introduces a generalizable, scalable framework for transactive energy trading in microgrid networks and is built upon to include decision making and trading preferences

in Chapter 4. Throughout the dissertation, specific attention is given to how individual node-level behaviors affect network-level behaviors and outcomes including economic metrics (e.g., levelized-cost-of-energy, maximum and minimum buying/selling prices) and behavioral metrics (e.g., number of successful negotiations, number of consistent trading groups). These control techniques are evaluated in a range of network configurations to maximize generalizability. Chapter 5 provides a discussion of scientific implications of the dissertation, followed by a brief discussion of physical deployment and future work.

Below is a summary of each chapter:

- Chapter 1: Introduction – An introduction to microgrid control concepts, self-organizing control techniques, transactive energy, and the present state of the research space. Objectives of the dissertation research are identified, as well as a brief description of the work completed in Chapters 2, 3, and 4.
- Chapter 2: Implications of High-penetration Renewables for Ratepayers and Utilities in the Residential Solar Photovoltaic (PV) Market – A journal article examining the combined effect electric rate structures and local environmental conditions have on optimal solar home system size, ratepayer financials, utility financials, and electric grid ramp rate requirements as the amount of installed solar PV increases. Analyses are conducted for three urban regions in the United States that provide both generalizable and site-specific findings. This article was published in *Applied Energy* in October 2016. Permissions by co-author visible in Appendix B.
- Chapter 3: Scalable Multi-Agent Microgrid Negotiations for a Transactive Energy Market – A journal article introducing a generalizable method for negotiation and

energy trading between microgrids in a grid-connected network. Multi-agent techniques enable information sharing between nodes and scalability of the network architecture. Year-long simulations of 3-node and 9-node networks with varying local energy storage capacities are implemented to examine the impact on levelized cost of energy and trading behaviors. This article was published in *Applied Energy* in November 2018.

- Chapter 4: Reputation-based Competitive Pricing Negotiation and Power Trading for Grid-Connected Microgrid Networks – A journal article describing how microgrids in a grid-connected network can be modeled as a competitive game of negotiations between agents to determine energy pricing with energy trades offered by each agent based on most utility (or payoff) for themselves. Negotiation strategies are affected by reputation, which considers the agent's familiarity, success rate, and value attributed to other agents. Year-long 9-node networks with varying levels of connectivity are analyzed. This article will be submitted for publication January 2020.
- Chapter 5: Discussion – Results from Chapters 2, 3, and 4 are discussed in aggregate. Trends in nodal and network behavior with respect to self-organizing control techniques are described. Implications to the energy industry are described and future research spaces are defined, including implementation of the control techniques described in Chapter 3 and Chapter 4 in hardware

CHAPTER 2

IMPLICATIONS OF HIGH-PENETRATION RENEWABLES FOR RATEPAYERS AND UTILITIES IN THE RESIDENTIAL SOLAR PHOTOVOLTAIC (PV) MARKET

Authored by Samantha A. Janko, Michael R. Arnold, & Nathan G. Johnson

Published in *Applied Energy* Vol. 180 October 2016

https://doi.org/10.1016/j.apenergy.2016.07.041

Abstract

Residential energy markets in the United States are undergoing rapid change with increasing amounts of solar photovoltaic (PV) systems installed each year. This study examines the combined effect of electric rate structures and local environmental forcings on optimal solar home system size, ratepayer financials, utility financials, and electric grid ramp rate requirements for three urban regions in the United States. Techno-economic analyses are completed for Chicago, Phoenix, and Seattle and the results contrasted to provide both generalizable findings and site-specific findings. Various net metering scenarios and time-of-use rate schedules are investigated to evaluate the optimal solar PV capacity and battery storage in a typical residential home for each locality. The net residential load profile is created for a single home using BEopt and then scaled to assess technical and economic impacts to the utility for a market segment of 10,000 homes modeled in HOMER. Emphasis is given to intraday load profiles, ramp rate requirements, peak capacity requirements, load factor, revenue loss, and revenue recuperation as a function of the number of ratepayers with solar PV. Increases in solar PV penetration reduced the annual system load factor by an equivalent percentage yet had little to no impact on peak power requirements. Ramp rate requirements were largest for Chicago in

October, Phoenix in July, and Seattle in January. Net metering on a monthly or annual basis had a negligible impact on optimal solar PV capacity, yet optimal solar PV capacity reduced by 20-50% if net metering was removed altogether. Technical and economic data are generated from simulations with solar penetration up to 100% of homes. For the scenario with 20% homes using solar PV, the utility would need a 16%, 24%, and 8% increase in time-of-use electricity rates ($/kWh) across all ratepayers to recover lost revenue in Chicago, Phoenix, and Seattle, respectively. The $15 monthly connection fee would need to increase by 94%, 228%, or 50% across the same cities if time-of-use electricity rates were to remain unchanged. Batteries were found to be cost-effective in simulations without net metering and at cost reductions of at least 55%. Batteries were not cost-effective—even if they were free—when net metering was in effect. As expected, Phoenix had the most favorable economic scenario for residential solar PV, primarily due to the high solar insolation.

2.1. Introduction

Addressing the societal demand for low-carbon energy is an ongoing challenge that will persist for several decades. It has been suggested that a zero-carbon economy can be realized in the United States by 2050 through changes in technology, policy, economics, business models, and consumer behavior (Lovins 2013). Yet that year is far away, and much progress is needed. For now, the increasing amount of research and practice in reducing carbon emissions hint that a zero-carbon future may be possible (EIA 2014; Roosa and Jhaveri 2009; Damiani et al. 2011).

The long-term vision for carbon-free energy has been pursued with research in renewables design and integration (Nemet et al. 2012; Purohit and Purohit 2010), grid

stability at high levels of renewable penetration (Carrasco et al. 2006; Kempton and Tomić 2005; Lund 2005; Yan et al. 2015; Lund and Münster 2003), building energy systems design and analysis (Nguyen et al. 2014; Wang et al. 2011; Salpakari and Lund 2016), energy efficiency in end-use devices (Abramson et al. 1990; Negrão and Hermes 2011; Finn et al. 2013), thermal energy storage to offset air conditioning loads (Ruddell et al. 2014; Arteconi et al. 2012), and studies of the social, political, and economic implications of transitioning to a low-carbon future (Laird 2013; Miller and Richter 2014; Yun and Steemers 2011; Mills and Wiser 2015; Brouwer et al. 2016). The diversity of topics covered in the literature is an indication of the complexity and the challenges faced when integrating distributed energy resources (DER) from the individual circuit to the larger grid.

Household solar photovoltaic (PV) systems have become increasingly common in the United States, with a current annual growth rate of 58% (SEIA 2014). Solar home systems commonly produce excess electricity during the daytime to displace grid purchases during off-sun hours. This excess electricity can be stored in batteries for later use, or credited to the customer through a feed-in tariff or net metering. Net metering is a billing agreement that allows customers to use the credited electricity at another time when solar PV generation is less than the household load. Net metering is a major factor in solar PV adoption (Darghouth et al. 2011). The ability to use the grid as a "zero cost lossless battery" is unquestionably an economic advantage for the consumer (ratepayer). A feed-in tariff is another form of billing agreement (Couture and Gagnon 2010). In a feed-in tariff billing agreement, the ratepayer is compensated monetarily for excess production, whereas in net metering the ratepayer receives kilowatt-hour energy credits by "rolling back the meter" during periods of excess production.

The technical and economic implications of small amounts of household solar PV are minimal to the utility, but at higher penetration levels, solar PV is expected to cause grid instability and disrupt utility business models (Denholm and Margolis 2007). A primary concern is managing the significant rise in electrical demand that occurs during the late afternoon when solar output declines and residential loads increase as people arrive home from work or school. This increases the ramp rate requirement from dispatchable generation as popularized in the "duck curve" or "duck chart" (California ISO 2013). Intermittency in renewables is another point of concern when noting that utilities must keep sufficient reserves (e.g., dispatchable generation, storage, and demand response) online to displace potential disruptions in solar PV power output caused by clouding or other effects (Denholm and Margolis 2007; Evans et al. 2016). These issues may become more prevalent over time as distributed solar PV capacity continues to increase.

2.2. Background

A growing body of research has explored the technical and economic implications of high-penetration distributed residential solar PV (Cai et al. 2013; Darghouth et al. 2011; Katiraei and Aguero 2011; Liu et al. 2014; Mondol et al. 2009; Østergaard 2009; Pillai et al. 2014; Reichelstein and Yorston 2012). It is clear that the declining costs of solar modules have contributed to increases in the installed capacity of solar PV (EA 2008). Total hardware costs have dropped from $3.30 per watt to $1.83 per watt between 2010 and 2012, with current module prices at under $1.00 per watt (Ardani 2014; Hernández-Moro and Martínez-Duart 2012). Recent work is seeking to reduce costs further by targeting the "soft costs" of solar installation such as labor, supply chain, permitting, and transaction costs. Soft costs comprised approximately two-thirds of the total installed cost

of $5.22 per watt in 2012 (Ardani 2014). Additional reductions in cost to the end-user were available through tax incentives, subsidies, and rebates offered by governments and utilities (Mulder et al. 2013; Reichelstein and Yorston 2012). Leasing is also an attractive option that offers a no-money-down solution with low financing charges. Current systems can be leased on 20-year or 25-year agreements for as little as $3.00 per watt to the end-user after accounting for rebates, incentives, financing charges, and maintenance and warranty costs (DSIRE 2015; Liu et al. 2014; SolarCity 2015).

The economic advantage of home solar is not universal for all ratepayers. An analysis of local electric rate structures must be performed to determine if solar PV reduces the levelized cost of electricity (LCOE) for the end-user vis-à-vis grid power alone (Cai et al. 2013; Mondol et al. 2009). Areas with higher costs of electricity and favorable distributed generation policies—such as Hawaii (USA), Germany, and Denmark—have experienced substantial increases in solar PV penetration whereas regions with lower electricity costs and more strict owner-side generation policies—such as fossil-fuel rich industrialized economies—have seen solar PV penetration grow at a slower rate (Anaya and Pollitt 2014; IEA 2014, 2015). Net metering has been suggested as one of the leading contributors to the growth of the residential solar PV market (Darghouth et al. 2011). Feed-in tariffs have also contributed to solar PV adoption and often begin with a high feed-in tariff to spur the installation of solar and then reduce the tariff's value over time as a way to slow down the rate of solar PV adoption (Mondol et al. 2009; Wand and Leuthold 2011; Wirth 2015).

Electric utility business models will not be insolated from the rise in distributed solar PV. Instead, it has been surmised that solar PV consumers will have the strongest

effect on utility revenue (Pillai et al. 2014). According to a scoping study conducted by Lawrence Berkeley National Laboratory, a solar PV penetration rate reducing 10% of retail sales at a Northeast wires-only distribution utility was found to reduce the return on equity by 40% with a corresponding 15% reduction in achieved earnings and an average rate increase of 2.7% for ratepayers (Satchwell et al. 2014). This suggests that the loss of revenue from solar PV customers could be recouped through rate increases for all customers—solar and non-solar homes.

Aside from revenue loss, uncontrolled renewables can create over-production issues within a region when thermal base-loading power plants need to operate at a minimum load or provide reserve capacity (Wirth 2015). In addition, fluctuations in solar PV output can cause disturbances in voltage and frequency that fatigue hardware and reduce equipment lifetime (Bhat et al. 2014; Kern et al. 1989; Patsalides et al. 2007; Sadineni et al. 2012). Further studies are needed to explore these and other challenges of high-penetration solar PV integration (Katiraei and Aguero 2011). Yet for now, it can be surmised that the unfolding of the residential solar PV market will not continue business as usual for utilities, customers, and technology providers. Modeling approaches and stakeholder engagement efforts that represent, contrast, and integrate the perspectives of various parties can facilitate energy planning decisions for mutual gain (Browne et al. 2010; Løken 2007).

This article contrasts the objectives of residential ratepayers and an electric utility by simulating the combined effect of electric rate structures and local environmental forcings on optimal home energy system size, ratepayer financials, and utility technical and financial factors. Analyses are completed of three urban cities (Chicago, Phoenix, and

Seattle) in the United States and then contrasted to provide both generalizable findings and site-specific findings. Various time-of-use pricing schedules are investigated, and the effect of net metering is evaluated to determine the optimal capacity of solar PV and battery storage in a typical residential home. The residential load profile is scaled to assess system-wide technical and economic merits of interest to a utility at low-, medium-, and high-penetration solar PV scenarios.

2.3. Methodological Approach

A variety of models are available for evaluating changes in the residential solar PV market. These include elements of expansion planning for modeling system-wide effects of load growth and generation assets, and production cost modeling and economic dispatch for dispatching energy sources to deliver the least cost energy. In this analysis, two software packages were employed: Building Energy Optimization (BEopt) was used to simulate household load profiles for each study location (Christensen et al. 2006, U.S. Department of Energy 2014), and Hybrid Optimization Model for Electric Renewables (HOMER®) (Lambert et al. 2006) was used to aggregate and evaluate system-wide effect of solar PV on the net system load. Finally, sensitivity analyses were performed on hardware cost parameters, solar PV penetration, and utility electricity rates.

BEopt, commonly used to evaluate whole-building energy savings, provides important information about a building, such as size and orientation, materials composition and structure, location, occupancy data, along with a library of technologies for lighting, heating, cooking, and other end-use energy needs. BEopt can be used to describe the costs and benefits of renewable energy options for new or existing residential homes (Anderson et al. 2006; Christensen et al. 2006). Building energy calculations are completed in an

underlying simulation engine, such as EnergyPlus (Crawley et al. 2001). The computed hourly time series data and aggregate energy use data are reported in BEopt's graphical user interface.

The HOMER software can be used for power system topology selection and sizing against uncertain constraints that are explored through sensitivity analyses on hardware cost, performance, resource availability, and other data used in economic feasibility studies (Fulzele and Dutt 2011; Hafez and Bhattacharya 2012; Roy et al. 2014). HOMER models a power system using chronological hourly simulations over a one-year period and quantifies the total cost of the power system over its multi-year lifespan. Although HOMER was developed primarily for off-grid micro-grid systems, the software can be used to simulate residential-scale grid-connected systems and model a simplified representation of the electric grid as a single circuit to calculate aggregate load and economic statistics (Johnson et al. 2011). The latter use case demonstrates the primary role of HOMER in this study.

2.3.1. Electric Load Profile and Solar Irradiance Simulation

A residential load profile (without renewables or batteries) was simulated for a household created in BEopt. The selection of a single, common home design subjected to local environmental forcings permits a more direct comparison of results, and therefore generalizable findings, across the case study locations for optimal solar home system size, ratepayer financials, utility financials, and electric grid ramp rate requirements as a function of electric rate structures.

The two-story square home of 11.58 meters by 11.58 meters (38 feet by 38 feet) equates to a total of 221 square meters (2,388 square feet) after subtracting the garage space

of 7.62 meters by 6.10 meters (25 feet by 20 feet) on the first floor (Fig. 2.1). This home size is within 0.2% of the national average for the United States (U.S. Census Bureau 2010a). Many of the standard industry values listed in the Building America House Simulation Protocols were chosen for simulation (Hendron and Engebrecht 2010). Points of deviation include: gas water heater, gas cooking range, electric clothes dryer, and spacing of 6.10 meters (20 feet) between neighboring households. The BEopt model can be reproduced using default values with edits to such values described as deviations from default settings.

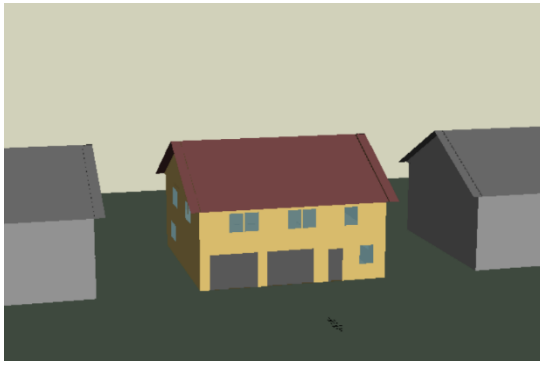

Figure 2.1: Household visualization in BEopt.

The BEopt household model was run for three separate locations using BEopt's predefined TMY2 solar and temperature profile data for Chicago, Phoenix, and Seattle (Christensen et al. 2006). These cities were chosen to provide dataset diversity in location, solar insolation, climate, and weather as shown in Fig. 2.2 and Table 2.1. The Chicago metropolitan area, home to 9.7 million people in the mid-western region of the United States, experiences colder winters relative to the other two cities. Seattle is further north in latitude, yet its proximity to the Pacific Ocean in the northwestern region of the country provides more consistent year-round temperatures and milder winters. The 3.7 million people living in the metropolitan area of Seattle have overcast skies for approximately one-

quarter to one-third of the year, and consequently receive the least solar insolation of any city. Phoenix has a desert climate and is located in the southwestern United States. The 4.2 million people in the Phoenix metropolitan area experience the greatest solar insolation and hottest temperatures of any study location (U.S. Department of Energy 2014; U.S. Census Bureau 2010b). Figure 3 summarizes the annual solar profile for all three cities in a heat map of all hours in a one-year period.

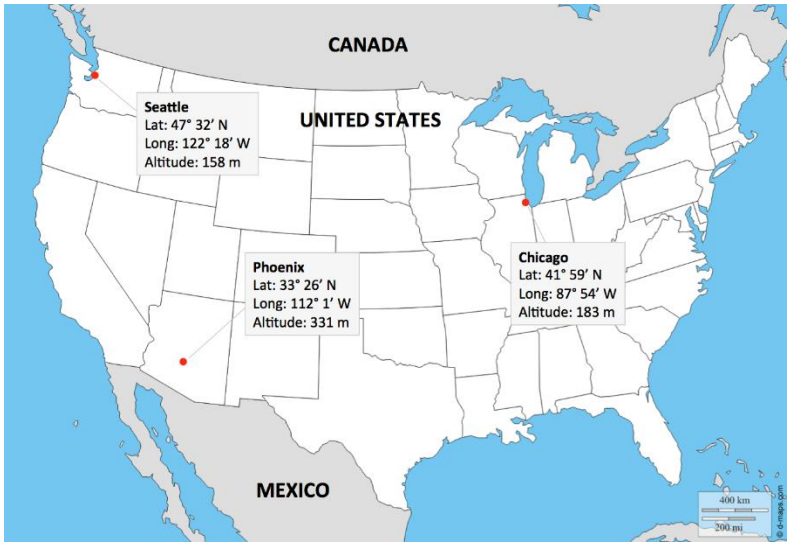

Figure 2.2: Geographic data for case study locations (d-maps 2016).

Table 2.1: Solar and Temperature Data for Case Study Locations (U.S. Department of Energy 2014)

Location	Average solar insolation (kWh/m^2/day)	Average daily temperature (°C)	Average daily minimum temperature (°C)	Average daily maximum temperature (°C)
Chicago	3.83	10.0	4.8	14.9
Phoenix	5.71	23.8	17.6	30.1
Seattle	3.31	11.8	8.3	15.6

Household energy use statistics are summarized in Table 2.2. It can be seen that Phoenix has a higher peak power demand and average load relative to Chicago and Seattle. This is principally caused by the increase in cooling loads in the warm desert climate. While households in Chicago and Seattle have similar total energy usage, Chicago experiences a

higher peak load. The minimum load is similar across all locations, suggesting that non-cooling loads provide similar base load profiles across all regions. This is expected since the BEopt model input parameters were held constant for each study location.

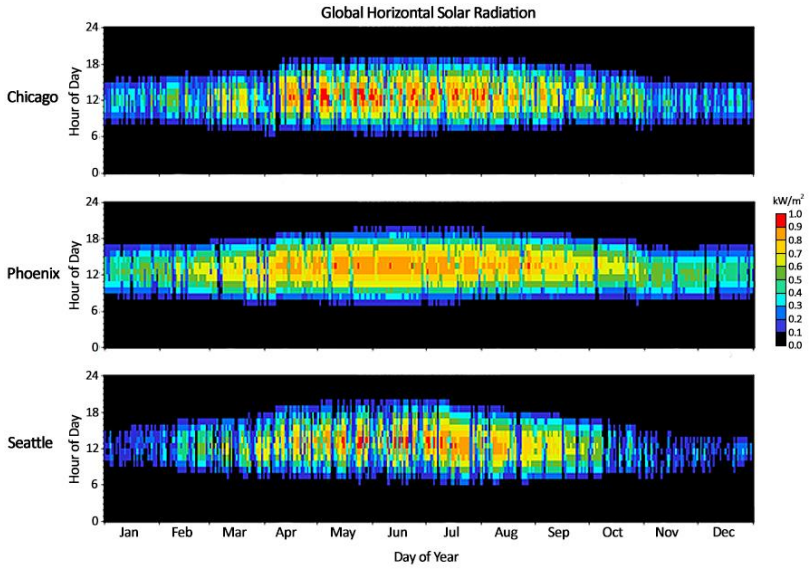

Figure 2.3: Hourly global horizontal solar radiation at study locations in BEopt.

Table 2.2: Household Energy Use Summary

Location	Average (kW)	Peak (kW)	Min (kW)	Total (kWh)
Chicago	1.00	2.84	0.41	8,765
Phoenix	1.57	5.29	0.44	13,750
Seattle	0.90	2.09	0.41	7,887

2.3.2. Household Solar PV System Sizing and Energy Costs

Residential load (kW) and global horizontal irradiance (kW/m^2) profiles from the BEopt building energy model were inputted into the HOMER economic model. HOMER includes algorithms to generate synthetic solar data. These algorithms were overridden using hourly data from BEopt to maintain consistency across the two modeling packages. The HOMER model can be reproduced by changing values listed herein away from default values loaded in HOMER.

The DC capacity of the solar array was selected to create a net-zero energy home on an annual basis—the solar array DC capacity was varied until the AC inverter output matched the household AC electricity use, thereby offsetting the total annual energy use for the home so that the net grid in/out was zero. Annual household energy use was taken from BEopt, PV capacity factor from HOMER, and the inverter efficiency assumed a constant 95% in Eq. 2.1. The maximum allowable PV array capacity was calculated to be 7.57 kW for Chicago, 7.93 kW for Phoenix, and 7.68 kW for Seattle. Solar PV array capacities were similar despite higher loads in Phoenix since the city has a higher solar PV capacity factor.

$$P_{max} = \frac{E_{tot}}{CF \times \eta_{inv}} \tag{2.1}$$

P_{max} = maximum allowable PV array capacity (kW)

CF = capacity factor (%)

E_{tot} = total annual household energy use (kWh/yr)

η_{inv}= inverter efficiency (%)

Net home energy profiles and energy costs were simulated for each study location using the following HOMER input parameters:

- Solar PV—The array was mounted facing due south at a slope equivalent to the latitude in each study site to achieve maximum energy output over a one-year period. Shading and temperature effects were not considered. A conservative derating factor of 80% was selected to account for soiling and line loss, panel degradation, diodes and connections, and other discrepancies between the rated power output and installed power output (Deline et al. 2011; National Renewable Energy Laboratory

2016a). Rooftop array capacities were evaluated at 5% increments ranging from 0% to 100% of the maximum capacity permitted in each study site. Installed solar PV cost was assumed at $3.00 per watt after rebates and incentives (DSIRE 2015; SolarCity 2015). Annual operating and maintenance costs were 1% of the installed system capital cost. Replacement costs were ignored given that the PV system lifetime and simulation timeframe (20 years) were equivalent (National Renewable Energy Laboratory 2016b).

- Inverter—The DC-to-AC conversion efficiency was assumed to be a constant 95% through a review of manufacturer specifications from common home solar inverters (ABB 2016; Fronius USA LLC 2016; SMA Solar Technology AG 2016). Inverter sizes were selected to be equivalent to solar PV sizes evaluated in each study site. The initial capital cost and replacement costs incurred for inverter failure were included in the $3.00 per watt cost of the solar home system.
- Battery—A Surrette 4KS25P battery was used with a nominal 7.6 kWh capacity. Costs data included initial costs of $1,200, replacement costs of $800, and annual operation and maintenance costs of $40. The effects of battery cost on energy cost and optimal system topology were explored through sensitivity analyses. Battery replacement occurs after reaching a maximum energy throughput as calculated in Eq. 2.2. HOMER assumes the lifetime of the modeled battery is independent of cycle depth, and uses the annual energy throughput to estimate the battery lifetime, as in Eq. 2.3.

$$E_{life} = E_{nom} \frac{1}{m} \sum_{i=1}^{m} n_i d_i \quad (2.2)$$

E_{nom} = nominal capacity of battery (kWh)

E_{life} = lifetime battery throughput (kWh)

m = number of manufacturer data points for lifetime tests (%)

n_i = manufacturer data on number of cycles till failure (-)

d_i = manufacturer data on depth of discharge (%)

$$t_{life} = \frac{E_{life}}{E_{ann}} \tag{2.3}$$

E_{ann} = annual battery throughput (kWh/yr)

t_{life} = battery lifetime (yr)

- Grid electricity price—Three time-of-use (TOU) rate schedules were selected as shown in Table 2.3. The price of electricity differed between summer months (June-September) and non-summer months, with peak pricing between 1:00 PM and 7:00 PM (weekdays only). Case 1 is the reference case with no intraday TOU price increase, Case 2 represents a 50% TOU increase, and Case 3 represents a 100% TOU increase. Rates in Table 2.3 include all taxes and fees. A grid connection fee of $15 per month was applied to all scenarios. Although HOMER is not able to evaluate grid price escalation over the simulated 20-year project lifetime, increases in grid price can be modeled implicitly using a negative annual real interest rate and by compensating for that formulation of the time-value of money when selecting equipment replacement costs encumbered over the system's lifetime. This method allowed the study to consider grid rate increases, but did not accurately reflect the time value of money for other operating costs incurred. This was deemed an acceptable simplifying assumption given that operating and maintenance costs

for home energy equipment were negligible relative to grid purchases. A grid price escalation of 3.0% per annum was assumed and was based on the observed 3.2% per annum increase in the average retail price of electricity from 2002–2015 for residential customers in the United States. It is worth noting that the price of electricity increased 5.0% per annum and 1.7% per annum, between 2002–2008 and 2009–2015, respectively, with a maximum annual increase of 10.1% and minimum annual increase of 0.3% over the observed period of 2002–2015 (EIA 2016). It is assumed that future price volatility will be driven by global events, energy policy, the price of natural gas, and new technology. The average increase of 3.0% per annum was considered as representative of the multi-year historical data including such events and input into HOMER as a negative discount rate as discussed previously.

Table 2.3: Grid Rate Structures ($/kWh)

Rate period	No TOU	TOU	
	Case 1	Case 2	Case 3
Non-summer	0.12	0.12	0.12
Summer off-peak	0.16	0.16	0.16
Summer on-peak	0.16	0.24	0.32

- Net metering—The effect of net metering policy was explored as follows: a) no net metering, b) net metering calculated on a monthly basis, and c) net metering calculated on an annual basis. A flat sell-back rate of $0.03/kWh was applied across all scenarios to reflect the sale of any net excess generation from the household PV array at the end of a net metering period. This rate approximates a typical wholesale electricity value in the United States (EIA 2015).

Optimal array capacities that produce least-cost energy for the consumer were evaluated using the LCOE formulation (Eq. 2.4) from HOMER, which discounts future energy use at the same rate as cash flow terms.

$$LCOE = \frac{\sum_{t=0}^{n} \frac{C_t}{(1+i)^t}}{\sum_{t=1}^{n} \frac{E_t}{(1+i)^t}} \tag{2.4}$$

$LCOE$ = levelized cost of energy ($/kWh)

t = increment of time (yr)

n = lifetime of the system (yr)

i = discount rate (%)

C_t = net cash flow in year *t* ($)

E_t = useful energy provided in year *t* (kWh)

2.3.3. Aggregate Utility-scale Effects

Utility-scale effects of solar PV were investigated by calculating the net system-wide load profile as a summation of 10,000 individual homes. The number of homes selected does not affect conclusions of the study achieved on a *relative* basis with respect to input parameters when noting the linear scaling in Eq. 2.1 and Eq. 2.5. Stated otherwise, the same relative findings emphasized in this comparative study can be achieved by simulating 100 homes or 500,000 homes. The quantity of 10,000 homes is a small subset of homes in each city, yet is large enough to illustrate 5–50 MW swings in utility net load that affect the output of committed assets and still sufficiently small to have no effect or minor effect on utility unit commitment decisions and transmission scheduling to a metropolitan area.

The net load profile was calculated for various levels of PV penetration using the affine combination given in Eq. 2.5. Households with solar PV used the maximum allowable solar PV capacity calculated from Eq. 1.

$$P_{utility} = n_h\left[(1-\gamma)P_{res} + \gamma P_{res,PV}\right] \quad (2.5)$$

$P_{utility}$ = utility net power (kW)

P_{res} = net power of a household without PV installed (kW)

$P_{res,PV}$ = net power of a household with PV installed (kW)

n_h = number of households simulated (-)

γ = residential PV adoption rate (%)

2.4. Results and Analysis

Hourly time series data were generated for a one-year period in each simulation. Data was selected from January, April, July, and October to visualize effects to the net system load profile over various parts of the year.

2.4.1. Utility Implications

Implications of solar PV for utilities were first explored by examining the net system load profile and economic metrics for residential PV penetration rates of 0%, 5%, 10%, 15%, 20%, and 25%. This utility-focused analysis assumed that ratepayers install sufficient solar PV to make their home net-zero.

Simulation results for net load profiles exhibit “duck curve” behavior at higher solar PV penetrations that differ by location and season. Figure 2.4 shows the average daily load profile for selected months in the year with these findings easily identifiable based on location, time of day, and time of year. It can be seen that net load profiles overlap in the early and late hours of the day due to a lack of sunlight, as expected. The

effect of solar PV on the net profile is clearly the greatest in Phoenix, yet Phoenix displays no negative net load in July due to the high use of electric air conditioning units. Chicago and Seattle, conversely, experience the greatest drop in net load in July, given a reduced air conditioning load when compared to Phoenix. The minimum annual net load for Chicago and Seattle occurs in April and July, respectively, due to their slightly higher cooling load requirements in the summer. The minimum annual net load for Phoenix occurs in April due to its high solar insolation and relatively minimal cooling load, when compared to July at the same location. The dynamics of the net load profile clearly vary by season, indicating that a utility must adapt operational strategies throughout the year to handle additional ramp rate requirements.

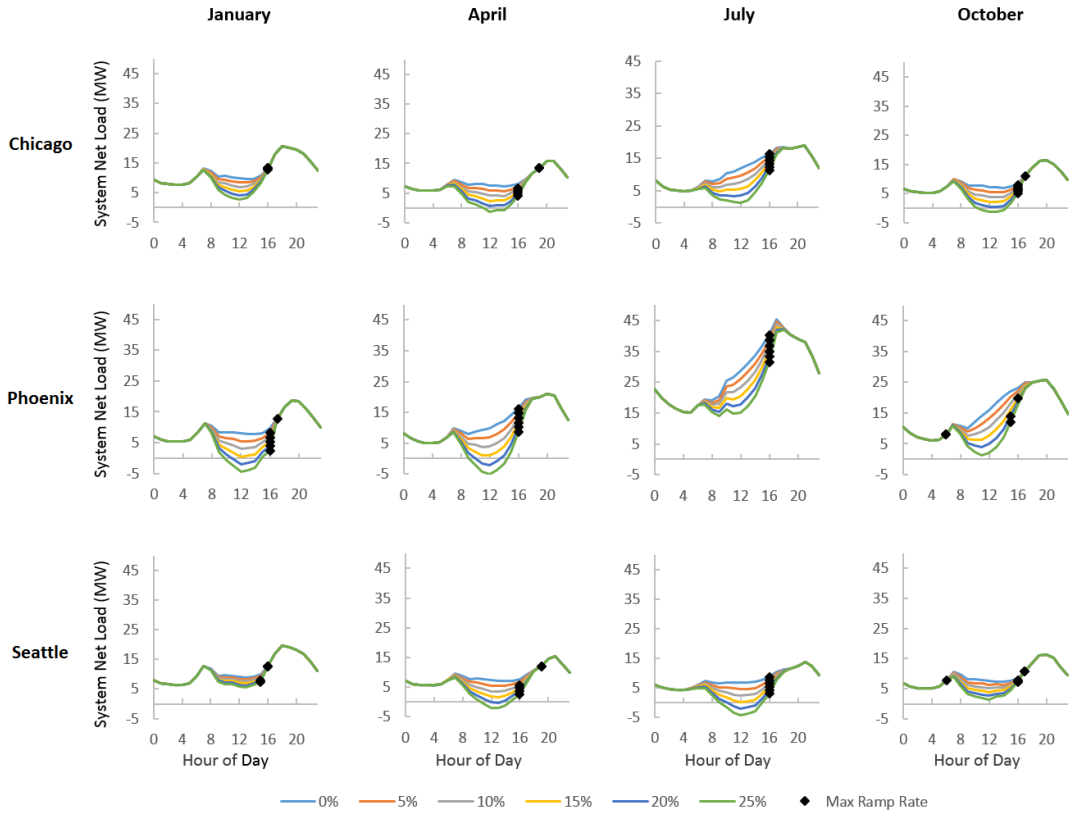

Figure 2.4: Grid load profiles at various solar PV penetration rates with net-zero solar PV capacity for the ratepayer.

Figure 2.4 depicts the time of day when the maximum ramp rate occurs. The maximum positive ramp rate occurred at 4:00 PM or 5:00 PM in almost all scenarios. Exceptions are Chicago and Seattle in April (7:00 PM) and Phoenix and Seattle in October (6:00 AM). The morning peak in October is smaller in magnitude than the evening peak, yet larger ramp rates occur in the morning. Table 4 summarizes the ramp rates quantitatively across various solar PV penetration rates and provides the percentage change compared to the no-solar (0% penetration) scenario. The largest ramp rates occurred during January (winter) for Chicago and Seattle for the no-solar reference case. This is considered an artifact of the simulated household load data with lighting loads turning on earlier in the day during the winter months. However, the no-solar reference case for Phoenix exhibited higher ramp rates in July (summer) when cooling loads are peaking.

A clear trend exists between the maximum ramp rate and solar PV penetration rate—an increase in residential solar PV causes an increase in utility ramp rate requirements. An exception occurs during October when the ramp rate requirements decline and shift from morning to evening. These ramp rate reductions were minimal and only occurred for the 5% and 10% solar penetration scenarios in October of the months shown for Phoenix and Seattle. This behavior discontinued as solar PV penetration reached 15% and exhibited positive changes in the maximum ramp rate.

Ramp rates requirements over the year were affected differently by the solar PV penetration rate. The relative change in the ramp rate magnitude was greatest for Phoenix in January and greatest for Chicago and Seattle in July. This is an important finding for scheduling peaker plants that are not typically online and ready to provide power within existing grid networks with lower solar PV penetration rates. As expected, ramp rate

characteristics for Chicago and Seattle are fairly similar, on an average daily basis, using the household energy model evaluated in each location with similar environmental forcings.

Table 2.4: Maximum System Ramp Rate Evaluated at Various Solar PV Penetration Rates with Net-zero Solar PV Capacity for the Ratepayer

Month	Homes with PV (%)	Ramp Rate Magnitude [MW/h] (Change in Magnitude Relative to Reference Case of 0% Homes with Solar [%])		
		Chicago	Phoenix	Seattle
January	0	4.57 (-)†	3.87 (-)‡	4.41 (-)†
	5	4.66 (2%)†	4.60 (19%)†	4.42 (0%)†
	10	4.75 (4%)†	5.96 (54%)†	4.44 (1%)†
	15	4.84 (6%)†	7.31 (89%)†	4.46 (1%)†
	20	4.93 (8%)†	8.66 (124%)†	4.53 (3%)**
	25	5.02 (10%)†	10.2 (159%)†	5.03 (14%)**
April	0	2.42 (-)§	3.02 (-)†	2.45 (-)§
	5	2.42 (0%)§	3.81 (26%)†	2.45 (0%)§
	10	2.77 (14%)†	4.61 (53%)†	2.56 (5%)†
	15	3.33 (38%)†	5.40 (79%)†	3.12 (28%)†
	20	3.89 (61%)†	6.20 (105%)†	3.69 (51%)†
	25	4.45 (84%)†	6.99 (132%)†	4.25 (74%)†
July	0	1.93 (-)†	5.13 (-)†	1.74 (-)†
	5	2.52 (31%)†	6.02 (17%)†	2.29 (32%)†
	10	3.12 (62%)†	6.91 (35%)†	2.85 (64%)†
	15	3.71 (92%)†	7.80 (52%)†	3.40 (96%)†
	20	4.30 (123%)†	8.69 (69%)†	3.96 (128%)†
	25	4.90 (154%)†	9.58 (87%)†	4.51 (160%)†
October	0	2.99 (-)‡	3.49 (-)*	2.95 (-)*
	5	3.21 (7%)†	3.39 (-3%)*	2.83 (-4%)‡
	10	3.86 (29%)†	3.28 (-6%)*	2.84 (-4%)‡
	15	4.52 (51%)†	3.92 (12%)†	3.08 (5%)†
	20	5.18 (73%)†	4.60 (32%)**	3.34 (13%)†
	25	5.84 (95%)†	5.47 (57%)**	3.59 (22%)†

Note: Ramp rate time of day denoted by * 6:00 AM, ** 3:00 PM, † 4:00PM, ‡ 5:00PM, § 7:00PM

0-49%	50-99%	100-149%	150%+	Negative

Seasonal ramp rate values in Table 2.4 are complemented by additional metrics in Table 2.5 including the average system load, peak system load, minimum system load, maximum ramp rate, total energy usage, and load factor over the entire year. Increased PV

penetration had a strong effect on all metrics—except peak system load—across the study locations. Solar PV penetration had a negligible effect on peak system load in Seattle and exhibited a minor decrease in the peak load observed in Chicago and Phoenix. The relative change in the ramp rate was another point of departure across study locations. The change in ramp rate for Chicago and Seattle was approximately twice that of Phoenix. This suggests that Phoenix already exhibits high ramp rates due to existing peaks in the load profile—a point corroborated by the lower load factor (higher peak power relative to average power) across all simulations for Phoenix. These data provide further evidence that utilities may need to place more dispatchable resources online to accommodate higher ramp rate requirements caused by increases in distributed renewables. Such dispatchable generation could include peaker plants, storage, demand response, or other controllable assets.

Table 2.5: Annual Technical Metrics at Various Solar PV Penetration Rates with Net-zero Solar PV Capacity for the Ratepayer

Location	Metrics	Solar PV Penetration (Change Relative to Reference Case of 0% Solar [%])					
		0%	5%	10%	15%	20%	25%
Chicago	Average (MW)	10.0 (-)	9.5 (-5%)	9.0 (-10%)	8.5 (-15%)	8.0 (-20%)	7.5 (-25%)
	Peak (MW)	28.4 (-)	28.0 (-1%)	27.6 (-3%)	27.2 (-4%)	26.8 (-6%)	26.5 (-7%)
	Min (MW)	4.1 (-)	1.4 (-65%)	-1.3 (-132%)	-4.1 (-199%)	-6.8 (-266%)	-9.6 (-333%)
	Total (GWh)	87.7 (-)	83.3 (-5%)	78.9 (-10%)	74.5 (-15%)	70.1 (-20%)	65.7 (-25%)
	Ramp Rate (MW/h)	4.8 (-)	5.1 (6%)	5.6 (17%)	6.8 (41%)	9.0 (88%)	11.3 (134%)
	Load Factor	0.35 (-)	0.34 (-4%)	0.33 (-7%)	0.31 (-11%)	0.30 (-15%)	0.28 (-20%)
Phoenix	Average (MW)	15.7 (-)	14.9 (-5%)	14.1 (-10%)	13.3 (-15%)	12.6 (-20%)	11.8 (-25%)
	Peak (MW)	52.9 (-)	52.1 (-2%)	51.2 (-3%)	51.0 (-4%)	50.9 (-4%)	50.8 (-4%)
	Min (MW)	4.4 (-)	2.7 (-39%)	-0.2 (-106%)	-3.2 (-172%)	-6.5 (-248%)	-9.9 (-324%)
	Total (GWh)	137.5 (-)	130.6 (-5%)	123.7 (-10%)	116.9 (-15%)	110.0 (-20%)	103.1 (-25%)
	Ramp Rate (MW/h)	7.3 (-)	8.4 (15%)	9.5 (30%)	10.5 (45%)	11.6 (60%)	12.7 (75%)
	Load Factor	0.30 (-)	0.29 (-4%)	0.30 (-7%)	0.26 (-12%)	0.25 (-17%)	0.23 (-22%)
Seattle	Average (MW)	9.0 (-)	8.6 (-5%)	8.1 (-10%)	7.7 (-15%)	7.2 (-20%)	6.8 (-25%)
	Peak (MW)	20.9 (-)	20.9 (0%)	20.9 (0%)	20.9 (0%)	20.9 (0%)	20.9 (0%)
	Min (MW)	4.1 (-)	1.3 (-67%)	-1.5 (-136%)	-4.3 (-206%)	-7.2 (-275%)	-10.0 (-344%)
	Total (GWh)	78.9 (-)	74.9 (-5%)	71.0 (-10%)	67.0 (-15%)	63.1 (-20%)	59.1 (-25%)
	Ramp Rate (MW/h)	4.7 (-)	5.5 (18%)	7.2 (55%)	8.9 (92%)	10.6 (129%)	13.2 (184%)
	Load Factor	0.43 (-)	0.41 (-5%)	0.39 (-10%)	0.37 (-15%)	0.34 (-20%)	0.32 (-25%)

Table 2.6 provides financial metrics to consider alongside the technical metrics in Table 2.5. Changes in utility annual revenue are given for various solar PV penetration rates and TOU rate structures. Data in the table was selected for simulations using monthly net metering, common for residential net metering agreements. As expected, increases in PV penetration decrease utility revenue. Utility revenue dropped 0.88–1.04% for every one-percent increase in PV penetration. However, increases in the on-peak price of electricity had little to no effect on the relative change in utility revenue across solar PV penetration rates. The smaller change in utility revenue for Phoenix is explained by the greater amount of net-negative months in Phoenix relative to the other two cities—each additional kWh generated in net-negative months yields revenue loss equivalent to the sell-back rate ($0.03/kWh) whereas in net-positive months an additional kWh of generation yields revenue loss equivalent to the TOU electric rate.

Table 2.6: Annual Utility Revenue at Various Solar PV Penetration Rates with Net-zero Solar PV Capacity for the Ratepayer

Location	On-Peak Price ($/kWh)	Utility Revenue [$ 000,000/yr] (Change Relative to Reference Case of 0% Solar [%])					
		0%	5%	10%	15%	20%	25%
Chicago	0.16	13.4 (-)	12.8 (-4%)	12.2 (-9%)	11.6 (-13%)	11.0 (-18%)	10.4 (-22%)
	0.24	14.1 (-)	13.5 (-5%)	12.8 (-9%)	12.1 (-14%)	11.5 (-19%)	10.8 (-23%)
	0.32	14.8 (-)	14.1 (-5%)	13.4 (-10%)	12.6 (-15%)	11.9 (-20%)	11.2 (-24%)
Phoenix	0.16	21.2 (-)	20.2 (-4%)	19.3 (-9%)	18.4 (-13%)	17.5 (-17%)	16.5 (-22%)
	0.24	23.1 (-)	22.1 (-4%)	21.1 (-9%)	20.1 (-13%)	19.0 (-18%)	18.0 (-22%)
	0.32	25.1 (-)	24.0 (-4%)	22.9 (-9%)	21.7 (-13%)	20.6 (-18%)	19.5 (-22%)
Seattle	0.16	12.2 (-)	11.6 (-5%)	11.1 (-9%)	10.5 (-14%)	10.0 (-18%)	9.4 (-23%)
	0.24	12.6 (-)	12.0 (-5%)	11.4 (-10%)	10.8 (-15%)	10.2 (-19%)	9.5 (-24%)
	0.32	13.1 (-)	12.4 (-5%)	11.7 (-10%)	11.0 (-16%)	10.4 (-21%)	9.7 (-26%)

2.4.2. Ratepayer Implications

This analysis assumed that ratepayers are rational agents seeking to minimize their energy expenditures by selecting the least-cost energy source. The optimal home energy system provided the lowest LCOE for the ratepayer. Solar PV system capacities were

evaluated from 0% (no solar) to 100% (net-zero home) in 5% increments. The analysis was repeated under various net metering agreements (monthly, annually, none) and three TOU rate structures (Table 2.3). Figure 2.5 provides a graph of the LCOE for each simulation completed. The minima shown in Fig. 2.5—lowest LCOE for the ratepayer—are also given in Table 2.7. There is a clear difference in the optimal PV capacity by location and net metering policy.

Larger solar home systems were economical in Phoenix due to excellent solar insolation. Optimal array sizes in Chicago and Seattle were smaller, with solar providing minimal financial benefit to the ratepayer in cases where there is no net metering.

Simulations with net metering on a monthly or annual basis had the same effect on LCOE and hence the optimal solar array capacity, indicating that ratepayers can size their solar PV system regardless of whether net metering occurs on a monthly or annual timeframe. It is clear, however, that completely removing net metering reduces the optimal array capacity appreciably. Optimal array capacities reduced by 20–50% when net metering was removed because the value of excess solar is credited to the ratepayer at the comparatively low sell-back rate of $0.03/kWh. An interesting finding is that Phoenix had a relatively flat LCOE curve in the absence of net metering, suggesting that ratepayers could size a solar PV system with little consideration for the magnitude of financial gain or loss.

Ratepayers can select the solar PV system size with minimal consideration for the specific TOU rate schedule when noting the minor effect of TOU peak rate on optimal array capacity. TOU pricing curves converge at higher PV capacities because solar PV costs contribute to a larger portion of total costs.

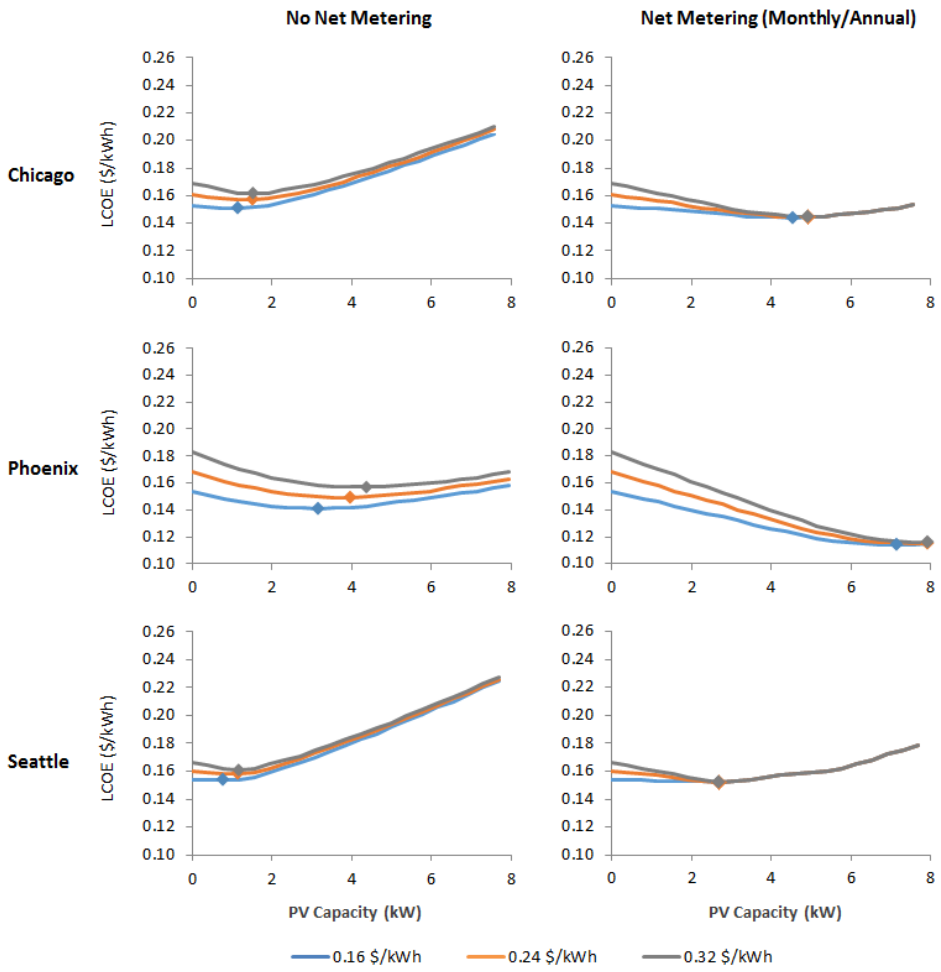

Figure 2.5: Levelized cost of energy for solar PV systems under various rate structures.

An analysis of solar-storage systems indicated that batteries were not cost-effective under present grid rate structures and equipment prices. Figure 2.6 provides a graphical representation of the analysis showing the optimal system type—set of power system components with least cost energy—indicated by shaded regions on the sensitivity graph. TOU peak prices are shown on the y-axis and battery prices on the x-axis at 0% to 100% of battery cost. Batteries were only cost-effective in cases without net metering, at a high on-peak grid price, and at a greatly reduced battery cost (>55%). Batteries were never cost-effective in cases when net metering was in effect (monthly or annually). This is expected since ratepayers can use the grid as a "zero cost lossless battery" under a net metering

agreement. Cycling grid power through a battery increases the cost of energy discharged (Eq. 2.6), suggesting that a battery may not be cost-effective for dispatch purposes even if the battery is free. In scenarios with higher on-peak grid prices, a battery can be useful for storing low-cost energy from off-peak times and discharging the energy during higher on-peak times. Batteries had the most favorable business case in Phoenix because solar PV could not fully meet electricity loads during summer peak hours. However, the value of storage could increase if other ancillary benefits such as backup power or power quality control are considered and monetized.

Table 2.7: Optimal Solar PV Array Capacities for the Ratepayer

Location	**Peak Price ($/kWh)**	**Optimal PV Capacity [kW] (Relative to Net-zero Home Solar PV Capacity [%])**	
		No Net Metering	**Net Metering (Monthly/Annually)**
Chicago	0.16	1.14 (15%)	4.54 (60%)
	0.24	1.51 (20%)	4.92 (65%)
	0.32	1.51 (20%)	4.92 (65%)
Phoenix	0.16	3.17 (40%)	7.14 (90%)
	0.24	3.97 (50%)	7.93 (100%)
	0.32	4.36 (55%)	7.93 (100%)
Seattle	0.16	0.77 (10%)	2.69 (35%)
	0.24	1.15 (15%)	2.69 (35%)
	0.32	1.15 (15%)	2.69 (35%)

$$C_{e,o} = \frac{C_{e,i}}{\eta_{bat}\eta_{inv}\eta_{rec}} \tag{2.6}$$

$C_{e,o}$ = cost of AC grid energy taken from the battery ($/kWh)

$C_{e,}$ = cost of AC grid energy put into the battery ($/kWh)

η_{bat} = battery efficiency (%)

η_{inv} = inverter efficiency (%)

η_{rec} = rectifier efficiency (%)

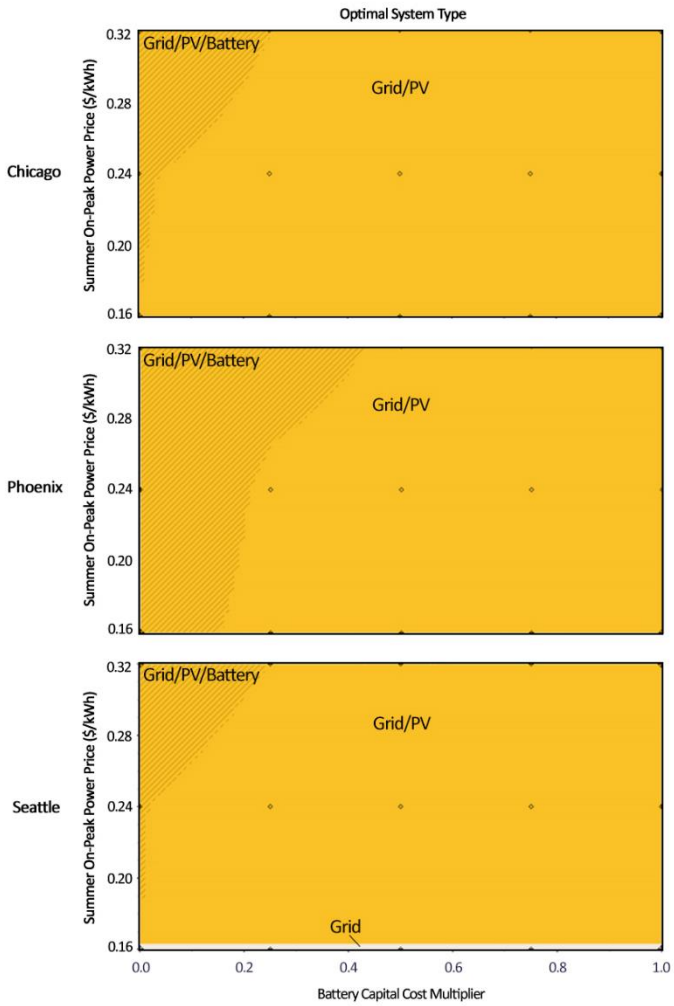

Figure 2.6: Least-cost solar-storage power system configurations without net metering.

2.4.3. Combined Analysis

The utility analysis with net-zero homes was reevaluated using optimal solar array capacities for each study location. This scenario explores solar PV penetration rates up to 100% by assuming the decision to install solar PV lies solely in the hands of the ratepayer. In specific terms, utilities and policy makers have no direct authority or control over ratepayer choice and therefore ratepayers have the freedom to install any amount of PV and batteries. A second assumption is that ratepayers make decisions to minimize energy expenditures when selecting home energy system size. The least-cost optimal solar PV

array capacities were used for the 0.24 $/kWh case—65% for Chicago, 100% for Phoenix, 35% for Seattle. Batteries were not cost-effective and were therefore not considered. Monthly net metering was applied.

The duck curves in Fig. 2.7 have similar profiles to those in Fig. 2.4, yet are more prominent at higher solar PV penetration rates. As expected, the duck curve behavior is more pronounced in areas with higher installed solar PV capacity—Phoenix, Chicago, and then Seattle. Ramp rate data by month is provided in Table 2.8. It is again noted that the largest ramp rates for Phoenix occur in January (winter), suggesting that high air conditioning loads in July (summer) offset the high solar insolation. The visible difference in Seattle's net load profiles between January and July illustrates the discrepancy in solar insolation received between the winter and summer months, respectively. Chicago has the most consistent net load profile across the year with minimal difference in its peak and minimum loads in the observed months. Figure 2.8 summarizes these and other metrics for each location. Solar PV adoption rate had little effect on peak power yet produced a steady negative trend in the average power and hence the load factor. For Phoenix, the 100% solar PV adoption rate yielded a 100% reduction in the average power and load factor—making each equivalent to zero—because the optimal solar array capacity for Phoenix produced a net-zero energy home.

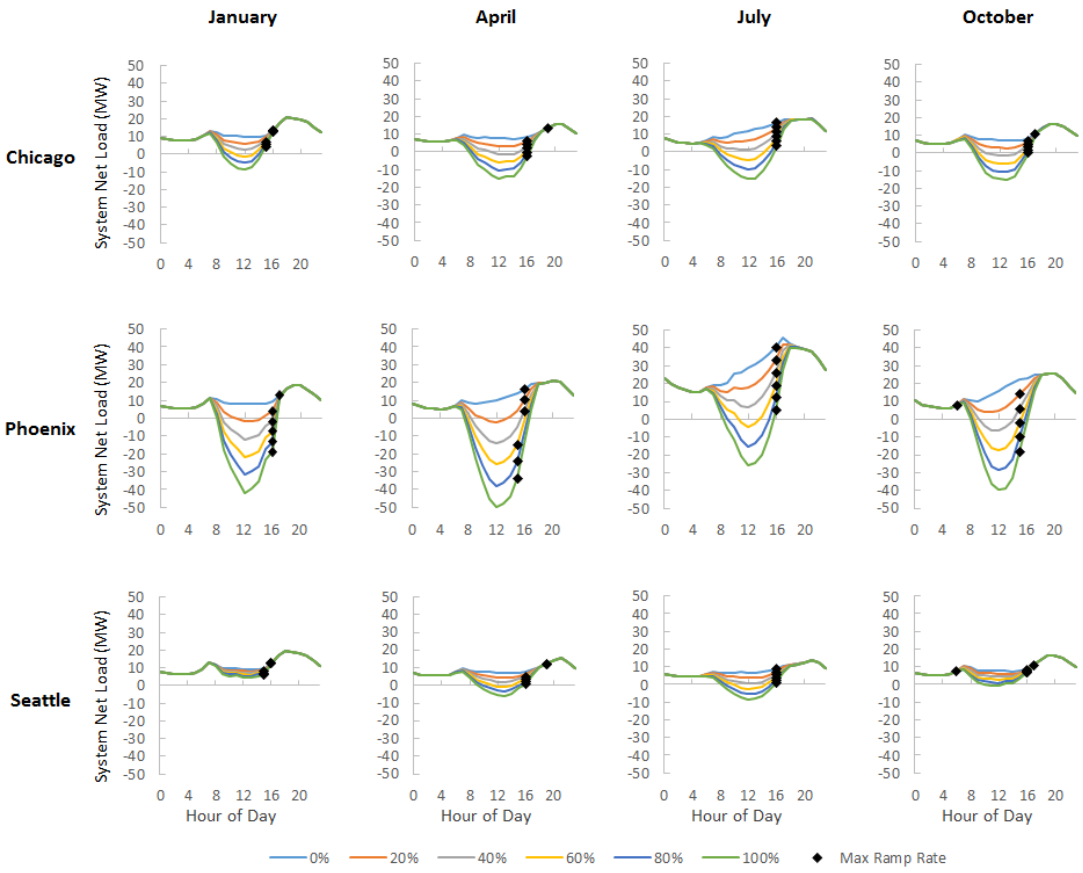

Figure 2.7: Grid load profiles at various solar PV penetration rates with optimal solar PV capacity for the ratepayer.

Table 2.8: Maximum System Ramp Rate Evaluated at Various Solar PV Penetration Rates with Optimal Solar PV Capacity for the Ratepayer

Month	Homes with PV (%)	Ramp Rate Magnitude [MW/h] (Change in Magnitude Relative to Reference Case of 0% Homes with Solar [%])		
		Chicago	Phoenix	Seattle
January	0	4.57 (-)†	3.87 (-)‡	4.41 (-)†
	20	4.80 (5%)†	8.66 (124%)†	4.43 (1%)†
	40	5.04 (10%)†	14.08 (264%)†	4.45 (1%)†
	60	5.70 (25%)**	19.49 (404%)†	4.63 (5%)**
	80	6.73 (47%)**	24.90 (543%)†	5.33 (21%)**
	100	7.76 (70%)**	30.27 (682%)†	6.02 (37%)**
April	0	2.42 (-)§	3.02 (-)†	2.45 (-)§
	20	3.10 (29%)†	6.20 (105%)†	2.45 (0%)§
	40	4.56 (89%)†	9.38 (211%)†	3.01 (23%)†
	60	6.02 (149%)†	12.70 (321%)**	3.80 (55%)†
	80	7.48 (210%)†	16.22 (437%)**	4.59 (88%)†
	100	8.94 (270%)†	19.70 (553%)**	5.38 (120%)†
July	0	1.93 (0%)†	5.13 (-)†	1.74 (-)†
	20	3.47 (80%)†	8.70 (69%)†	2.52 (45%)†
	40	5.02 (160%)†	12.26 (139%)†	3.29 (89%)†
	60	6.56 (240%)†	15.82 (208%)†	4.07 (134%)†
	80	8.10 (320%)†	19.38 (278%)†	4.85 (179%)†
	100	9.65 (400%)†	22.91 (346%)†	5.62 (224%)†
October	0	2.99 (0%)‡	3.50 (-)*	2.95 (-)*
	20	4.26 (42%)†	4.61 (32%)**	2.84 (-4%)‡
	40	5.97 (100%)†	8.09 (131%)**	3.03 (3%)†
	60	7.68 (157%)†	11.57 (231%)**	3.39 (15%)†
	80	9.39 (214%)†	15.05 (330%)**	3.74 (27%)†
	100	11.10 (271%)†	18.50 (429%)**	4.09 (39%)†

Note: Ramp rate time of day denoted by * 6:00 AM, ** 3:00 PM, † 4:00PM, ‡ 5:00PM, § 7:00PM

0-49%	50-99%	100-199%	200%+	Negative

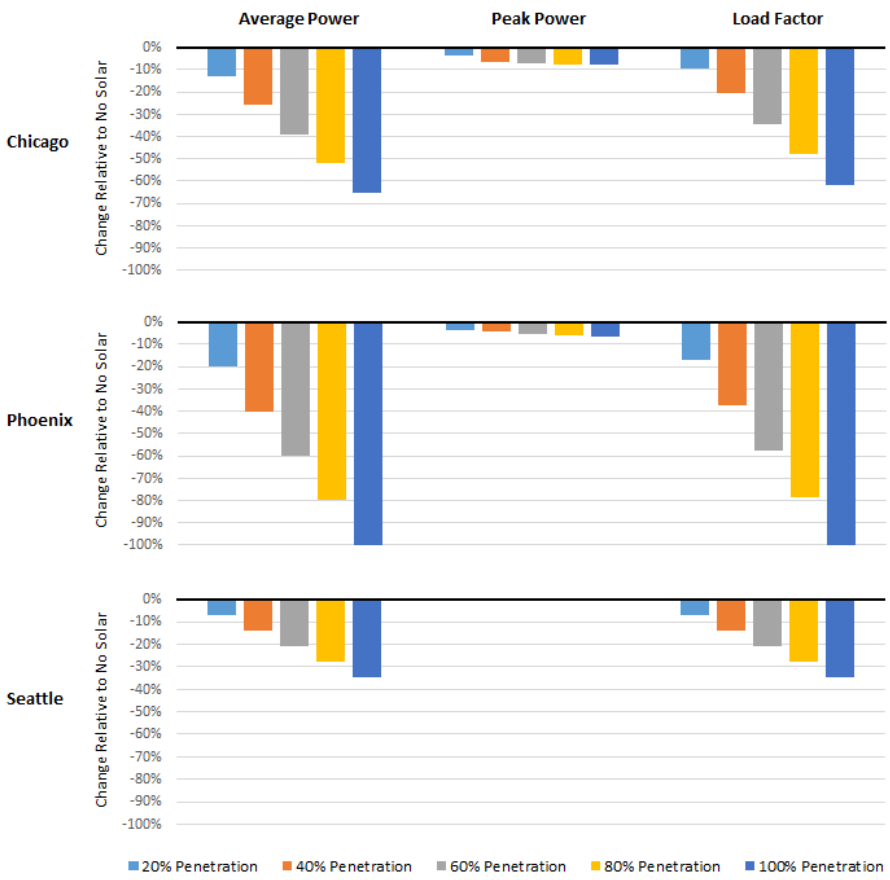

Figure 2.8: Change in grid metrics at various solar PV penetration rates with optimal solar PV capacity for the ratepayer.

Utility revenue loss summarized in Table 2.9 displays a fairly steady negative trend with respect to solar penetration for each location. This trend becomes weaker for Phoenix at higher solar PV penetration rates because the fixed monthly connection fee comprises a larger percentage of total annual revenue.

Table 2.10 lists the requisite increase in electric rates to recover the revenue losses reported in Table 2.9. Rate increases were applied to all customers and applied evenly across each rate period (non-summer, summer off-peak, and summer on-peak). To take an example, if 20% of homes install solar PV under a 0.24 $/kWh peak power price, the utility would need a 16%, 24%, and 8% increase in rates across all ratepayers to recover lost

revenue in Chicago, Phoenix, and Seattle, respectively. These rises in electric rates were a quadratic function of the solar PV penetration rate because a kWh generated by the ratepayer has a doubling effect on utility revenue when net metering is in effect—one kWh of lost revenue plus one kWh credit to ratepayer per one kWh generated by home solar. It is important to note that these results only consider revenue loss and do not consider potential cost savings associated with a reduction in utility operating expenses.

Table 2.11 shows results from a complementary analysis using the monthly connection fee to recover lost revenue. Showing results for the selected penetration rate of 20%, a utility would need to increase the base connection fee of $15.00 per month to an average of $29.17, $49.17, and $22.50 per month for Chicago, Phoenix, and Seattle, respectively. Phoenix requires the greatest rise in the monthly connection fee based on the fact that homes in Phoenix have larger solar arrays relative to Chicago and Seattle. If the connection fee increase were applied to solar customers only, the resulting connection fee would equate to an average of $85.83, $185.83, and $52.50 per month for Chicago, Phoenix, and Seattle, respectively. Looking further at the Phoenix scenario with 20% solar PV market penetration, the utility would need to increase the connection fee by 228% for all customers or 1139% for solar customers, which is an average fee increase of 11.39% and 56.94% for each one-percent rise in solar PV penetration, respectively.

Table 2.9: Annual Utility Revenue at Various Solar PV penetration Rates with Optimal Solar PV Capacity for the Ratepayer

Location	On-Peak Price ($/kWh)	Utility Revenue [$ 000,000/yr] (Change Relative to Reference Case of 0% Solar [%])					
		0%	20%	40%	60%	80%	100%
Chicago	0.16	13.4 (-)	11.9 (-12%)	10.3 (-23%)	8.8 (-35%)	7.3 (-46%)	5.9 (-56%)
	0.24	14.1 (-)	12.4 (-12%)	10.7 (-24%)	9.0 (-37%)	7.3 (-48%)	5.9 (-58%)
	0.32	14.8 (-)	12.9 (-13%)	11.0 (-26%)	9.2 (-38%)	7.4 (-50%)	5.9 (-60%)
Phoenix	0.16	21.2 (-)	17.5 (-17%)	13.8 (-35%)	10.1 (-52%)	7.1 (-66%)	4.9 (-77%)
	0.24	23.1 (-)	19.0 (-18%)	14.9 (-36%)	10.9 (-53%)	7.4 (-68%)	5.0 (-78%)
	0.32	25.1 (-)	20.6 (-18%)	16.1 (-36%)	11.6 (-54%)	7.7 (-69%)	5.0 (-80%)
Seattle	0.16	12.2 (-)	11.4 (-6%)	10.6 (-13%)	9.8 (-19%)	9.1 (-25%)	8.3 (-32%)
	0.24	12.6 (-)	11.7 (-7%)	10.9 (-14%)	10.0 (-20%)	9.2 (-27%)	8.3 (-34%)
	0.32	13.1 (-)	12.1 (-7%)	11.2 (-15%)	10.2 (-22%)	9.3 (-29%)	8.3 (-36%)

Table 2.10: Electric Rate Increase Required to Recover Utility Revenue Loss at Various Solar PV Penetration Rates with Optimal Solar PV Capacity for the Ratepayer (Reference case shown for 0.24 $/kWh summer on-peak price)

Location	Homes with PV (%)	Rate Increase (%)	Rate Price [$/kWh] Required to Recoup Revenue Loss		
			Non-Summer	Summer Off-Peak	Summer On-Peak
Chicago	0	-	0.120	0.160	0.240
	20	16	0.139	0.186	0.278
	40	38	0.166	0.221	0.331
	60	72	0.206	0.275	0.413
	80	120	0.264	0.352	0.528
	100	192	0.350	0.497	0.701
Phoenix	0	-	0.120	0.160	0.240
	20	24	0.149	0.198	0.298
	40	63	0.196	0.261	0.391
	60	135	0.282	0.376	0.564
	80	268	0.442	0.589	0.883
	100	466	0.680	0.906	1.358
Seattle	0	-	0.120	0.160	0.240
	20	8	0.130	0.173	0.259
	40	19	0.143	0.190	0.286
	60	32	0.158	0.211	0.317
	80	47	0.176	0.235	0.353
	100	66	0.199	0.266	0.398

Table 2.11: Increase to Fixed Monthly Connection Fee to Recover Utility Revenue Loss at 20% Solar PV Penetration for Homes with Optimal Solar PV Capacity for the Ratepayer

		Applied to All Customers			Applied to Only Solar Customers		
Location	**On-Peak Price [$/kWh]**	**Additional Fee [$/mo]**	**Total Fee [$/mo]**	**Relative Change [%]**	**Additional Fee [$/mo]**	**Total Fee [$/mo]**	**Relative Change [%]**
Chicago	0.16	12.50	27.50	83	62.50	77.50	417
	0.24	14.17	29.17	94	70.83	85.83	472
	0.32	15.83	30.83	106	79.17	94.17	528
Phoenix	0.16	30.83	45.83	206	154.17	169.17	1028
	0.24	34.17	49.17	228	170.83	185.83	1139
	0.32	37.50	52.50	250	187.50	202.50	1250
Seattle	0.16	6.67	21.67	44	33.33	48.33	222
	0.24	7.50	22.50	50	37.50	52.50	250
	0.32	8.33	23.33	56	41.67	56.67	278

2.5. Discussion and Conclusions

This study examined the implications of high penetration solar PV systems in the residential market across three cities in the United States by exploring the combined effect of electric rate structures and local environmental forcings on optimal solar home system size, ratepayer financials, utility financials, and net electric loads. The analyses first considered net-zero energy homes with solar capacities equated at 7.57 kW for Chicago, 7.93 kW for Phoenix, and 7.68 kW for Seattle, with utility metric calculations that included ramp rate requirements, intraday load profiles, load factor, and revenue loss with solar PV penetration rates up to 25%. Retail electricity sales (kWh) dropped by approximately 1% for each 1% increase in solar PV penetration. This is comparable to the loss of sales reported in other studies and provides further evidence that new rate structures with revenue decoupling should be developed and piloted (Satchwell et al. 2014). This analysis was repeated for each location using the optimal array capacity that provided the minimum LCOE for the ratepayer with installed capacities of 4.92 kW for Chicago, 7.93 kW for Phoenix, and 2.69 kW for Seattle with solar PV penetration rates up to 100%. Some of the major findings include:

- Net metering had a significant effect on the optimal amount of solar PV installed. Removing net metering decreased solar array capacities by 20−50% when selecting the optimal capacity by the lowest LCOE. Monthly and annual net metering simulations yielded the same optimal solar PV sizing.
- Optimal solar PV array capacities were unchanged or increased slightly (0−15%) at higher TOU rates (50−100%). The optimal capacity may increase further if solar

panel orientation is not due south; other studies have reported economic gains of 3−4% for panels facing 30 degrees west of due south (Sadineni et al. 2012).

- Batteries were not cost-effective—even if they were free—when net metering was in effect. Batteries were found to be cost-effective in simulations without net metering and at cost reductions of at least 55%. This decrease in consumer purchase price could be achieved through subsidies that improve home storage economics. Findings corroborate other studies, i.e., the requisite size of subsidies to reach break-even will decrease as grid electricity prices increase (Mulder et al. 2013). Further, ancillary benefits of storage may improve economics beyond a pure consumer-focused analysis (Denholm and Margolis 2007; Evans et al. 2016).
- Intraday load profiles with "duck curve" behavior were more prominent as solar PV penetration rates increased. The largest ramp rates for each location occurred in the late afternoon as solar insolation decreased and occupancy loads increased with residents returning home from work or school.
- Increases in the solar PV penetration rate changed the time of year in which the maximum ramp rate was observed: July to January for Phoenix, January to October for Chicago, with no change for Seattle.
- Utility revenue loss can be recovered by increasing the electricity rate ($/kWh) or the fixed monthly connection fee ($ per month). Taking Phoenix as an example with 20% solar penetration and 0.24 $/kWh peak power price, a utility would need to increase electricity rates by 24% or increase the fixed connection by 228% ($15.00 per month to $49.17 per month) across all residential ratepayers to recoup lost revenue if 20% of homes in the region installed solar PV. The connection fee

would need to be raised by 1139% ($15.00 per month to $185.83 per month) if revenue was recovered from only the solar customers. Other revenue generation options include demand charges or energy-as-a-service business models.

These site-specific findings emphasize the interplay between technical, economic, and policy considerations within the context of local environmental forcings, energy use behaviors, and grid rate structures. Pertinent generalizable findings to other study locations include:

- Solar PV penetration had little effect on peak power draw.
- There was little observed difference between monthly and annual net metering.
- Net metering was shown to negate the cost-effectiveness of batteries under the modeled parameters. The grid can be effectively characterized as a "zero cost lossless battery" with both technical and economic advantages over battery storage if used for energy management alone.
- Utilities may need to place more dispatchable resources online to accommodate higher ramp rate requirements caused by increases in distributed renewables. Such dispatchable generation could include peaker plants, storage, demand response, or other controllable assets. Generation units may need to operate at partial load to meet operating capacity and reserve requirements during periods of high solar insolation and thereby produce power at lower efficiency and higher emissions factors.
- Demand response capabilities may serve a greater role in the residential energy market as system-wide operating reserve capacity requirements increase with

increases in renewables penetration. Demand response also offers a mechanism to reduce peak power draw at lower cost than on-site battery storage.

Reaching a zero-carbon economy is a challenge that will require technology innovation, new policy approaches, alternative value propositions and rate agreements, new energy business models, and changes in consumer behavior. This study is one of many studies needed to explore that complex decision space, yet it is clear that a business-as-usual approach to distributed solar PV will yield an untenable future for the utility on both technical and financial metrics. Unit commitment and power flow studies could extend this study using a generic generation fleet. Further opportunities for investigation include an analysis of utility-side emissions and economics from running nonrenewable generation at lower loads, evaluating the techno-economic performance of electric vehicles, developing load management scenarios to smooth residential load profiles, and evaluating the consumer-side and utility-side effects of alternative rate structures including tiered rate structures or shorter-duration net metering timeframes (e.g., daily or hourly). Those explorations will take additional computational functionality outside of that currently provided by HOMER or BEopt. Results and findings from this study can be reproduced in HOMER and BEopt using default values and updating the values of variables listed in Section 3.1 and 3.2 away from default settings.

The provided methods can be applied to other locations using simulated or measured data. Model parameters in BEopt and HOMER can be updated to reflect various building designs, local environmental forcings, rate structures, and equipment costs to recreate and apply a simulated study of other locations around the world. Measured load and solar PV data can also be obtained for a single home or consumer segment to complete

a site-specific study of a real scenario. Such case studies are needed to better understand and guide the changing shape of the United States residential energy market.

References

ABB. (2016). Solar inverters - power converters and inverters | ABB. Retrieved from http://new.abb.com/power-converters-inverters/solar

Abramson, D. S., Turiel, I., & Heydari, A. (1990). Analysis of refrigerator-freezer design and energy efficiency by computer modeling: DOE perspective. *ASHRAE Transactions*, *96*(Part I), 1354–1358.

Anderson, R., Christensen, C., & Horowitz, S. (2006). Program design analysis using BEopt (Building Energy Optimization) software: Defining a technology pathway leading to new homes with zero peak cooling demand. *ACEEE Summer Study on Energy Efficiency in Buildings. Panel 2*, 23–35.

Anaya, K. L. & Pollitt, M. G. (2014). Integrated distributed generation: Regulation and trends in three leading countries (EPRG Working Paper No. 1423). Retrieved from University of Cambridge Energy Policy Research Group website: http://www.eprg.group.cam.ac.uk/wp-content/uploads/2015/01/EPRG-WP-1423.pdf

Ardani, K. (2014). Benchmarking non-hardware balance-of-system (soft) costs for US photovoltaic systems using a bottom-up approach and installer survey. National Renewable Energy Laboratory, USA.

Arteconi, A., Hewitt, N. J., & Polonara, F. (2012). State of the art of thermal storage for demand-side management. *Applied Energy*, *93*, 371–389.

Bhat, R., Begovic, M., Kim, I., & Crittenden, J. (2014). Effects of PV on conventional generation. *2014 47th Hawaii International Conference on System Sciences (HICSS)*, 2380–2387.

Brouwer, A. S., van den Broek, M., Zappa, W., & Turkenburg, W. C. (2016). Least-cost options for integrating intermittent renewables in low-carbon power systems. *Applied Energy*, *161*, 48–74.

Browne, D., O'Regan, B., & Moles, R. (2010). Use of multi-criteria decision analysis to explore alternative domestic energy and electricity policy scenarios in an Irish city-region. *Energy*, *35*(2), 518–528.

Cai, D. W., Adlakha, S., Low, S. H., De Martini, P., & Mani Chandy, K. (2013). Impact of residential PV adoption on retail electricity rates. *Energy Policy*, *62*, 830–843.

California ISO. (2013). Demand response and energy efficiency roadmap: Maximizing preferred resources. California ISO, USA.

Carrasco, J. M., Franquelo, L. G., Bialasiewicz, J. T., Galván, E., Guisado, R. P., Prats, M. A. & Moreno-Alfonso, N. (2006). Power-electronic systems for the grid integration of renewable energy sources: A survey. *IEEE Transactions on Industrial Electronics, 53*(4), 1002–1016.

Christensen, C., Anderson, R., Horowitz, S., Courtney, A., & Spencer, J. (2006). BEopt software for building energy optimization: Features and capabilities. National Renewable Energy Laboratory, USA.

Crawley, D. B., Lawrie, L. K., Winkelmann, F. C., Buhl, W. F., Huang, Y. J., Pedersen, C. O., Strand, R. K., Liesen, R. J., Fisher, D.E., Witte, M. J., & Glazer, J. (2001). EnergyPlus: Creating a new-generation building energy simulation program. *Energy and Buildings, 33*(4), 319–331.

Couture, T. & Gagnon, Y. (2010). An analysis of feed-in tariff remuneration models: Implications for renewable energy investment. *Energy Policy, 38*(2), 955–965.

D-maps (2016). United States of America. Retrieved from: http://d-maps.com/carte.php?num_car=1682&lang=en

Damiani, D., Litynski, J. T., McIlvried, H. G., Vikara, D. M., & Srivastava, R. D. (2012). The US Department of Energy's R&D program to reduce greenhouse gas emissions through beneficial uses of carbon dioxide, *Greenhouse Gases Science and Technology*, *2*(1), 9–19.

Database of State Incentives for Renewables & Efficiency® - DSIRE. (2015). Retrieved from: http://www.dsireusa.org

Darghouth, N. R., Barbose, G., & Wiser, R. (2011). The impact of rate design and net metering on the bill savings from distributed PV for residential customers in California. *Energy Policy*, *39*(9), 5243–5253.

Deline, C., Marion, B., Granata, J., Gonzalez, S. (2011). A performance and economic analysis of distributed power electronics in photovoltaic systems. National Renewable Energy Laboratory, USA.

Denholm, P. & Margolis, R. M. (2007). Evaluating the limits of solar photovoltaics (PV) in electric power systems utilizing energy storage and other enabling technologies. *Energy Policy*, *35*(9), 4424–4433.

Evans, A., Strezov, V., & Evans, T. J. (2016). Assessment of utility energy storage options for increased renewable energy penetration. *Renewable & Sustainable Energy Reviews*, *16*(6), 4141–4147.

Finn, P., O'Connell, M., & Fitzpatrick, C. (2013). Demand side management of a domestic dishwasher: Wind energy gains, financial savings and peak-time load reduction. *Applied Energy*, *101*, 678–685.

Fronius USA LLC. (2016). Fronius USA LLC - products - grid-connected PV inverters. Retrieved from https://www.fronius.com/en-us/usa#.Vxu8tWPWzzI

Fulzele, J. B. & Dutt, S. (2011). Optimum planning of hybrid renewable energy system using HOMER. *International Journal of Electrical and Computer Engineering (IJECE)*, *2*(1), 68–74.

Hafez, O. & Bhattacharya, K. (2012). Optimal planning and design of a renewable energy based supply system for microgrids. *Renewable Energy*, *45*, 7–15.

Hendron, R. & Engebrecht, C. (2010). Building America House Simulation Protocols. National Renewable Energy Laboratory, USA.

Hernández-Moro, J. & Martínez-Duart, J. M. (2013). Analytical model for solar PV and CSP electricity costs: Present LCOE values and their future evolution. *Renewable and Sustainable Energy Reviews*, *20*, 119–132.

International Energy Agency (IEA). (2014). Technology Roadmap Solar Photovoltaic Energy. OECD/IEA, France.

International Energy Agency (IEA). (2015). Energy Prices & Taxes: Quarterly Statistics; 2015 IIS 2380-P2; ISSN 0256–2332. OECD/IEA, France.

Johnson, N., Lilienthal, P., & Schoechle, T. (2011). Modeling distributed premises-based renewables integration using HOMER. *2011 Grid-Interop Conference, Phoenix, AZ.*

Katiraei, F. & Aguero, J. R. (2011). Solar PV integration challenges. *Power and Energy Magazine, IEEE*, *9*(3), 62–71.

Kempton, W. & Tomić, J. (2005). Vehicle-to-grid power implementation: From stabilizing the grid to supporting large-scale renewable energy. *Journal of Power Sources*, *144*(1), 280–294.

Kern, E. C., Gulachenski, E. M., & Kern, G. A. (1989). Cloud effects on distributed photovoltaic generation: Slow transients at the Gardner, Massachusetts, photovoltaic experiment. *IEEE Transactions on Energy Conversion*, *4*(2), 184–190.

Laird, F. N. (2013). Against transitions? Uncovering conflicts in changing energy systems. *Science as Culture*. *22*(2), 149–156.

Lambert, T., Gilman, P., & Lilienthal, P. (2006). Micropower system modeling with HOMER. *Integration of Alternative Sources of Energy*, *1*(15), 379–418.

Liu, X., O'Rear, E. G., Tyner, W. E., & Pekny, J. F. (2014). Purchasing vs. leasing: A benefit-cost analysis of residential solar PV panel use in California. *Renewable Energy*, *66*, 770–774.

Løken, E. (2007). Use of multicriteria decision analysis methods for energy planning problems. *Renewable and Sustainable Energy Reviews*, *11*(7), 1584–1595.

Lovins, A. (2013). Reinventing fire: Bold business solutions for the new energy era. Chelsea Green Publishing.

Lund, H. (2005). Large-scale integration of wind power into different energy systems. *Energy*, *30*(13), 2402–2412.

Lund, H. & Münster, E. (2003). Management of surplus electricity-production from a fluctuating renewable-energy source. *Applied Energy*, *76*(1), 65–74.

Miller, C. A. & Richter, J. (2014). Social planning for energy transitions. *Current Sustainable/Renewable Energy Reports*, *1*(3), 77–84.

Mills, A. D. & Wiser, R. H. (2015). Strategies to mitigate declines in the economic value of wind and solar at high penetration in California. *Applied Energy*, *147*, 269–278.

Mondol, J. D., Yohanis, Y. G., & Norton, B. (2009). Optimising the economic viability of grid-connected photovoltaic systems. *Applied Energy*, *86*(7), 985–999.

Mulder, G., Six, D., Claessens, B., & Broes, T. (2013). The dimensioning of PV-battery systems depending on the incentive and selling price conditions. *Applied Energy*, *111*, 1126–1135.

National Renewable Energy Laboratory. (2016a). PVWatts calculator. Retrieved from http://pvwatts.nrel.gov

National Renewable Energy Laboratory. (2016b). NREL: Energy analysis - distributed generation energy technology operations and maintenance costs. Retrieved from http://www.nrel.gov/analysis/tech_cost_om_dg.html

Negrão, C. O. & Hermes, C. J. (2011). Energy and cost savings in household refrigerating appliances: A simulation-based design approach. *Applied Energy*, *88*(9), 3051–3060.

Nemet, A., Klemeš, J. J., Varbanov, P. S., & Kravanja, Z. (2012). Methodology for maximising the use of renewables with variable availability. *Energy*, *44*(1), 29–37.

Nguyen, A. T., Reiter, S., & Rigo, P. (2014). A review on simulation-based optimization methods applied to building performance analysis. *Applied Energy*, *113*, 1043–1058.

Østergaard, P. A. (2009). Reviewing optimisation criteria for energy systems analyses of renewable energy integration. *Energy*, *34*(9), 1236–1245.

Patsalides, M., Evagorou, D., Makrides, G., Achillides, Z., Georghiou, G. E., Stavrou, A., Efthymiou, V., Zinsser, B., Schmitt, W. and Werner, J. H. (2007). The effect of solar irradiance on the power quality behaviour of grid connected photovoltaic systems. *International Conference on Renewable Energies and Power Quality, ICREPQ, La Coruña, ES, 25 - 27 Mar 2007*.

Pillai, G. G., Putrus, G. A., Georgitsioti, T., Pearsall, N. M. (2014). Near-term economic benefits from grid-connected residential PV (photovoltaic) systems. *Energy*, *68*, 832–843.

Purohit, I. & Purohit, P. (2010). Techno-economic evaluation of concentrating solar power generation in India. *Energy Policy*, *38*(6), 3015–3029.

Reichelstein, S. & Yorston, M. (2013). The prospects for cost competitive solar PV power. *Energy Policy*, *55*, 117–127.

Roosa, S. A. & Jhaveri, A. G. (2009). Carbon Reduction: Policies, Strategies and Technologies. Lilburn, GA, USA: Fairmont Press, Incorporated.

Roy, B., Basu, A. K., & Paul, S. (2014). Techno-economic feasibility analysis of a grid connected solar photovoltaic power system for a residential load. *2014 First International Conference on Automation, Control, Energy and Systems (ACES)*, 1–5.

Ruddell, B. L, Salamanca, F., & Mahalov, A. (2014). Reducing a semiarid city's peak electrical demand using distributed cold thermal energy storage. *Applied Energy*, *134*, 34–44.

Sadineni, S. B., Atallah, F., & Boehm, R. F. (2012). Impact of roof integrated PV orientation on the residential electricity peak demand. *Applied Energy*, *92*, 204–210.

Salpakari, J. & Lund, P. (2016). Optimal and rule-based control strategies for energy flexibility in buildings with PV. *Applied Energy*, *161*, 425–436.

Satchwell, A., Mills, A. D., Barbose, G. L., Wiser, R. H., Cappers, P., and Darghouth, N. (2014). Financial Impacts of Net-Metered PV on Utilities and Ratepayers: A Scoping

Study of Two Prototypical U.S. Utilities. Lawrence Berkeley National Laboratory, USA.

SMA Solar Technology AG. (2016). Solar Inverters. Retrieved from http://www.sma-america.com/products/solarinverters.html

Solar Energy Industries Association (SEIA). (2014). Solar Market Insight Report 2014 Q3.

SolarCity. (2015). How Much Do Solar Panels Cost? Find the Cost of Solar Energy. Retrieved from: http://www.solarcity.com/residential/how-much-do-solar-panels-cost

U.S. Census Bureau. (2010a). Median and Average Square Feet of Floor Area in New Single-Family Houses Completed by Location. Retrieved from http://www.census.gov/const/C25Ann/sftotalmedavgsqft.pdf

U.S. Census Bureau. (2010b). Census data – 2010 Census. Retrieved from http://www.census.gov/2010census/data/

U.S. Department of Energy: Energy Efficiency & Renewable Energy (EERE). (2014). Weather Data for Simulation.

U.S. Energy Information Administration (EIA). (2014). December 2014 Monthly Review. Washington, DC: U.S. Energy Information Administration, DOE/EIA-0035; 2014. P. 1–201.

U.S. Energy Information Administration (EIA). (2015). Wholesale Electricity and Natural Gas Market Data.

U.S. Energy Information Administration (EIA). (2016). Electricity Data Browser – Average Retail Price of Electricity. Retrieved from http://www.eia.gov/electricity/data.cfm

Wand, R. & Leuthold, F. (2011). Feed-in tariffs for photovoltaics: Learning by doing in Germany, *Applied Energy*, *88*(12), 4387–4399.

Wang, J., Zhai, Z. J., Jing, Y., Zhang, X., & Zhang, C. (2011). Sensitivity analysis of optimal model on building cooling heating and power system. *Applied Energy*, *88*(12), 5143–5152.

Wirth, H. (2015). Recent Facts about Photovoltaics in Germany. Fraunhofer Institute for Solar Energy Systems.

Yan, R., Saha, T. K., Modi, N., & Masood, N. (2015). The combined effects of high penetration of wind and PV on power system frequency response. *Applied Energy*, *145*, 320–330.

Yun, G. Y. & Steemers, K. (2011). Behavioural, physical and socio-economic factors in household cooling energy consumption. *Applied Energy*, *88*(6), 2191–2200.

CHAPTER 3

SCALABLE MULTI-AGENT MICROGRID NEGOTIATIONS FOR A TRANSACTIVE ENERGY MARKET

Authored by Samantha A. Janko & Nathan G. Johnson

Published in *Applied Energy* Vol. 229 July 2018

https://doi.org/10.1016/j.apenergy.2018.08.026

Abstract

Distributed energy resources are becoming increasingly common and forcing change in conventional energy markets with growing attention given to transactive energy networks that allow power trading between neighboring microgrids or distributed energy resources customers to supplement transactions with an electric utility. This study develops and evaluates a generalizable method for managing energy trading between microgrids in a grid-connected network through multi-agent techniques. The approach is demonstrated for a 3-node network and a 9-node network for a simulated year with hourly load and solar data for each unique microgrid agent. Results are compared against baseline networks without trading enabled to quantify a 3.6% and 5.4% reduction in the levelized cost of energy, respectively, with trading enabled for the 3-node and 9-node cases. Local energy storage capacities are varied to examine impact on the levelized cost of energy and trading behaviors. Results indicate that trading between microgrids reduces the levelized cost of energy for each individual node and the whole network, and that certain trends emerge between agents that allow some microgrids to operate at a lower cost than others.

Nomenclature

Variable	Units	Description
L	kW	Electrical load at current time step
L_n	kW	Electrical load of microgrid node *n* at current time step
P_s	kW	Solar production at current time step
S_D	kWh	Dispatchable energy from storage at current time step
S_A	kWh	Available storage for energy at current time step
S	kWh	Total energy in storage at current time step
S_{max}	kWh	Maximum storage capacity
S'	kWh	Total energy in storage at current time step after accounting for local loads and generation
L_N	kW	Net load at current time step
L'_N	kW	Net load at current time step after accounting for local loads, generation, and storage
$L_{N,p}$	kW	Net load of producer agent at current time step
$L_{N,c}$	kW	Net load of consumer agent at current time step
Δt	hour	Time step increment
ε	$/kWh	Minimum difference in energy rate to permit trading between agents
R_g	$/kWh	Grid electricity rate at current time step
$R_{i,c}$	$/kWh	Initial rate offer for consumer agent at current time step
$P_{i,c}$	kW	Initial power offer for consumer agent at current time step
$V_{c\rightarrow p}$	$/kWh	Energy valuation from consumer agent to producer agent at current time step and bargaining session
β_c	-	Convexity of consumer valuation curve
$V_{p\rightarrow c}$	$/kWh	Energy valuation from producer agent to consumer agent at current time step and bargaining session
β_p	-	Convexity of producer valuation curve
k	-	Current bargaining session
$k_{max,c}$	-	Maximum number of bargaining sessions for consumer agent
$k_{max,p}$	-	Maximum number of bargaining sessions for producer agent
$R_{min,c}$	$/kWh	Minimum rate consumer agent will accept
$R_{max,c}$	$/kWh	Maximum rate consumer agent will accept
$R_{min,p}$	$/kWh	Minimum rate producer agent will accept
$R_{max,p}$	$/kWh	Maximum rate producer agent will accept
$LCOE$	$/kWh	Levelized cost of energy
C_n	$/kWh	Cost of power for node *n* at current time step

3.1. Introduction

Distributed energy resources (DERs) are becoming increasingly common with the global capacity of installed systems expected to increase from 132.4 GW to 528.4 GW between 2017 and 2026, respectively (Navigant 2017). This growth will force change in conventional energy markets as distributed solar photovoltaics (PV) and wind displace centralized generation and create financial challenges for electric utilities such as disrupted

business models (Janko, Arnold, and Johnson 2016), politically-driven investment strategies (Institute for Energy Research 2014), and increased marginal costs of electricity (Goop, Odenberger, and Johnsson 2017), as well as technical challenges such as grid congestion (Goop, Odenberger, and Johnsson 2017), grid instability (Schmietendorf, Peinke, and Kamps 2017; Lam & Yeh 2014), overgeneration (Denholm, Clark, and O'Connell 2016), reduced power quality (Bank et al. 2013; Schmietendorf, Peinke, and Kamps 2017), and decreased reliability (Eber and Corbus 2013). These challenges increase when individual consumers become net energy producers over a year, with excess generation credited using feed-in tariffs ($) or net metering (kWh) (Arnette 2013). With net metering, consumers use the grid as a "zero cost lossless battery" for excess generation that can be used later in the day, month, or year to offset power purchases from the utility. This form of virtual storage is becoming less common, however, as utilities around the world reduce incentives as the solar PV market matures (Herbes et al. 2017). This trend in policy change has been demonstrated in both Germany and Arizona (Leepa and Unfried 2013; Energy Monitor Worldwide 2016). Consumers are now looking to localized energy storage (Tesla 2018; LG Chem ESS Battery Division n.d.), load management, programmable thermostats, and other DER devices to manage energy expenditures (Shen, Jiang, and Li 2015), with uninterrupted power supplies and generators providing back-up power for critical load applications such as hospitals (Professional Services Close-up 2012), military bases, and data centers (Kirchner 2012) that require high reliability if the main grid is compromised (Luo et al. 2015; Zachel 2013). A special case of these systems is known as a microgrid. The US Department of Energy and the Microgrid Exchange Group describe a microgrid as "a group of interconnected DERs and loads with clearly defined

electrical boundaries that act as a single controllable entity with respect to the grid" (Ton and Smith 2012). This is a useful, but expensive, solution to maintain reliability in the event of a grid outage. Microgrid owners and net energy producers have also begun seeking new value streams to offset costs of their microgrid asset base. One option is trading power between neighboring microgrids or DER customers with lower rates than the grid using an approach known as transactive energy.

3.1.1. Transactive Energy

The GridWise Architecture Council provides a general definition for transactive energy as an approach that assigns value to facilitate dynamic balancing between supply and demand across electrical infrastructure, typically between independent power producers (IPP) (GridWise Architecture Council 2015). This balance is achieved by trading energy, power, and ancillary services within the network, with the value of traded resources assigned through negotiation between nodes. Several techniques are available to determine value such as an organized market, self-optimization, tariffs, and bilateral contracts. Transactive energy markets seek optimal system-wide results by dynamically aligning individual and global objectives (Liu et al. 2017; Holmberg et al. 2016) for applications including scheduling energy management across adjacent microgrids, mitigating voltage fluctuations caused by high penetration renewables (Chassin et al. 2017), managing motor start-up currents (e.g., air conditioning) (Behboodi et al. 2018), and reducing the use of limited fossil fuel reserves in an islanded microgrid (Martínez Ceseña et al. 2018). A well-known transactive energy pilot project was initiated in 2006 by GridWise for an installation on Olympic Peninsula, Washington, United States with sponsorship from the U.S. Department of Energy (Hammerstrom 2007). The network consisted of controllable assets

including residential demand response from 112 homes, five water pumps, and two diesel generators. Each home was equipped with an energy management system accessing real-time data on grid prices updated every five minutes, with consumer demand response preferences to manage real-time energy purchases from the grid. Generators were controlled using price signals from an incentivizing shadow market. Water pumps bid into the market based on water-reservoir height. The project successfully demonstrated a transactive energy system containing both the technical network and financial market using technologies to manage bidding and load dispatch with consideration for wholesale energy costs, line congestion, and consumer needs. Though this project included demand response and some distributed generation, it did not incorporate home-based solar PV and energy storage that could provide additional grid services and a finer degree of control at individual nodes and across the electrical network. Additionally, power trading between home systems was not permitted.

3.1.2. Microgrid Operation and Coordination

Recent literature has demonstrated how microgrids can use transactive energy trading during real-time operations to achieve node-level and network-level benefits. Several studies have shown that coordination between multiple microgrids can reduce overall energy costs by improving DER utilization (Qu and Guan 2013; Khodaei 2015; Zenginis et al. 2017). A recent study by Yang and Hu explored this opportunity further by developing and comparing four operation decision models that demonstrated how total energy cost can be reduced for clusters of microgrids based on node-level or network-level economic minimization routines (Chen and Hu 2016). Moayedi and Davoudi (2016) expanded work beyond economic performance to show that power transfer and load

sharing between microgrids improves utilization of DERs across a network, improves reliability, and extends component lifespan. Further studies indicate that power exchange through coupled microgrids reduces node-level load shedding and network-level congestion in overloaded lines (Pashajavid, Shahnia, and Ghosh 2017; Shahnia, Bourbour, and Ghosh 2017). Power quality improvements have also been demonstrated using linear quadratic gaussian techniques for cooperative control of a simulated microgrid network (Minciardi and Sacile 2012). Microgrids can also support the main grid to self-heal and prepare for contingency events through reallocation of power and reconfiguration of network topology (Wu et al. 2018; Rivera, Farid, and Youcef-Toumi 2014). These benefits were achieved using control approaches for interconnected microgrids including bilevel model predictive control (Minciardi and Robba 2017), sequentially coordinated operation (Song et al. 2015), and robust optimization (Zhang et al. 2018). Similar approaches have been applied to optimize scheduling of energy assets within microgrids including mixed integer linear programming (Silvente et al. 2015), parametric mixed-integer linear programming (Umeozor and Trifkovic 2016), and receding horizon model predictive control (Holjevac et al. 2017). In recent work by Nikmehr, Najafi-Ravadenegh, and Khodaei (2017), a bi-level, stochastic optimization algorithm was used to achieve optimal asset scheduling in a network of microgrids over a one-day period. The energy management system used a combination of centralized and decentralized control that resulted in a 17.3% reduction in operating cost under a time-of-use pricing scenario. Other work by Rahmani-Andebili (2017; 2018) suggests a multi-time scale stochastic model predictive control technique for distributed energy scheduling of both energy resources and

deferrable appliances. This approach reduced weekly operation cost by a half when compared to a case without scheduling.

3.1.3. Approaches to Transactive Energy

Multi-agent control has emerged as a prominent technique for transactive energy trading due to its ability to increase system scalability, flexibility, autonomy, and resiliency (Divshali, Choi, and Liang 2017; Babar et al. 2018; Ghorbani, Rahmani, and Unland 2017; Jun et al. 2011). Logenthiran, Srinivasan, and Khambadkone (2011) proposed a multi-agent system to schedule energy resources within an islanded power network through three steps: (i) internal demand management, (ii) bidding to export power to the network, and (iii) rescheduling to meet total system demand. Network scheduling was accomplished through a wholesale energy market with centralized economic dispatch controlled by a market operator that provided a single market clearing price using the highest bid. This technique was tested on a simulated network of three microgrids and five loads to minimize operating cost, but were not tested with a grid connection or utility rate structures. Another approach to transactive energy focused on grid-connected microgrids and used agent-based trading and a priority index to rank customers to receive lower cost energy by participating in demand response (Nunna and Doolla 2012). A continuous double auction market strategy was used to determine power cost, which cleared one unit of goods per round. The theoretical framework was demonstrated on a simulated system of two microgrids containing two loads each. Though this work successfully reduced system peak and cost, it did not include consideration for local generation assets such as solar PV or energy storage assets. More recent work by Rivera, Farid, and Youcef-Toumi (2014) included storage in grid-connected microgrids and incorporated agent-based control for power grid

modeling and distributed decision-making techniques with a focus on transient stability and self-healing behaviors. The JAVA Agent Development Framework (JAVA-JADE) was used for multi-agent peer-to-peer messaging and MATLAB was used for simulating power transients. Microgrid interactions were autonomous and demonstrated how microgrids could be dispatched using local, decentralized control algorithms to benefit network-level objectives for grid stability and ancillary services. Further work is needed for transactive negotiation of power trading to support real-time operation. The decentralized nature of multi-agent control has also proven to be robust against communication failures through techniques such as consensus + innovation algorithms (Hug, Kar, and Wu 2015; Kar, Moura, and Ramanan 2012; Kar and Hug 2012) and diagonal quadratic approximation (Mohammadi, Mehrtash, and Kargarian 2018). In traditional centralized control schemas, sharing sensitive information and access rights to a central authority can leave the system vulnerable to cyber-attacks. Distributed techniques such as multi-agent control provide a means for coordination in large-scale systems while preserving the privacy of energy stakeholders (Mohammadi, Mehrtash, and Kargarian 2018).

3.1.4. Article Contributions and Organization

This study develops and evaluates a generalizable method to manage energy trading using multi-agent techniques for microgrids in a grid-connected network. Economic transactions are simulated in time steps with each microgrid acting as its own negotiating agent within the energy market. Annual simulations are performed with datasets from existing and simulated buildings on an electrical network with a ring configuration to demonstrate the proposed technique and explore agent-level and network-level behaviors

for application to real distribution circuits. This work is differentiated from existing microgrid control and operation literature by focusing on transactive energy negotiations between sub-groups of microgrids as a means to lower the cost of energy for both individual nodes and the network.

The major contributions of this work are summarized below.

- A generalizable mathematical framework is introduced for handling economic transactions between microgrids using a multi-agent negotiation approach scalable to n-many agents.
- Demonstration case studies are developed, simulated, and analyzed for a 3-node network and a 9-node network of heterogeneous microgrid nodes including different loads, solar, and storage.
- Baseline data from a network that disallows trading is compared with a transactive network to quantify the financial value of energy trading for individual agents and the entire network.
- Microgrid agent trading behaviors are identified and discussed with supporting data from a one-year techno-economic performance analysis.
- Sensitivity analysis of storage sizing uncovers further trends in trading behavior with different outcomes observed due to agent load factor and renewables penetration.

The remaining sections of the paper are organized as follows: Section 3.2 describes the theoretical approach and mathematical formulations, Section 3.3 discusses two case studies for simulation and comparison, Section 3.4 introduces and analyzes results, and

Section 3.5 concludes the paper with a summary of findings and a description of application opportunity spaces and future research extensions.

3.2. Methods

Communication and negotiation between nodes is managed by a multi-agent framework where each microgrid is represented by a single agent in a transactive energy marketplace. Each agent has the same basic microgrid components, as shown in Fig. 3.1, but with different component capacities and load profiles to produce a heterogeneous set of agent characteristics. Electrical feeder architecture was limited to a grid-connected ring network, a standard circuit configuration for secondary power distribution (Naval Facilities Engineering Command 1990). Though several other electrical feeder architectures exist such as radial, parallel, and tie structures, the ring structure is a common distribution architecture used around the world to improve reliability (Glover, Sarma, and Overbye 2012) and was selected to increase applicability to real networks. Abstract graph theory topologies such as wheel graphs and complete graphs were not considered. An example 3-node case is shown in Fig. 3.2 with electrical and communication lines noted. The ring configuration shown be extended to any number of nodes.

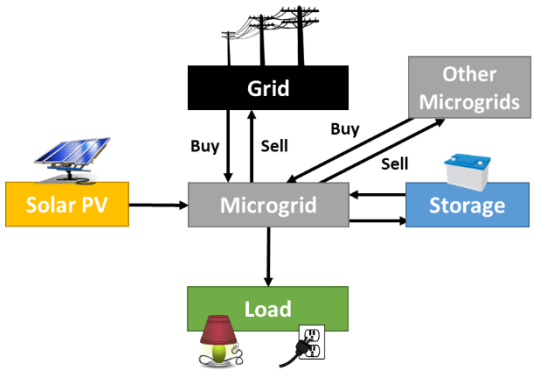

Figure 3.1: Microgrid agent configuration.

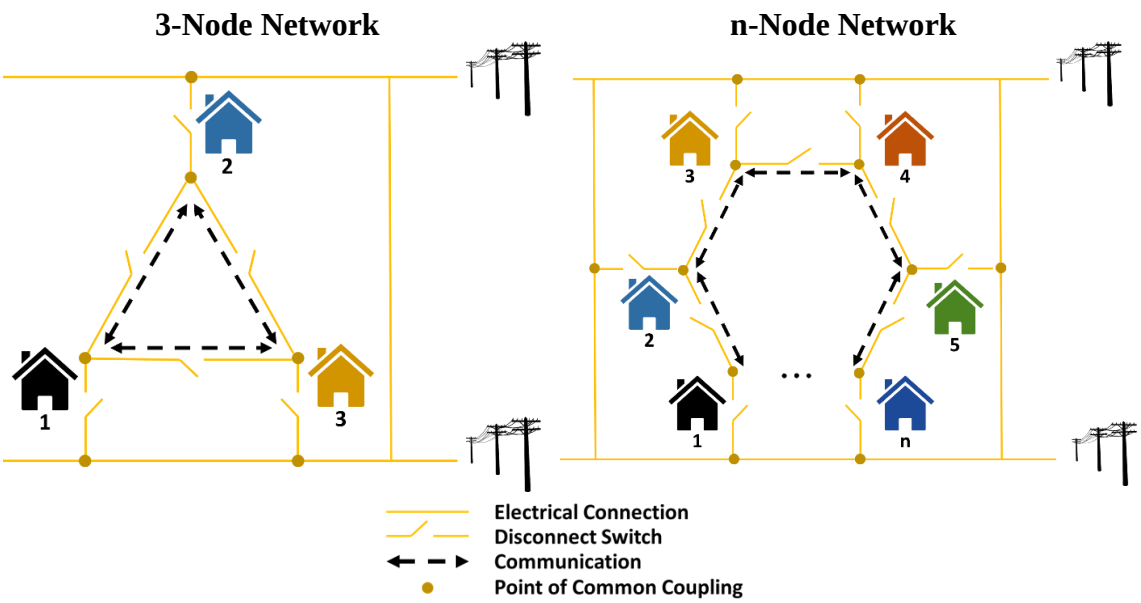

Figure 3.2: Scalability of simulated ring network for 3-node case (left) and n-node case (right).

Negotiations and trading occur each time step following the processes described in Fig. 3.3. A microgrid agent first determines its own operational status as a consumer (needs power from neighbors or the grid) or a producer (wants to sell power to neighbors or the grid) based on its net load after applying local generation and storage to meet electrical loads. A net load of zero means the microgrid is in a neutral state and does not participate in trading for that time step. Next, agents share operational status with one another and form trading groups. Agents within each trading group then negotiate with one another until an energy price is accepted or until the maximum number of bargaining sessions is reached. After bargaining is complete, consumer agents with any remaining load purchase power from the grid at rates dictated by the utility rate structure. Producer agents with remaining excess generation sell power to the grid at the wholesale price of electricity in the absence of net metering or a higher feed-in tariff. This self-organizing distributed approach models each agent as an independent decision-making entity that ensures its own

loads are met and any excess generation is sold off before the end of each time step, in contrast to other approaches with centralized dispatch and an auction to set a market clearing price in a competitive environment.

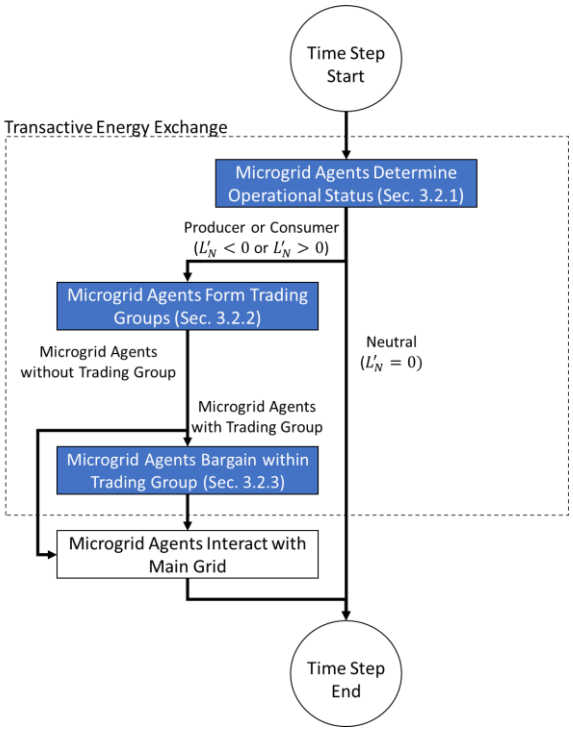

Figure 3.3: Microgrid agent processes within a time step.

Several assumptions maintain the generality of this approach for managing energy trading in a simulated transactive market framework:

1. Network topology remains the same throughout the time series simulation (no outages or switching).
2. All microgrid nodes are on a single distribution network with no efficiency losses for power conversion or transfer between nodes.
3. Capacity limits are ignored for distribution transformers and power lines.
4. All loads must be met at the instant of power use (no dispatchable loads, deferrable loads, or load shedding).

5. Each microgrid is a rational financial agent that seeks to lower expenses by purchasing power at the lowest available price and selling at the highest possible price.
6. There is no cost for utilizing local generation and storage.
7. Each microgrid agent utilizes local generation and storage to meet its loads prior to seeking outside resources (interconnected microgrid or grid power).
8. Each microgrid agent can be a consumer or a producer at any time step based on the microgrid's instantaneous loads, generation, and storage.
9. Any excess generation is first sent to local storage before the microgrid agent attempts to sell excess externally.
10. Each microgrid uses the same electric utility rate structure.
11. Microgrid agents do not have global information on network status. They only know the information they receive from neighboring microgrid agents.
12. Storage charging and discharging is limited to a maximum 1C rate based on commonly available battery technologies (McLaren et al. 2016).
13. Microgrid agents always attempt to trade with one another when they have neighbors with compatible operational statuses (a consumer and a producer).

A Python script was developed to simulate microgrid agent transactions, manage communications between agents, and solve optimization routines. Input data includes hourly load and solar profiles, storage size, and bargaining parameters for each microgrid agent, and a rate structure for transactions with the utility. Additional input data includes the incidence matrix that defines network structure (agent connections); the incidence matrix can be modified to create various electrical circuit configurations other than the ring

network simulated in this study. Model parameters and all simulated data were saved in an SQL database for fast access. Several Python packages were utilized including osBrain 0.4.4 for multi-agent programming, sqlite 3.22.0 for database management, and scipy 0.19.0 for optimization (osBrain n.d.; SQLite n.d.; SciPy.org 2018).

3.2.1. Microgrid Agents Determine Operational Status

At each time step, each microgrid agent first identifies its operational status as a producer or consumer based on the net load calculation in Eq. 3.1 that expresses the difference between local loads and generation. If the net load is positive ($L_N > 0$), the agent attempts to discharge available storage to meet the load and recalculates the new battery state of charge and net load to be met by external purchases (Eqs. 3.2a1-3.2b2). If the net load is negative ($L_N < 0$), the agent has excess generation and attempts to charge its storage and recalculates the new battery state of charge and net load for potential external sale (Eqs. 3.3a1-3.3b2).

$$L_N = L - P_s \tag{3.1}$$

A positive net load indicates there is insufficient local generation, and the available battery storage for discharge is then calculated as $S_D = S - S_{min}$ to try meet this deficit. If storage cannot meet the load ($S_D/\Delta t < |L_N|$) then Eqs. 3.2a1 and 3.2a2 apply and if storage can meet the load ($S_D/\Delta t \geq |L_N|$) then Eqs. 3.2b1 and 3.2b2 apply.

$$S' = S_{min} \text{ and } L'_N = L_N - S_D/\Delta t \qquad \text{(3.2a1 and 3.2a2)}$$

$$S' = S - L_N \Delta t \text{ and } L'_N = 0 \qquad \text{(3.2b1 and 3.2b2)}$$

A negative net load indicates there is excess local generation, and the available battery storage to accept energy is calculated as $S_C = S_{max} - S$. If storage cannot accept

all excess generation ($S_C/\Delta t < |L_N|$) then Eqs. 3.3a1 and 3.3a2 apply and if storage can accept excess generation ($S_C/\Delta t \geq |L_N|$) then Eqs. 3.3b1 and 3.3b2 apply.

$$S' = S_{max} \text{ and } L'_N = L_N + S_C/\Delta t \qquad \text{(3.3a1 and 3.3a2)}$$

$$S' = S - L_N \Delta t \text{ and } L'_N = 0 \qquad \text{(3.3b1 and 3.3b2)}$$

An agent will act as a producer agent when the recalculated net load is negative ($L'_N < 0$) and act as a consumer agent when the recalculated net load is positive ($L'_N > 0$). The agent is in a neutral state if the recalculated net load is zero ($L'_N = 0$) and the agent will not participate in bargaining while they are self-sufficient.

3.2.2. Microgrid Agents Form Trading Groups

Trading groups are formed as each agent sends its status (producer or consumer) and net load value to all neighboring, electrically connected agent nodes. Producer agents may group and negotiate with multiple consumer agents but each consumer agent may only negotiate with one producer. This divides the network into unique negotiating subgroups with bargaining managed as separate simulations independent of the larger network. Separate trading groups also reduce computational complexity and simulation time to reach network consensus by constraining negotiations to agents with direct physical connections. Physical limitations in the model are also better preserved by limiting trading between microgrid nodes on opposite sides of the ring network. If a consumer agent is connected to two producer agents, then the consumer agent chooses to group with the producer agent that has the largest amount of excess power to sell. This is a rational action because consumer agents want the highest probability of meeting all their load with power from other microgrids, given that trading may be cheaper than purchasing power from the main

grid. Once the group is formed, producer agents are classified as group leaders and are responsible for beginning trading sessions with an initial offer.

3.2.3. Microgrid Agents Bargain within Trading Group

Bargaining between the producer agent and each consumer agent within a trading group is completed separately from one another. Consumer agents in a single trading group do not interact with one another and do not have the opportunity to actively compete against one another's bids to the producer agent. Consumer agents also do not have knowledge of separate negotiations between the producer agent and other consumer agents. Producer agents must, however, have knowledge of all negotiations in a bargaining group to maintain conservation of energy laws by not selling the same power to two (or more) consumer agents. If more than one consumer agent reaches a negotiated price and requests all available power from the producer agent, then the producer sells power in such a way to maximize revenue. Bargaining is accomplished in two processes: making an initial offer and considering offers before making a counter offer. Both consumer agents and producer agents can choose to accept an offer, but the producer agent must make the final trading decision to conclude the bargaining process.

Making initial offer: The producer agent makes an initial offer just below the grid price (Eq. 3.4) in an attempt to maximize revenue. An epsilon of 0.0001 $/kWh is the smallest increment in energy price across which transactions are made. The amount of power traded is limited by the total capacity available from the producer and the total load requested by a consumer (Eq. 3.5). The amount of power offered for trading will remain the same during the negotiation process until a consensus is reached by one or more agents and that power

is sold, or bargaining ends and the power is sold to the grid. This study models electricity price that changes during the day with time-of-use (TOU) utility rates.

$$R_{i,c} = R_g - \varepsilon \tag{3.4}$$

$$P_{i,c} = \min\left(-L_{N,p}, L_{N,c}\right) \tag{3.5}$$

Considering offers and making counter offers: Consumer agents and producer agents consider an offer and decide to accept, reject, or make a counter offer (Winoto 2007). This decision is based on each agent's unique valuation of energy that defines the maximum and minimum rate that the agent will accept for purchase and sale, respectively. The relationship between the high and low bound is a function of the maximum number of allowable bargaining sessions, the net load and electrical load of the agent, and the current grid purchase and sellback rates. The consumer agent valuation curve is modeled as a positive exponential function (Faratin, Sierra, and Jennings 1998) that represents willingness to negotiate (Eq. 3.6a). Producer agent valuation is modeled similarly but with a decreasing exponential curve (Eq. 3.7a). Each agent is assigned a maximum number of bargaining sessions to prevent negotiations from continuing indefinitely, at which point an agent decides to conduct business with the grid instead. The parameter α expresses the exponential relationship between energy valuation and bargaining session at the current time step with the reservation value offered when the maximum number of bargaining sessions is reached (Eq. 3.6b and 3.7b). The parameter β determines the convexity of the exponential curve. For consumer agents, β_c is calculated as the ratio of the agent's net load during the current time step to its electrical load in that time step (Eq. 3.6c). This demonstrates behavior that consumer agents are more inclined to make a deal when they can serve less of their load with local generation or storage as indicated by Fig. 3.4. For

producer agents, β_p is calculated as the ratio of the power offered to a consumer agent to the electrical load of the producer in that time step (Eq. 3.7c) with a different β_p calculated for each consumer. This demonstrates behavior that producer agents are more inclined to make a deal with consumers that can purchase the most power (Fig. 3.5). Consumer and producer valuation curves are not static given that the net load or excess power, respectively, will be different each time step. This indicates that a single consumer or producer could exhibit any of the behaviors in Fig. 3.4 and 3.5.

From consumer agent "c" to producer agent "p"

$$V_{c\to p}(k) = R_{min,c} + \alpha_c(k)\left(R_{max,c} - R_{min,c}\right) \tag{3.6a}$$

$$\alpha_c(k) = e^{\left(1-\frac{\min(k,k_{max,c})}{k_{max,c}}\right)^{\beta_c}\ln(\lambda_c)} \tag{3.6b}$$

$$\beta_c = \frac{L_{N,c}}{L_c} \tag{3.6c}$$

From producer agent "p" to consumer agent "c"

$$V_{p\to c}(k) = R_{max,p} - \alpha_p(k)\left(R_{max,p} - R_{min,p}\right) \tag{3.7a}$$

$$\alpha_p(k) = e^{\left(1-\frac{\min(k,k_{max,p})}{k_{max,p}}\right)^{\beta_p}\ln(\lambda_p)} \tag{3.7b}$$

$$\beta_p = \frac{P_{i,c}}{L_p} \tag{3.7c}$$

Where:

$$0 \le \alpha(k) \le 1$$

$$\alpha(k_{max}) = 1$$

$$\lambda = \alpha(0)$$

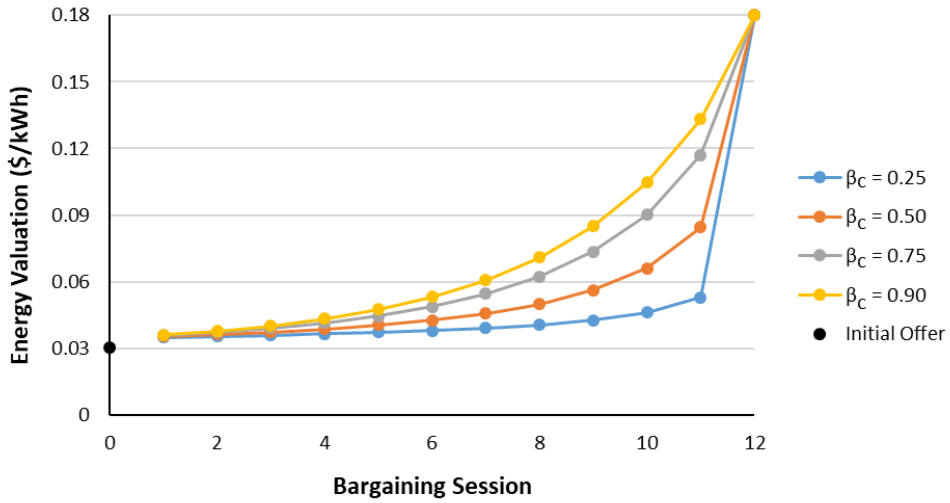

Figure 3.4: Example consumer agent valuation curves with a grid purchase rate of $0.18/kWh, grid sellback rate of $0.03/kWh, and maximum of 12 bargaining sessions.

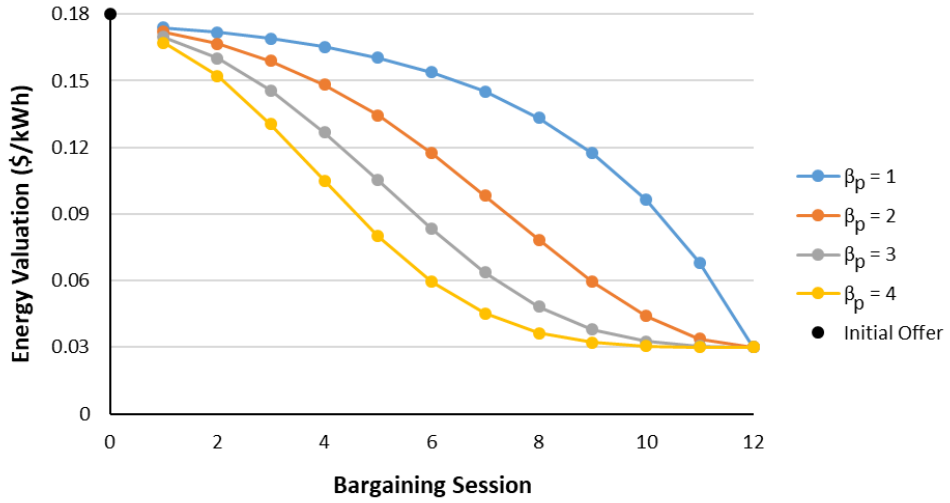

Figure 3.5: Example producer agent valuation curves with a grid purchase rate of $0.18/kWh, grid sellback rate of $0.03/kWh, and maximum of 12 bargaining sessions.

Each agent quantifies energy valuation from their unique valuation curve. This occurs for each agent, in each time step, and for the current bargaining session within that time step. A consumer agent accepts an offer that is less than or equal to its valuation. A producer agent accepts an offer that is greater than or equal to its valuation. Otherwise, the agent makes a counter offer or rejects the offer if the maximum number of bargaining sessions has been reached. Fig. 3.6 provides an illustrative example of the bargaining space

between two negotiating agents. The acceptable ranges for producer and consumer offers overlap after bargaining session 7 to provide a feasible set for negotiation. In general, an agent can offer any value within its acceptable set for a bargaining session. This work assumes the extreme case in which valuation in a bargaining session is equal to the valuation curve. Trading is therefore more likely to occur because it is easier for a consumer and producer to reach consensus and thus reduce overall network energy cost relative to the baseline case without trading.

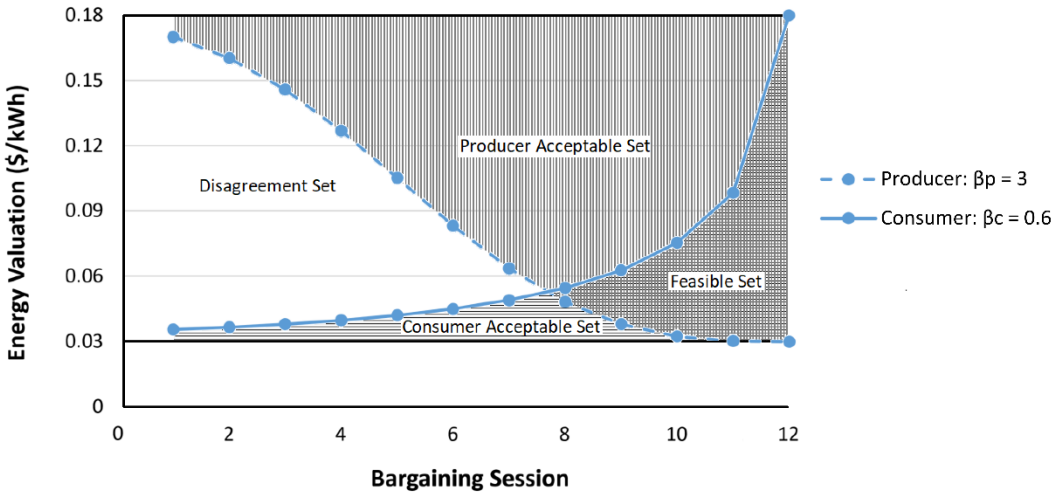

Figure 3.6: Example bargaining space with a grid purchase rate of $0.18/kWh, grid sellback rate of $0.03/kWh, and maximum of 12 bargaining sessions. Figure adapted from (Winoto 2007).

Fig. 3.7 portrays the bargaining process between a producer agent and a consumer agent with the same valuation curves as Fig. 3.6. The producer agent sets an initial offer of $0.1799/kWh that is sent to the consumer agent for consideration in bargaining session 1. Since the offer is far above the consumer's valuation, the consumer agent provides a counter offer equal to its own energy valuation. This negotiation continues until bargaining session 8 where the producer accepts the consumer's offer of $0.055/kWh, which is higher than the producer's valuation of $0.048/kWh.

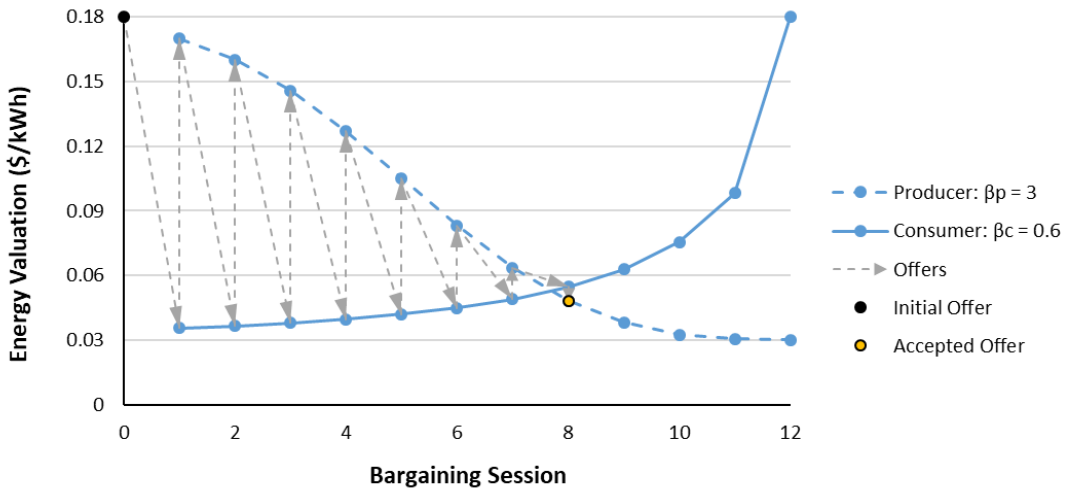

Figure 3.7: Example showing offer progression during a negotiation with a grid purchase rate of $0.18/kWh, grid sellback rate of $0.03/kWh, and maximum of 12 bargaining sessions. The offer is settled at bargaining session 8.

For trading groups with more than one consumer, the producer first sells power to the consumer that most quickly agrees upon a negotiated price and then continues negotiations with other consumer(s) to sell any remaining power as demonstrated in Fig. 3.8 for a two-consumer example. For instances in which both consumers agree upon a sale price in the same bargaining session, the producer sells all possible power at the highest negotiated rate first and sells any remaining power at the lower negotiated rate as demonstrated in Fig. 3.9 with Consumer 2 offering a higher price than Consumer 1. This is another characteristic of an agent's behavior to maximize revenue. In the uncommon case where acceptance is reached by multiple consumer agents within the same bargaining session and at the same rate, the producer agent splits power between the consumer agents.

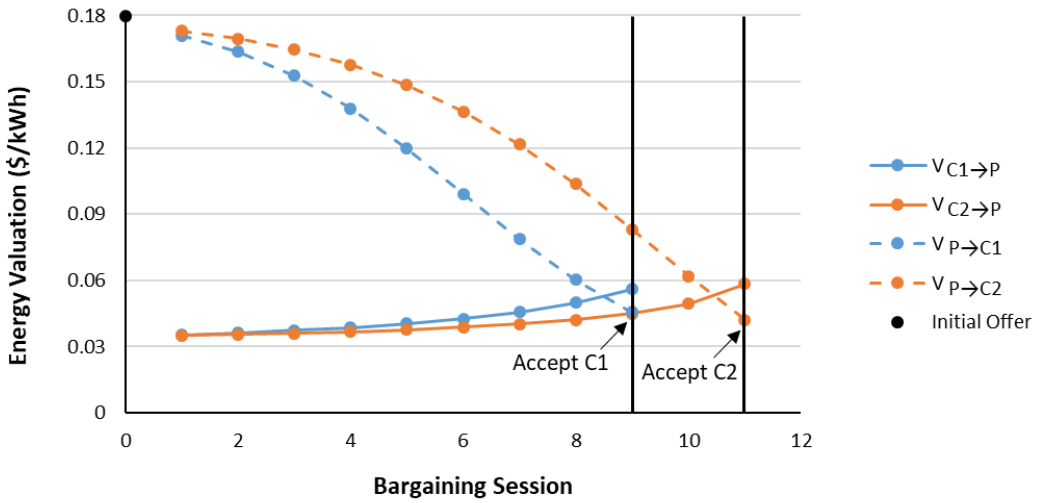

Figure 3.8: Example negotiation between a producer agent and two consumer agents with a grid purchase rate of $0.18/kWh, grid sellback rate of $0.03/kWh, and maximum of 12 bargaining sessions. The offer is settled with C1 at bargaining session 9 and C2 at bargaining session 11.

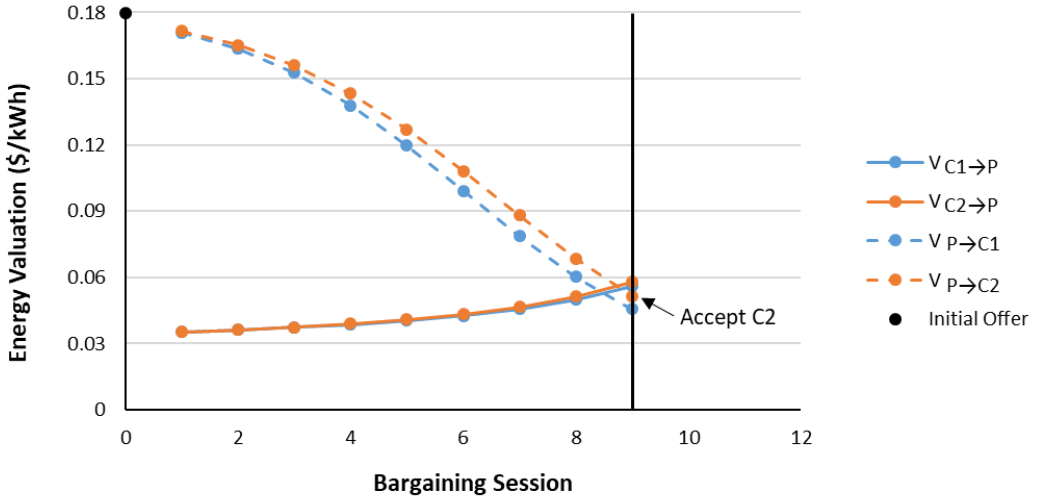

Figure 3.9: Example negotiation between a producer agent and two consumer agents with a grid purchase rate of $0.18/kWh, grid sellback rate of $0.03/kWh, and maximum of 12 bargaining sessions. The offer is settled at bargaining session 9.

3.3. Data Inputs

Two ring networks were developed and simulated with results compared to demonstrate the generalizable mathematical approach. The 3-node network included a school, a neighborhood, and a commercial building. The 9-node network included the same

nodes from the 3-node network plus six additional nodes including three neighborhoods, three commercial buildings, an industrial building, a hospital, and a school. These networks are illustrated in Figs. 3.10 and 3.11, respectively, with load and generation statistics summarized in Tables 3.1 and 3.2. Average load for each node was summed to equate the network average load with the network peak load reported as the maximum coincident load observed in a single time step. Simulations were performed with varying amounts of storage at each microgrid node sized to meet peak load for durations of 0, 1, 2, 3, and 4 hours. Batteries were modeled with a conservative 20% minimum state of charge for lithium-ion chemistries (Barkholtz et al. 2017). Negotiations within a single time step were completed out to a maximum of 12 bargaining sessions for each node and all time steps.

Simulations were completed using hourly time step data, a common resolution for trading and dispatch studies in literature (Hobbs 1995; Lynch et al. 2013). Hourly load and solar data were sourced from existing physical systems or simulated data sources for one full year (8760 hourly time steps). Open access data were used to permit replication and extension of this research. Hourly loads and solar PV generation data for node 1 were sourced from recorded building data on the Arizona State University Polytechnic and Tempe campuses (Arizona State University Campus Metabolism 2018). Neighborhood data for nodes 2, 6, and 9 were generated from different individual household load and solar profiles selected from OpenEI and scaled linearly to create three distinct neighborhoods (OpenEI.org n.d.). The number of houses, solar PV penetration, and locations of each neighborhood were varied to increase network heterogeneity and better illustrate the bargaining and negotiation process. Commercial building load and solar data for node 3 were measured at the National Renewable Energy Laboratory Research and

Support Facility (OpenEI.org 2011). Building load data for nodes 4, 5, and 7 were simulations of a large hotel, large office building, and supermarket, respectively, available on OpenEI (OpenEi.org n.d.), and paired with solar PV data recorded from several solar-covered parking structures on the ASU Tempe campus (Arizona State University Campus Metabolm 2018). Node 8 had simulated hospital building data with no solar PV.

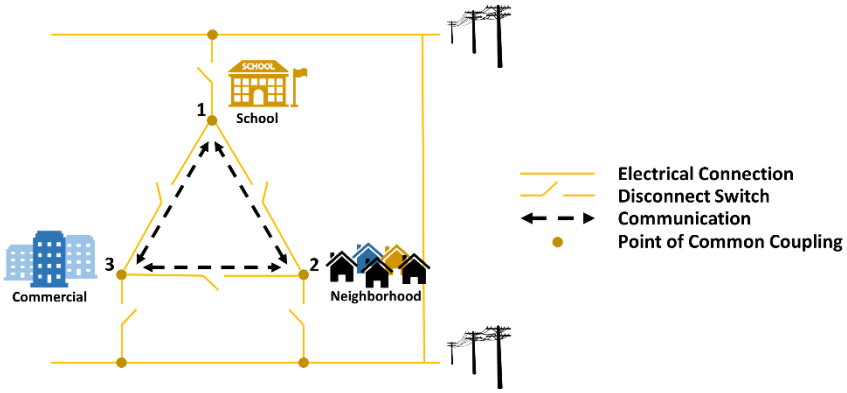

Figure 3.10: Example 3-node microgrid ring network.

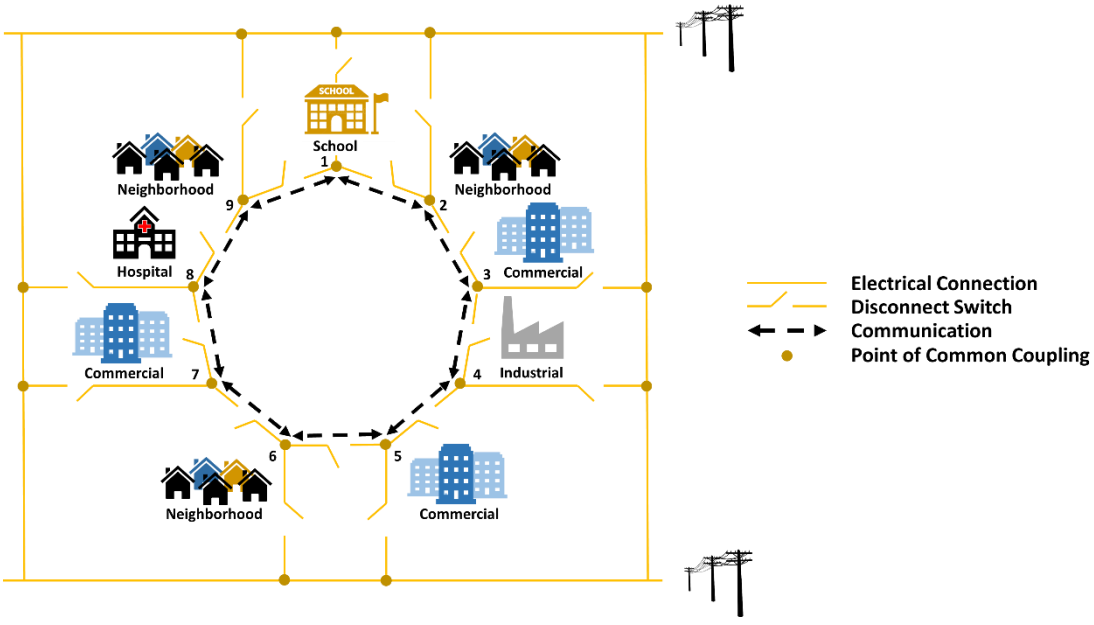

Figure 3.11: Example 9-node microgrid ring network.

Table 3.1: 3-Node Network Summary

Parameter	Microgrid Node			
	1	2	3	Network
Average Load (kW)	1109	885	268	2261
Peak Load (kW)	1577	2637	1852	4239
Solar Production (kWh/day)	13714	16433	2519	32666
Load Factor (-)	0.703	0.336	0.145	0.534
Renewables Fraction (-)	0.515	0.774	0.392	0.602

Table 3.2: 9-Node Network Summary

Parameter	Microgrid Node									
	1	2	3	4	5	6	7	8	9	Network
Average Load (kW)	1109	885	268	310	873	820	209	1156	373	6003
Peak Load (kW)	1577	2637	1852	501	1688	1863	403	1576	1244	10079
Solar Production (kWh/day)	13714	16433	2519	1935	8849	29911	2260	0	2789	78410
Load Factor (-)	0.703	0.336	0.145	0.619	0.517	0.440	0.518	0.734	0.300	0.596
Renewables Fraction (-)	0.515	0.774	0.392	0.260	0.422	1.520	0.451	0.000	0.311	0.544

Load and solar profiles for each microgrid affect grouping and bargaining behaviors between agents in the network. The neighborhood in node 6 produces more solar on average than is required to meet its load. This results in node 6 acting as a producer agent during most daylight hours, which directly affects trading for nodes 5 and 7 and indirectly affects the trading of nodes 4 and 8 because nodes 5 and 7 prefer to group with the producer agent that has the most excess generation to offer. Additionally, the hospital at node 8 has no local generation and is a consumer agent at all hours. By rank, nodes 8, 1, and 4 have the highest load factors and therefore have a more consistent or flatter load profile than other nodes in the network. Conversely, nodes 3, 9, and then 2 have the lowest load factors indicating that they tend to operate far lower than their annual peak power consumption.

Transactions with the main grid were modeled using the TOU rate structure given in Table 3.3. The sellback rate is representative of the wholesale price of electricity on the grid (United States Energy Information Administration 2018), which is a common value to resell power back to the utility in the absence of net metering or a higher feed-in tariff. Peak hours are between 1PM and 8PM for every day in the year.

Table 3.3: Grid Rate Structure

Price Structure	Rate ($/kWh)
Off-peak	0.09
On-peak (1PM-8PM daily)	0.18
Sellback Rate	0.03

3.4. Results

A baseline case was simulated with grid-only transactions and compared against a second case with microgrid trading permitted. The primary metric for comparison was the levelized cost of energy (LCOE) evaluated for each node and the entire network. Node LCOE was evaluated for each day of the year as described in Eq. 3.8 with the annual LCOE evaluated similarly over all 8760 hours in the year. Network LCOE was calculated alongside node LCOE values to represent the average cost of all power transactions on the network for each day and the entire year.

$$LCOE = \frac{\sum_{t=1}^{t=24} C_n}{\sum_{t=1}^{t=24} L_n} \tag{3.8}$$

3.4.1. 3-Node Network

Results in Table 3.5 and Fig. 3.12 show that network LCOE reduced with microgrid trading enabled when compared to the grid-only case. Individual results for each node in Table 3.5 show that the average daily cost of energy with trading enabled is 0.3% and 5.4% less than with grid-only transactions. Additionally, all nodes and the network benefited from a lower cost of energy as the amount of storage increased. This occurred because microgrids with storage could utilize their stored self-generated power at no cost rather than trading power with neighbors or interacting with the grid. If equipment costs or efficiency losses were assigned to dispatching local storage, the trend of decreasing LCOE in Fig. 3.12 would be less prominent and then vanish when storage costs become more

expensive than the cost of transactions with the grid or neighbors. Increasing storage size also narrows the difference in LCOE between grid-only and microgrid trading cases because trading occurrences reduce with increasing amounts of storage. Increasing storage size also permitted nodes 2 and 3 to store and sell power more often to node 1, thereby giving each node a profit (negative cost) in at least one day over the one-year period.

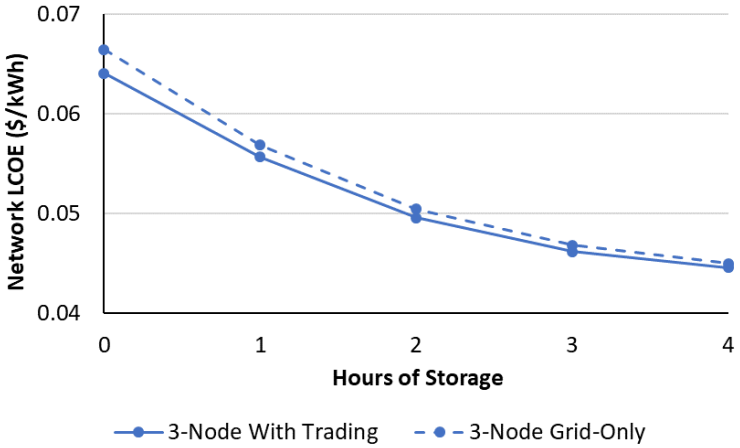

Figure 3.12: Network LCOE for 3-node network with trading and grid-only cases for varying amounts of storage.

Table 3.4: Average Daily Energy Cost ($/kWh) for 3-Node Network

Node		Hours of Storage									
		0		1		2		3		4	
		Grid-Only	**With Trading**	**Grid-Only**	**With Trading**	**Grid-Only**	**With Trading**	**Grid-Only**	**With Trading**	**Grid-Only**	**With Trading**
1	Min	0.033	0.031	0.025	0.024	0.020	0.018	0.017	0.016	0.014	0.012
	Max	0.124	0.124	0.124	0.124	0.124	0.124	0.124	0.124	0.124	0.124
	Range	0.091	0.093	0.099	0.100	0.104	0.106	0.107	0.108	0.110	0.112
	Average	0.066	0.064	0.060	0.059	0.055	0.055	0.052	0.052	0.051	0.051
	Savings		**2.7%**		**1.2%**		**0.9%**		**0.6%**		**0.3%**
2	Min	0.021	0.017	0.000	-0.003	-0.010	-0.013	-0.020	-0.023	-0.023	-0.027
	Max	0.114	0.114	0.114	0.114	0.114	0.114	0.114	0.114	0.114	0.114
	Range	0.093	0.097	0.114	0.117	0.124	0.127	0.134	0.137	0.137	0.141
	Average	0.061	0.058	0.044	0.043	0.033	0.031	0.026	0.025	0.022	0.021
	Savings		**5.2%**		**3.9%**		**4.3%**		**4.3%**		**3.6%**
3	Min	0.010	-0.007	-0.012	-0.024	-0.018	-0.027	-0.016	-0.025	-0.016	-0.025
	Max	0.126	0.118	0.126	0.119	0.126	0.119	0.126	0.119	0.126	0.119
	Range	0.115	0.125	0.138	0.143	0.144	0.146	0.142	0.144	0.142	0.144
	Average	0.067	0.064	0.055	0.053	0.053	0.051	0.052	0.051	0.052	0.051
	Savings		**5.4%**		**3.5%**		**2.5%**		**1.9%**		**1.2%**
Network	Min	0.036	0.034	0.022	0.021	0.015	0.015	0.007	0.007	0.005	0.005
	Max	0.116	0.116	0.116	0.116	0.116	0.116	0.116	0.116	0.116	0.116
	Range	0.080	0.082	0.094	0.095	0.100	0.100	0.109	0.109	0.111	0.111
	Average	0.066	0.064	0.057	0.055	0.050	0.049	0.046	0.046	0.044	0.044
	Savings		**3.6%**		**2.1%**		**1.8%**		**1.4%**		**1.0%**

Further examination into microgrid trading revealed trends in agent behaviors over the annual simulation. Fig. 3.13a summarizes the percentage of time steps resulting in grid-only, neighbors-only, grid and neighbors, and no transactions for nodes without storage. Fig. 3.13b summarizes the same information with four hours of storage at each node. Grid and neighbor transactions indicate time steps in which a node purchased power from neighbors and the grid to meet local loads. Time steps with no transactions indicate that a node met its own load and stored any excess generation without external export.

Without storage, nodes purchased power from only the grid in 83-86% time steps of the year. The remaining time steps were split between grid and neighbors transactions and neighbors-only transactions. There were minimal to no occurrences without any transactions because the node would need to exactly meet its load with local generation. Visual inspection of Fig. 3.13b indicates that nodes with storage had fewer transactions with the grid and fewer transactions between neighbors when compared to nodes without storage in Fig. 3.13a. Storage permitted a microgrid agent to more often serve its own load without importing or exporting power. This commonly occurred during daytime hours or shortly after sunset until storage was depleted. Results in Fig. 3.13b also show that the inclusion of storage increased the percentage of time steps with no transactions for node 2 as compared to nodes 1 and 3. This was due to the relatively high renewables fraction and low load factor for node 2 (refer to Table 3.1) that permitted node 2 to remain independent from the network for a longer duration of the year.

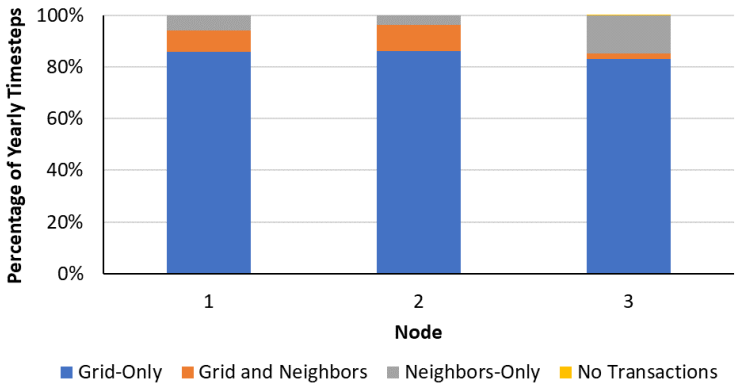

Figure 3.13a: Transaction types by percentage for 3-node network with 0 hours of storage.

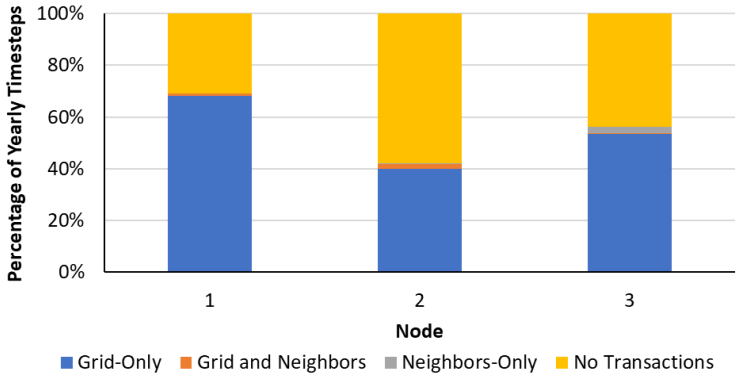

Figure 3.13b: Transaction types by percentage for 3-node network with 4 hours of storage.

Fig. 3.14 shows that the number of aggregate transactions between nodes decreased as storage was added because nodes were independent for a larger portion of the year. The proportion of unsuccessful transactions to successful transactions also dropped. Unsuccessful transactions were rejections by either the producer agent or consumer agent once the maximum number of bargaining sessions was reached, or when a producer agent sold all power to one of two consumer agents and rejected the second agent. After an unsuccessful transaction, the consumer agent would purchase power from the grid instead and result in a grid-only data point. If the unsuccessful transaction was caused by a rejection from the consumer agent, the producer agent would attempt to complete a transaction with

another consumer agent in its trading group or sell power to the grid. This could result in grid-only, grid and neighbors, or neighbors-only data points.

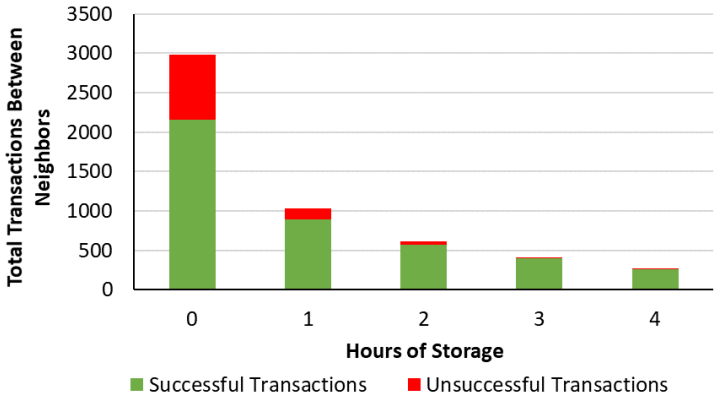

Figure 3.14: Frequency of successful and unsuccessful transactions between neighboring nodes in a 3-node network.

3.4.2. 9-Node Network

Trading in the 9-node network also yields financial benefits when noting the observed reductions in LCOE in comparison to the grid-only case. Fig. 3.15 shows that the benefit of trading decreases, however, as storage increases and nodes become more self-sufficient and trade less often. This finding is consistent with the 3-node case as observed in Fig. 3.12. The difference in the 9-node LCOE between microgrid trading and grid-only stays fairly consistent with increasing storage because nodes 5, 6, and 7 have almost the same number of neighbor transactions regardless of storage capacity.

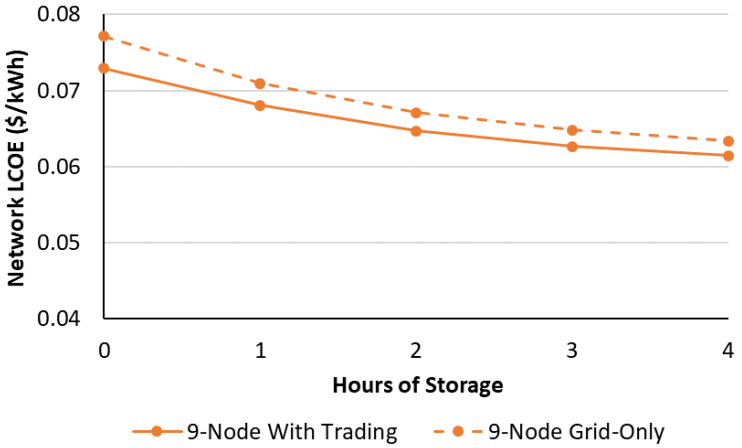

Figure 3.15: Network LCOE for 9-node network with trading and grid-only cases for varying amounts of storage.

Table 3.6 summarizes the average daily cost of energy for individual nodes within the 9-node network with Fig. 3.16a and Fig. 3.16b showing trading behavior with no storage and four hours of storage, respectively. Trading behavior is more complex in the 9-node network with trends in LCOE not strictly consistent with increasing storage size. The daily average cost of energy for nodes 4, 5, 7, 8, and 9 decreases monotonically with storage, decreases monotonically for node 2 except for the case with 2 hours of storage, increases once storage is added to nodes 1 and 3 and then decreases thereafter, and has a rapidly increasing spread in LCOE for node 6 between the baseline case and trading case because that microgrid node has significant excess solar generation. The deficit of generation in nodes 5 and 7 and the abundance of generation in node 6 lead to frequent successful transactions due to larger β_c and β_p values in their valuation curves. As storage increased node 6 actually made a profit, on average, over the entire year. This is not typically permitted in a utility rate structure due to a minimum charge for interconnection fees, but the observed trend in financial savings still holds true when trading is enabled. This is a mutually beneficial interconnection that frequently saved cost for nodes 5 and 7

by avoiding the need to buy power at a higher cost from the grid, and node 6 made a larger profit from selling its excess generation at a higher rate than the wholesale rate. Another interesting artefact is that node 8 had exclusively grid-only transactions when storage was given to all nodes. This is because node 8 had no generation for storage or trading. This lack of generation and storage created a fairly flat valuation curve relative to other consumer agents, and therefore node 8 commonly lost negotiations with its potential trading partners, node 7 and node 9, because those partners were able to complete bargaining sooner with other consumer agents, node 6 and node 1, respectively.

Table 3.5: Average Daily Energy Cost ($/kWh) for 9-Node Network

Node		Hours of Storage 0		1		2		3		4	
		Grid-Only	**With Trading**	**Grid-Only**	**With Trading**	**Grid-Only**	**With Trading**	**Grid-Only**	**With Trading**	**Grid-Only**	**With Trading**
1	Min	0.033	0.025	0.025	0.014	0.020	0.010	0.017	0.006	0.014	0.003
	Max	0.124	0.124	0.124	0.124	0.124	0.124	0.124	0.124	0.124	0.124
	Range	0.091	0.099	0.099	0.110	0.104	0.114	0.107	0.118	0.110	0.121
	Average	0.066	0.066	0.060	0.059	0.055	0.054	0.052	0.052	0.051	0.051
	Savings		**0.5%**		**2.6%**		**1.7%**		**1.0%**		**0.8%**
2	Min	0.021	0.009	0.000	-0.012	-0.010	-0.021	-0.020	-0.031	-0.023	-0.034
	Max	0.114	0.114	0.114	0.114	0.114	0.114	0.114	0.114	0.114	0.114
	Range	0.093	0.105	0.114	0.126	0.124	0.135	0.134	0.145	0.137	0.148
	Average	0.061	0.054	0.044	0.042	0.033	0.031	0.026	0.025	0.022	0.021
	Savings		**11.8%**		**5.7%**		**5.9%**		**5.6%**		**4.3%**
3	Min	0.010	-0.008	-0.012	-0.030	-0.018	-0.030	-0.016	-0.028	-0.016	-0.027
	Max	0.126	0.129	0.126	0.119	0.126	0.119	0.126	0.119	0.126	0.119
	Range	0.115	0.138	0.138	0.149	0.144	0.149	0.142	0.147	0.142	0.146
	Average	0.067	0.068	0.055	0.052	0.053	0.051	0.052	0.051	0.052	0.051
	Savings		**-1.1%**		**5.6%**		**3.4%**		**2.4%**		**1.5%**
4	Min	0.071	0.062	0.059	0.059	0.048	0.048	0.046	0.046	0.046	0.046
	Max	0.122	0.117	0.122	0.122	0.122	0.122	0.122	0.122	0.122	0.122
	Range	0.051	0.055	0.063	0.063	0.074	0.074	0.076	0.076	0.076	0.076
	Average	0.087	0.086	0.086	0.085	0.086	0.086	0.086	0.086	0.086	0.086
	Savings		**1.2%**		**1.0%**		**0.4%**		**0.2%**		**0.1%**
5	Min	0.021	0.019	0.000	0.000	-0.007	-0.007	-0.001	-0.001	0.003	0.003
	Max	0.135	0.125	0.135	0.127	0.135	0.127	0.135	0.127	0.135	0.127
	Range	0.114	0.106	0.135	0.128	0.142	0.134	0.136	0.128	0.132	0.125
	Average	0.073	0.065	0.068	0.062	0.067	0.061	0.066	0.061	0.066	0.062
	Savings		**10.3%**		**9.0%**		**8.2%**		**7.6%**		**7.3%**
6	Min	-0.012	-0.027	-0.027	-0.043	-0.034	-0.049	-0.040	-0.054	-0.048	-0.060
	Max	0.113	0.113	0.113	0.113	0.113	0.113	0.113	0.113	0.113	0.113
	Range	0.124	0.139	0.140	0.156	0.147	0.162	0.153	0.167	0.161	0.173
	Average	0.033	0.023	0.021	0.013	0.012	0.005	0.006	-0.001	0.001	-0.006
	Savings		**28.2%**		**38.7%**		**62.2%**		**124.6%**		**866.2%**
7	Min	0.043	0.027	0.031	0.018	0.023	0.013	0.018	0.016	0.018	0.018
	Max	0.132	0.125	0.132	0.125	0.132	0.125	0.132	0.125	0.132	0.125
	Range	0.088	0.097	0.100	0.107	0.109	0.112	0.113	0.109	0.113	0.107
	Average	0.070	0.067	0.065	0.064	0.064	0.063	0.064	0.063	0.064	0.064
	Savings		**4.8%**		**2.5%**		**1.3%**		**1.0%**		**0.9%**
8	Min	0.120	0.099	0.120	0.119	0.120	0.120	0.120	0.120	0.120	0.120
	Max	0.127	0.126	0.127	0.127	0.127	0.127	0.127	0.127	0.127	0.127
	Range	0.007	0.027	0.007	0.008	0.007	0.007	0.007	0.007	0.007	0.007
	Average	0.123	0.121	0.123	0.123	0.123	0.123	0.123	0.123	0.123	0.123
	Savings		**1.2%**		**0.1%**		**0.0%**		**0.0%**		**0.0%**
9	Min	0.063	0.050	0.037	0.031	0.033	0.033	0.033	0.033	0.033	0.033
	Max	0.124	0.123	0.124	0.124	0.124	0.124	0.124	0.124	0.124	0.124
	Range	0.061	0.073	0.087	0.093	0.091	0.091	0.091	0.091	0.091	0.091
	Average	0.091	0.083	0.082	0.081	0.081	0.081	0.081	0.081	0.081	0.081
	Savings		**8.7%**		**1.5%**		**0.6%**		**0.4%**		**0.3%**
Network	Min	0.055	0.052	0.045	0.044	0.039	0.038	0.035	0.035	0.034	0.034
	Max	0.119	0.119	0.119	0.119	0.119	0.119	0.119	0.119	0.119	0.119
	Range	0.064	0.066	0.074	0.075	0.080	0.081	0.083	0.083	0.085	0.085
	Average	0.077	0.073	0.071	0.068	0.067	0.065	0.065	0.063	0.063	0.061
	Savings		**5.4%**		**4.0%**		**3.5%**		**3.2%**		**3.0%**

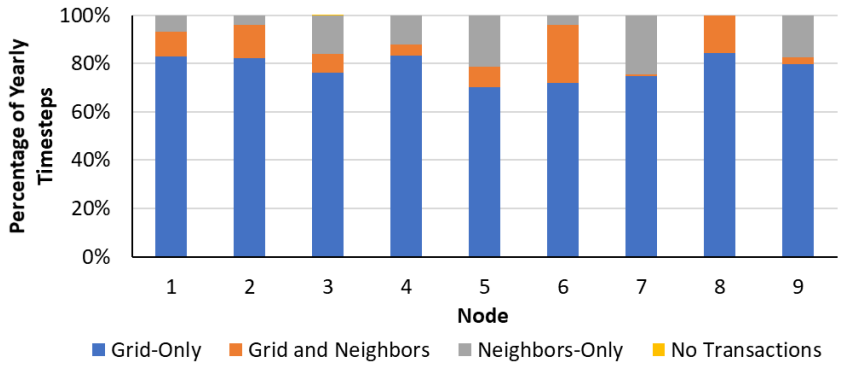

Figure 3.16a: Transaction types by percentage for 9-node network with 0 hours of storage.

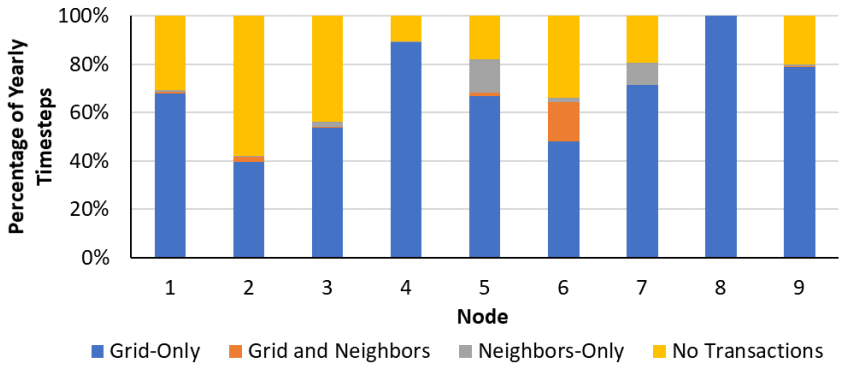

Figure 3.16b: Transaction types by percentage for 9-node network with 4 hours of storage.

The number of total transactions (successful and unsuccessful) decreased as storage was added to the 9-node case, similar to the 3-node case. Fig. 3.17 describes this trend, with 15.8% of transactions between neighbors being unsuccessful with no storage compared to 6.2% with 4 hours of storage. The number of unsuccessful transactions in the 9-node case was nearly constant for 2, 3, and 4 hours of storage, whereas in the 3-node case the number of unsuccessful transactions decreased to almost zero. This behavior emerged in the 9-node network because the number and type of transactions occurring between nodes 5, 6, and 7 remained consistent despite more storage being added to each node.

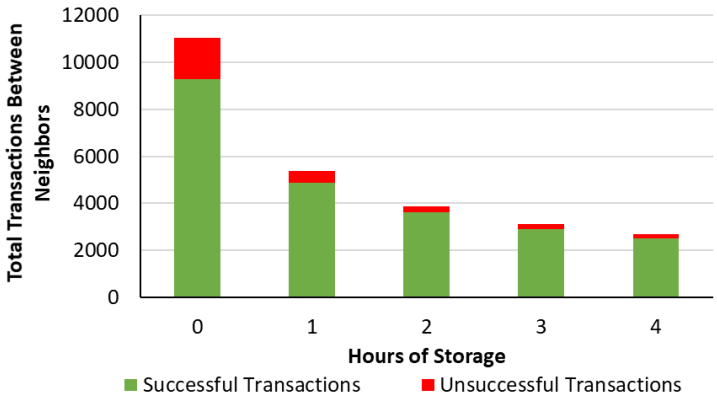

Figure 3.17: Frequency of successful and unsuccessful transactions between neighboring nodes in a 9-node network.

3.5. Conclusion

Agent-based techniques were developed and applied to manage energy transactions between neighboring microgrids in a grid-connected network. The transactive energy approach was developed using a generic mathematical framework and demonstrated for ring networks comprised of 3 nodes and 9 nodes with each node having a unique hourly load and solar profile for a one-year period. Microgrid agents complete three major processes within each simulated time step: (i) determine operational status as a producer, consumer, or neutral node, (ii) form trading groups with other agents, and (iii) bargain with other agents in a trading group. Any excess generation or unmet load was sold to or purchased from the main grid, respectively. Power was purchased according to a time-of-use rate structure with excess generation sold at the wholesale price of electricity. Negotiations between agents were modeled with exponential functions representing each node's unique valuation of energy. Consumers were represented with positive exponential functions that increased in convexity (willingness to buy) based on how much load they could serve with local generation, while producers were represented with negative exponential functions that increased in convexity (willingness to sell) based on how much

power they could sell to each consumer. Negotiations were successful when both agents reached consensus on an offered rate, and unsuccessful when the maximum number of bargaining sessions was reached or a producer traded all power to another node in a trading group.

Results from the transactive energy approach were compared to a baseline case that permitted grid-only transactions. Levelized cost of energy served as the primary metric of comparison. Secondary metrics included the type and frequency of agent transactions as well as the frequency of successful or unsuccessful bargaining attempts. A 3.6% and 5.4% decrease in network levelized cost of energy was observed in the 3-node and 9-node cases, respectively, when trading was enabled. Simulations were also completed with 1, 2, 3 and 4 hours of energy storage at each node sized to meet the peak load. As the amount of storage increased, the difference in levelized cost of energy between the grid-only and microgrid trading cases decreased because microgrids used their stored self-generated power at no cost rather than trading externally. Some adjacent nodes maintained their trading relationship as storage increased, however. This occurred more often within trading groups that included an aggressive producer agent with a high renewables penetration and an aggressive consumer agent(s) with a low load factor. It was found that as more storage was introduced in the network, the number of transactions with the grid and/or neighbors decreased due to nodes serving their loads locally more often. Additionally, the number of unsuccessful transactions decreased as the amount of storage was increased, as shown in the 9-node case with 15.8% unsuccessful transactions with no storage and 6.2% with four hours of storage.

The described case studies were developed with a ring network structure reminiscent of the conventional electric grid. Energy and asset data from real buildings were used to demonstrate real engineering applications. As a growing number of distributed energy resources and microgrids are integrated into the larger grid, transactive energy strategies such as those described in this text have demonstrated potential to manage energy and financial trading in the increasingly complex energy market. Application spaces such as Hawaii's Clean Energy Initiative (2018), California's recent requirement for solar photovoltaic installation on all new residential homes (California Energy Commission 2018), and Arizona's agreement to incentivize behind-the-meter battery systems (Salt River Project 2018) demonstrate direct relevance to markets in the United States, and further application spaces globally are emerging given Germany's Amendment of the Renewable Energy Sources Act that encourages wind resource installation (International Energy Agency 2017), Denmark's goal to reach 50% renewable energy by 2030 (State of Green 2017), and China's effort to increase renewables and curb emissions by 2030 (Climate Nexus 2017).

This work provided a generalized conceptual framework, mathematical expressions, and simulation methodology for use with any network configuration and any size of electrical network. The case study examples on ring networks can be expanded and contrasted with other types of configurations seen in real distribution networks, such as radial, parallel, or tie structures. Further, a more abstract comparison could be made by examining topologies from network theory including wheel and complete graphs. The inclusion of capacity constraints in distribution infrastructure and power flow modeling are planned extensions of this work that permit translation to larger systems. Additional studies

could expand financial and regulatory analyses to consider alternative electric rate agreements such as net metering, wheeling charges (trading charges) between microgrid agents, and demand charges. Research in forecasting and asset scheduling can be complemented by this work and integrated to improve short-term and real-time scheduling and trading as increasing amounts of distributed energy resources are installed on electric grids around the world.

Acknowledgements

This material is based upon work supported by the Office of Naval Research (ONR) Naval Enterprise Partnership Teaming with Universities for National Excellence (NEPTUNE) Program and the National Science Foundation Graduate Research Fellowship under Grant No. 026257-001.

References

Arizona State University Campus Metabolism. (2018). Retrieved from: https://cm.asu.edu/

Arnette, A. (2013). Integrating rooftop solar into a multi-source energy planning optimization model. *Applied Energy*, *111*, 456-467.

Babar, M., Grela, J., Ozadowicz, A. Nguyen, P.H., Hanzelka, Z., & Kamphuis, I.G. (2018). Energy flexometer: Transactive energy-based internet of things technology. *Energies, 11*(3), 568.

Bank, J., Mather, B., Keller, J., & Coddington, M. (2013). High Penetration Photovoltaic Case Study Report. National Renewable Energy Laboratory, Golden, CO. NREL/TP-5500-54742.

Barkholtz, H.M., Fresquez, A., Chalamala, B.R., & Ferreira, S.R. (2017). A Database for Comparative Electrochemical Performance of Commercial 18650-Format Lithium-Ion Cells. *Journal of the Electrochemical Society*, *164*(12), A2697-A2706.

Behboodi, S., Chassin, D.P., Djilali, N., & Crawford, C. (2018). Transactive control of fast-acting demand response based on thermostatic loads in real-time retail electricity markets. *Applied Energy, 210*, 1310-1320.

California Energy Commission. (2018). Energy Commission Adopts Standards Requiring Solar Systems for New Homes, First in Nation. Retrieved from: http://www.energy.ca.gov/releases/2018_releases/2018-05-09_building_standards_adopted_nr.html

Chassin, D., Behboodi, S., Shi, Y., & Djilali, N. (2017). H2 -optimal transactive control of electric power regulation from fast-acting demand response in the presence of high renewables. *Applied Energy*, *205*, 304-315.

Chen, Y. & Hu, M. (2016). Balancing collective and individual interests in transactive energy management of interconnected micro-grid clusters. *Energy*, *109*, 1075-1085.

Climate Nexus. (2017). China's Climate and Energy Policy. Retrieved from: https://climatenexus.org/international/international-cooperation/chinas-climate-and-energy-policy/

Denholm, P., Clark, K., & O'Connell, M. (2016). Emerging Issues and Challenges in Integrating High Levels of Solar into the Electrical Generation and Transmission System. National Renewable Energy Laboratory, Golden, CO. NREL/TP-6A20-65800.

Divshali, P.H., Choi, B.J., & Liang, H. (2017). Multi-agent transactive energy management system considering high levels of renewable energy source and electric vehicles. *IET Generation, Transmission & Distribution*, *11*(15), 3713-3721.

Eber, K. & Corbus, D. (2013). Hawaii Solar Integration Study: Executive Summary. National Renewable Energy Laboratory, Golden, CO. NREL/TP-5500-57215.

Energy Monitor Worldwide; Amman. (2016). Arizona regulators vote to stop net metering for solar. *SyndiGate Media Inc.*

Faratin, P., Sierra, C., & Jennings, N. R. (1998). Negotiation decision functions for autonomous agents. *Robotics and Autonomous Systems*, *24*(3–4), 159–182.

Ghorbani, S., Rahmani, R., & Unland, R. (2017). Multi-agent autonomous decision making in smart micro-grids' energy management: A decentralized approach. Lecture Notes in Computer Science (including Subseries Lecture Notes in Artificial Intelligence and Lecture Notes in Bioinformatics), 10413, 223-237.

Glover, J., Sarma, M., & Overbye, T. (2012). Power system analysis and design (5th ed.). Cengage Learning, Stamford, CT.

Goop, J., Odenberger, M., & Johnsson, F. (2017). The effect of high levels of solar generation on congestion in the European electricity transmission grid. *Applied Energy*, *205*, 1128-1140.

GridWise Architecture Council. (2015). GridWise Transactive Energy Framework Version 1.0. Pacific Northwest National Laboratory, Richland, WA. PNNL-22946 Ver1.0.

Hammerstrom, D. J. (2007). Pacific Northwest GridWise Testbed Demonstration Projects, Part I Olympic Peninsula Project. *Olympic Peninsula Project, National Technical Information Service*, 1–157.

Hawaii Clean Energy Initiative. (2018). Hawaii State Government. Retrieved from: http://www.hawaiicleanenergyinitiative.org/

Herbes, C., Brummer, V., Rognli, J., Blazejewski, S., & Gericke, N. (2017). Responding to policy change: New business models for renewable energy cooperatives – Barriers perceived by cooperatives' members. *Energy Policy*, *109*, 82-95.

Hobbs, B. (1995). Optimization methods for electric utility resource planning. European *Journal of Operational Research*, *83*(1), 1-20.

Holjevac, N., Capuder, T., Zhang, N., Kuzle, I., & Kang, C. (2017). Corrective receding horizon scheduling of flexible distributed multi-energy microgrids. *Applied Energy*, *207*, 176–194.

Holmberg, D., Hardin, D., Cunningham, R., Melton, R., & Widergren, S. (2016). Transactive Energy Application Landscape Scenarios. *Smart Electric Power Alliance*.

Hug, G., Kar, S., & Wu, C. (2015). Consensus + innovations approach for distributed multiagent coordination in a microgrid. *IEEE Transactions on Smart Grid*, *6*(4), 1893-1903.

Institute for Energy Research. (2014). Electricity Transmission.

International Energy Agency. (2017). 2017 Amendment of the Renewable Energy Sources Act (EEG 2017). IEA/IRENA Joint Policies and Measures Database.

Janko, S.A., Arnold, M.R., & Johnson, N.G. (2016). Implications of high-penetration renewables for ratepayers and utilities in the residential solar photovoltaic (PV) market. *Applied Energy*, *180*, 37-51.

Jun, Z., Junfeng, L., Jie, W., & Ngan, H.W. (2011). A multi-agent solution to energy management in hybrid renewable energy generation system. *Renewable Energy*, *36*(5), 1352-1363.

Kar, S. & Hug, G. (2012). Distributed robust economic dispatch in power systems: A consensus + innovations approach. *2012 IEEE Power Energy and Society General Meeting*.

Kar, S., Moura, J.M.F., & Ramanan, K. (2012). Distributed parameter estimation in sensor networks: Nonlinear observation models and imperfect communication. IEEE Transactions on Information Theory, 58(4), 3575–3605.

Khodaei, A. (2015). Provisional microgrids. *IEEE Transactions on Smart Grid*, *6*(3), 1107–1115.

Kirchner, M. (2012). Providing reliable data center backup power. Consulting - Specifying Engineer, N/a.

Lam, R. K. & Yeh, H. G. (2014). PV ramp limiting controls with adaptive smoothing filter through a battery energy storage system. *2014 IEEE Green Energy and Systems Conference*, 55-60.

Leepa, C. & Unfried, M. (2013). Effects of a cut-off in feed-in tariffs on photovoltaic capacity: Evidence from Germany. *Energy Policy*, *56*, 536-542.

LG Chem ESS Battery Division. (n.d.). Introducing Our RESU. Retrieved from: http://www.lgesspartner.com/front/normal/en/main/main.dev

Liu, Z., Wu, Q., Huang, S., & Zhao, H. (2017). Transactive energy: A review of state of the art and implementation. *2017 IEEE Manchester PowerTech, Manchester*.

Logenthiran, T., Srinivasan, D., & Khambadkone, A. M. (2011). Multi-agent system for energy resource scheduling of integrated microgrids in a distributed system. *Electric Power Systems Research*, *81*(1), 138–148.

Luo, X., Wang, J., Dooner, M., & Clarke, J. (2015). Overview of current development in electrical energy storage technologies and the application potential in power system operation. *Applied Energy*, *137*, 511-536.

Lynch, M.A.., Shortt, A., Tol, R.S.J., & Malley, M.J. (2013). Risk–return incentives in liberalised electricity markets. *Energy Economics*, *40*, 598-608.

Martínez Ceseña, E.A., Good, N., Syrri, A.L.A., & Mancarella, P. (2018). Techno-economic and business case assessment of multi-energy microgrids with co-optimization of energy, reserve and reliability services. *Applied Energy*, *210*, 896-913.

McLaren, J., Gagnon, P., Anderson, K., Elgqvist, E., Fu, R., & Remo, T. (2016). Battery Energy Storage Market: Commercial Scale, Lithium-ion Projects in the U.S. National Renewable Energy Laboratory, Golden, CO. NREL/PR-6A20-67235.

Minciardi, R. & Robba, M. (2017). A bilevel approach for the stochastic optimal operation of interconnected microgrids. *IEEE Transactions on Automation Science and Engineering*, *14*(2), 482–493.

Minciardi, R. & Sacile, R. (2012). Optimal control in a cooperative network of smart power grids. *IEEE Systems Journal*, *6*(1), 126–133.

Moayedi, S., & Davoudi, A. (2016). Distributed tertiary control of DC microgrid clusters. *IEEE Transactions on Power Electronics*, *31*(2), 1717–1733.

Mohammadi, A., Mehrtash, M., and Kargarian, A. (2018). Diagonal quadratic approximation for decentralized collaborative TSO+ DSO optimal power flow. *IEEE Transactions on Smart Grid*, *10*(3), 2358-2370.

Naval Facilities Engineering Command. (1990). Electric Power Distribution Systems Operations. NAVFAC MO-201.

Navigant. (2017). Global DER Deployment Forecast Database.

Nikmehr, N., Najafi-Ravadanegh, S., & Khodaei, A. (2017). Probabilistic optimal scheduling of networked microgrids considering time-based demand response programs under uncertainty. *Applied Energy*, *198*, 267–279.

Nunna, H. & Doolla, S. (2012). Demand response in smart distribution system with multiple microgrids. *IEEE Transactions on Smart Grid*, *3*(4), 1641–1649.

OpenEI.org. (2011). NREL RSF Measured Data 2011. Retrieved from: https://openei.org/datasets/dataset/nrel-rsf-measured-data-2011

OpenEI.org. (n.d.). Retrieved from: https://openei.org/datasets/files/961/pub/

osBrain. (n.d.). About osBrain. Retrieved from: https://osbrain.readthedocs.io/en/stable/about.html

Pashajavid, E., Shahnia, F., & Ghosh, A. (2017). Provisional internal and external power exchange to support remote sustainable microgrids in the course of power deficiency. *IET Generation, Transmission & Distribution*, *11*(1), 246–260.

Professional Services Close-up. (2012). Chicago's Rush University Medical Center Leverages GE's Emergency Power System. Business Insights: Global.

Rahmani-Andebili, M. (2017). Scheduling deferrable appliances and energy resources of a smart home applying multi-time scale stochastic model predictive control. *Sustainable Cities and Society*, *32*, 338-347.

Rahmani-Andebili, M. (Apr. 2018). Cooperative Distributed Energy Scheduling in Microgrids. *Electric Distribution Network Management and Control*, 235-254. Springer Nature Singapore.

Rivera, S., Farid, A. M., & Youcef-Toumi, K. (2014). A multi-agent system coordination approach for resilient self-healing operations in multiple microgrids. *Industrial Agents: Emerging Applications of Software Agents in Industry*, 269–285. Elsevier.

Salt River Project. (2018). SRP – Tesla Agreement. Retrieved from: https://www.srpnet.com/newsroom/releases/030718.aspx

Schmietendorf, K., Peinke, J., & Kamps, O. (2017). The impact of turbulent renewable energy production on power grid stability and quality. *The European Physical Journal B*, *90*(11), 1-6.

SciPy.org. (2018). Scientific Computing Tools for Python. Retrieved from: https://www.scipy.org/about.html

Shahnia, F., Bourbour, S., & Ghosh, A. (2017). Coupling Neighboring Microgrids for Overload Management Based on Dynamic Multicriteria Decision-Making. *IEEE Transactions on Smart Grid*, *8*(2), 969–983.

Shen, J., Jiang, C., & Li, B. (2015). Controllable load management approaches in smart grids. *Energies*, *8*(10), 11187-11202.

Silvente, J., Kopanos, G. M., Pistikopoulos, E. N., & Espuña, A. (2015). A rolling horizon optimization framework for the simultaneous energy supply and demand planning in microgrids. *Applied Energy*, *155*, 485–501.

Song, N. O., Lee, J. H., Kim, H. M., Im, Y., & Lee, J. (2015). Optimal energy management of multi-microgrids with sequentially coordinated operations. *Energies*, *8*(8), 8371–8390.

SQLite. (n.d.). About SQLite. Retrieved from: https://www.sqlite.org/about.html

State of Green. (2017). Denmark to be Coal-Free by 2030. Retrieved from: https://stateofgreen.com/en/partners/state-of-green/news/denmark-to-be-coal-free-by-2030/

Tesla. (2018). Powerwall. Retrieved from: https://www.tesla.com/powerwall

Ton, D. & Smith, M. (2012). The U.S. Department of Energy's Microgrid Initiative. *The Electricity Journal*, *25*(8), 84-94.

Umeozor, E. C., & Trifkovic, M. (2016). Operational scheduling of microgrids via parametric programming. *Applied Energy*, *180*, 672–681.

United States Energy Information Administration. (2018). Wholesale Electricity and Natural Gas Market Data.

Winoto, P. (2007). Modified Bargaining Protocols for Automated Negotiation in Open Multi-Agent Systems. University of Saskatchewan, Saskatoon.

Wu, J. & Guan, X. (2013). Coordinated multi-microgrids optimal control algorithm for smart distribution management system. *IEEE Transactions on Smart Grid*, *4*(4), 2174–2181.

Wu, P., Huang, W., Tai, N., & Liang, S. (2018). A novel design of architecture and control for multiple microgrids with hybrid AC/DC connection. *Applied Energy*, *210*, 1002-1016.

Zachel, C. (2013). Generators and transfer switches: Emergency power system solutions. *Consulting-Specifying Engineer*, *50*(8).

Zenginis, I., Vardakas, J.S., Echave, C., Morató, M., Abadal, J., & Verikoukis, C.V. (2017). Cooperation in microgrids through power exchange: An optimal sizing and operation approach. *Applied Energy*, *203*, 972-981.

Zhang, B., Li, Q., Wang, L., & Feng, W. (2018). Robust optimization for energy transactions in multi-microgrids under uncertainty. *Applied Energy*, *217*, 346-360.

CHAPTER 4

REPUTATION-BASED COMPETITIVE PRICING NEGOTIATION AND POWER TRADING FOR GRID-CONNECTED MICROGRID NETWORKS

Abstract

The integration of renewables and microgrids into the modern electric grid has forced financial, technical, and policy change. Control strategies that enable energy trading between microgrids provide more effective use of distributed energy resources. This study presents a decentralized, autonomous control approach to manage energy transactions between neighboring nodes of a grid-connected microgrid network. Agents in the network form relationships, with interactions between agents described by quantifying their reputation using historical knowledge of familiarity, acceptance, and value between nodes. Methods are demonstrated on a network of 9 nodes with varying levels of network connectivity for a simulated year. Results indicate that certain relationships between nodes form that allow some microgrids to receive more reduction in operating cost than others. A baseline case with no trading is used to compare results, with nodes experiencing anywhere from 3% to 71% reduction in LCOE depending on which node pairs were connected in the network. Node pair connections with the most opportunities to trade throughout the year had a significant effect on the amount of excess renewables successfully traded in the network, and network configurations containing those pairs also resulted in the lowest grid load factors.

4.1. Introduction

By the end of 2018, 92 countries, states, and provinces have established renewable energy targets for the electric power sector (Ren21 2019). This rapid growth in renewables

has been met with concerns about the intermittency of natural resources and subsequent effect on resource adequacy and power system stability. Additional control solutions are needed to handle power fluctuations and avoid cycling of large-scale power sources (MITei 2011; Van den Bergh and Delarue 2015). One solution is implementing energy storage and ultracapacitors to counteract variability in renewables and provide reserve capacity (Johnsotone and Haščič 2012; Zerrahn, Schill, and Kemfert 2018; Solomon, Kammen, and Callaway 2014). It has also become increasingly common to combine energy storage and renewable power generation into a microgrid, creating an integrated set of distributed energy resources (DERs) that can meet local loads as an independent controllable entity that can isolate and reconnect to the grid. Microgrids provide additional reliability for powering critical loads and enable flexible operational strategies to accommodate future changes to system architecture. However, business model and regulation strategy uncertainties introduce limitations (Hirsch, Parag, and Guerrero 2018). As microgrid technology and policy develop, generalizable and scalable control strategies are needed to coordinate microgrid operation in conjunction with large-scale grid systems.

Extensive research has been completed in the area of internal microgrid control and coordination of DERs. Techniques including transactive energy (Vaahedi et al. 2017; Akter, Mahmud, and Oo 2016; Ji, Zhang, and Cheng 2018), multi-agent control (Luo et al. 2017; Kantamneni et al. 2015; Eddy, Gooi, and Chen 2015; Li, Q. et al. 2016; Kouluri and Pandey 2011; Aung et al. 2010; Cossentino et al. 2011), game theory (Mei and Kirtley 2018; Sanjari and Gharehpetian 2014; Cintuglu, Martin, and Mohammed 2015; Maknouninejad et al. 2012; Ma et al. 2015; Chen et al. 2017), and model predictive control (Cominesi et al. 2018; Ghanbarian et al. 2017; Noroozi, Trip, and Geiselhart 2018; Zhang

et al. 2017) have shown simulated enhancements for economics, utilization of renewable resources, and reliability.

A natural extension of this early research is in the development of methods to coordinate interactions between multiple neighboring microgrids to meet common objectives. Interactions between microgrids can produce power trading, improved forecasting through information sharing, and increased flexibility and adaption to support changing network needs (Wang and Huang 2016; Akter, Mahmud, and Oo 2017; Shahnia, Bourbour, and Ghosh 2017; Mei et al. 2019). Off-grid microgrid networks can especially benefit from these interactions, since microgrid entities can support neighboring loads to improve network reliability where there is no larger grid or slack bus to draw from. Research in off-grid interacting microgrids has included techniques such as transactive control and pricing schemes to facilitate scheduling based on user participation (Prinsloo, Mammoli, and Dobson 2017), two-level control with support from both local storage and neighboring microgrids (Pashajavid, Shahnia, and Ghosh 2017), agent-based networks with control laws derived from the communication network (Li, Q. et al. 2016), and coalition formation (Hammad, Farraj, and Kundur 2015a; Hammad, Farraj, and Kundur 2015b). Simulation of these techniques were shown to achieve promising results such as improved network stability through overload detection and mitigation, improved pricing via demand-side management, and maintaining operation within voltage and frequency requirements (i.e. IEEE Standard 1547) (Pashajavid, Shahnia, and Ghosh 2017; Prinsloo, Mammoli, and Dobson 2017; Li, Q. et al. 2016). On-grid microgrids can benefit from this type of interaction as well with benefits including lowered cost of energy, better utilization of renewable energy resources, increased resilience, and increased operational flexibility

(Daneshvar, Pesaran, and Mohammadi-ivatloo 2018; Nikmehr, Najafi-Ravadanegh, and Khodaei 2017; Holjevac et al. 2017; Liu, Y. et al. 2018; Akter, Mahmud, and Oo 2017; Qu et al. 2018; Janko and Johnson 2018; Kumrai et al. 2017). Wang et. al. (2018) studied how a bi-level game model for an on-grid multi-microgrid network could be used to regulate voltage, with results showing an improvement in control speed and operating costs. In a paper by Wei et. al. (2014), coalition formation between on-grid microgrids enabled a reduction in average system power loss for each microgrid. This paper seeks to develop a scalable and generalizable approach to microgrid interaction and negotiation for on-grid microgrid applications.

Past research in microgrid interaction and multi-microgrid network control can be categorized as centralized or decentralized computation strategies. Centralized control has produced promising results such as algorithms that determine optimal operation by minimizing multiple objectives (Kumrai et al. 2017; Wang et al. 2018). However, it does not easily scale to include new nodes and communication pathways without significant computational tradeoffs. Chakraborty, Nakamura, and Okabe (2014) demonstrated centralized control techniques applied to microgrid networks. The results described how microgrid coalitions could reduce line losses, but also demonstrated a quadratic increase in average execution time based on the number of microgrids in the system. Decentralized control, where computation and decision-making are localized for each controllable entity, has improved scalability and creates a more robust network with no single point of failure (Prabaharan et al. 2018). Decentralized systems such as those introduced in (Liu, Y. et al. 2018; Wu et al. 2018; Harmouch, Krami, and Hmina 2018) distributed computational requirements across nodes, suggesting that they may be more practical for real-world

applications where hardware limitations are a contributing factor to successful operation. Combinations of centralized and decentralized strategies are also possible. For instance, Esfahani et. al. (2019) demonstrated a multi-level control technique that represented loads, energy storage, and generators as individual agents, with information passed to a local market agent and later to a general market agent that had information from all microgrids and the utility. This hierarchical structure created a three-level market framework for day-ahead, hour-ahead, and real-time markets. The work proposed in this paper utilizes a decentralized algorithm approach to bring computation time to a minimum and achieve better scalability.

Communication and interaction between microgrids are often implemented within a multi-agent framework, where each entity in the network can be represented by an agent or set of agents that interact to accomplish tasks (Pashajavid, Shahnia, and Ghosh 2017; Prinsloo, Mammoli, and Dobson 2017; Li, Q. et al. 2016; Liu Y. et al. 2018; Janko and Johnson 2018; Wang et a. 2018; Harmouch, Krami, and Hmina 2018; Rivera, Farid, and Youcef-Toumi 2014). Borrowing terminology from game theory, agent interaction can be modeled as cooperative or competitive games. Cooperative games involve strategic collaboration between players (or agents) with aligned interests, while competitive games involve agents with opposing interests (Colman 2014). Saad, Han, and Poor (2011) utilized a cooperative strategy for microgrid group formation that yielded up to a 31% reduction in distribution line power losses when compared to traditional power exchange with the grid. A competitive strategy demonstrated by W. Liu et al. (2018) simplified coordination and provided self-healing capabilities for microgrids while maintaining fairness in the network. Microgrids in the proposed work are considered independent power consuming and

producing entities with access to only local information or information provided to them by neighbors. Microgrids only have knowledge about and are concerned with their own objectives, which aligns best with competitive (or non-cooperative) game theory.

Information shared with an agent provides insight on environment status and contributes to the decisions made locally. The amount and order in which information is shared between agents can also change actions taken by each agent as well as the outcome of the overall game. Further research is needed in information sharing and its specific effect on agent behavior and network-wide benefit. However, work in social e-commerce considering similar questions suggests that a dynamic replication model for knowledge sharing can be used to analyze behavioral evolution and network-level behaviors and outcomes (Jiang et al. 2014). Additionally, agents can be capable of learning from previous encounters with other agents and can change their decision-making strategy based on the outcomes of those encounters. By keeping track of historical interactions, agents can form opinions about one another based on trends that affect the way they will interact with that specific agent in the future. Past research in computer science and artificial intelligence has described this as an association coefficient or reputation score (Yu, Van Der Schaar, and Sayed 2015; Haque 2010; Mihailescu, Vasirani, and Ossowski 2011).

Work presented in this paper extends past work (Janko and Johnson 2018) to model microgrid interactions as a competitive game of negotiations between agents to determine energy pricing with each agent seeking to minimize net expenses for themselves. Additionally, a reputation coefficient that considers an agent's familiarity, success rate, and value attributed to other agents is introduced to analyze the behavioral adaptation and changes in network-level outcomes based on environmental and situational parameters.

This technique is outlined and verified with several realistic case studies. Unique contributions of this paper include:

- Generalizable and scalable approach to microgrid price negotiation considering familiarity, acceptance, and value between nodes.
- Modeling multi-agent microgrid power trading as a competitive marketplace in which historical interactions affect the reputation of a node and the strategy taken with that node.
- Case studies demonstrating scalability and performance of the proposed method through network simulations with varying levels of connectivity.

4.2. Methods

4.2.1. Microgrid Node and Network Topology

Each microgrid interacting in the competitive network is modeled as a generic power system consisting of a production asset, storage asset, controller, and load to serve (see Fig. 4.1). Asset capacities and load profiles are varied to produce a heterogeneous set of participants in the network. At the beginning of the simulation, the network is configured in a pre-defined architecture of switches that enables microgrids to electrically connect to one another. Microgrid pairs connected by switches are called neighboring microgrids. Configurations of neighbors can range in complexity from a linear network to a completely connected network (see Fig. 4.2). The number of possible network configurations within an n-node network is $2^{\frac{n(n-1)}{2}}$. Communication and negotiation between nodes are managed within a multi-agent framework where each microgrid is represented as a single agent within the marketplace.

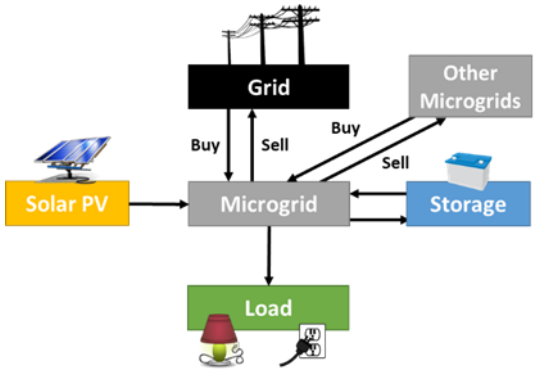

Figure 4.1: Generic microgrid topology.

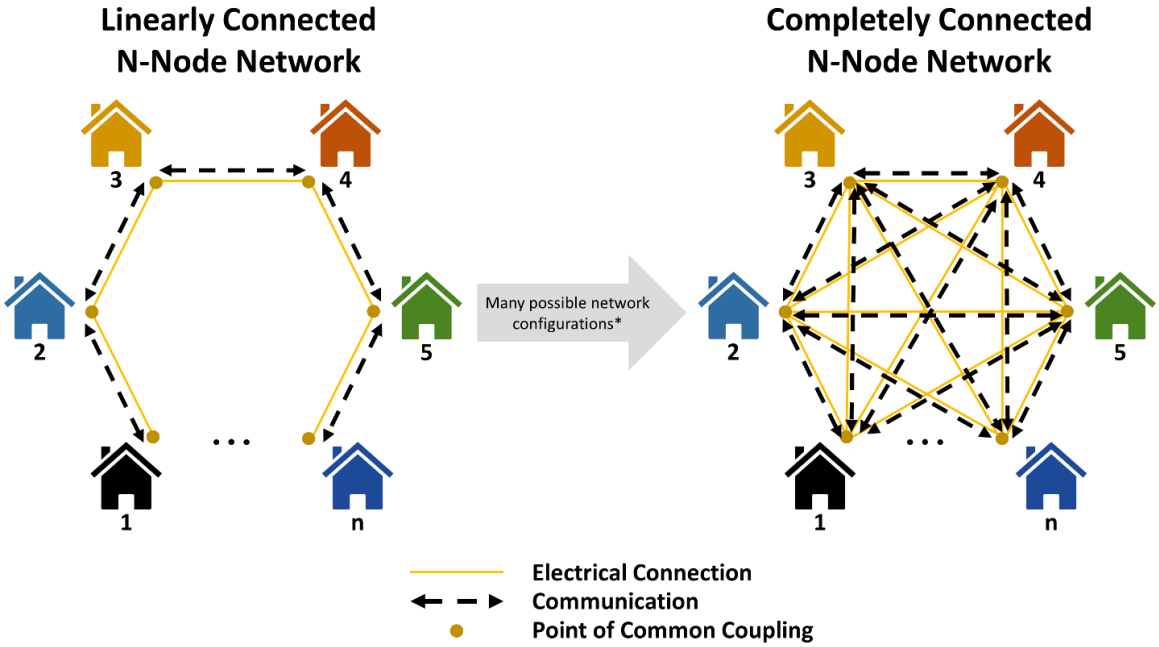

Figure 4.2: Range of network configurations possible for n-node network.

4.2.2. Multi-Microgrid Interactions and Negotiation

Microgrid agents complete several processes within each time step as described in Fig. 4.3. Similar to prior work (Janko and Johnson 2018), each agent first determines its operational status as either a power consumer or a power producer by calculating its net load after considering the local loads, generation, and energy storage. If the net load is zero, the microgrid has a neutral status and its agent does not participate in the power trading marketplace for that time step. Each agent transmits its status to neighbors and determines which of the neighbors is a compatible trading partner for that time step. Consuming agents must trade with producers and producers must trade with consumers. Agents then negotiate the price of power (in $/kWh) with only the compatible neighbors until consensus is reached or the maximum number of negotiation steps is reached. After negotiation, agents complete power trades with neighbors in priority order of most utility to least utility. Any remaining excess generation from producer agents is sold to the grid at the wholesale price of electricity, and any unmet load of consumer agents is purchased from the grid at rates dictated by their utility rate structure. Each process is described in detail within the sections 4.2.3 - 4.2.5.

Simulation of the multi-agent microgrid network and negotiations between agents is managed within a Python script and an accompanying local SQL database for each agent. Input data includes hourly load and solar profiles, storage size, negotiation parameters for each microgrid agent, and a rate structure for transactions with the utility. An incidence matrix defines network structure (agent connections) and allows for easy modification of the electrical and communication architecture. Model parameters and all simulated data are saved in local SQL databases for fast access. Several Python packages were utilized

including osBrain 0.4.4 for multi-agent programming, sqlite 3.22.0 for database management, and PuLP 1.6.0 for optimization (osBrain n.d.; SQLite n.d.; Mitchell et al. 2009).

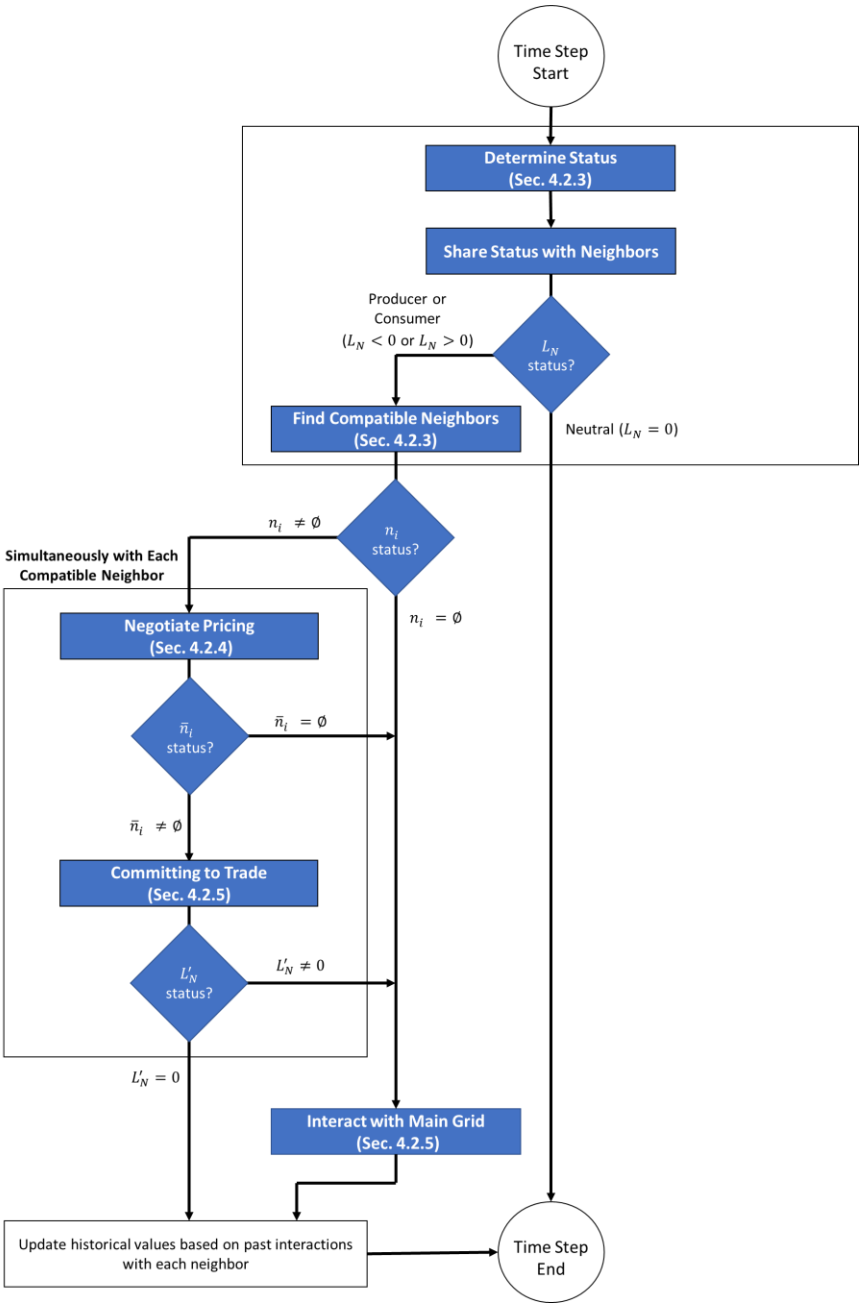

Figure 4.3: Process flow for an agent in one time step.

4.2.3. Status Determination and Finding Compatible Neighbors

An agent can act as a producer (excess generation is available to sell) or a consumer (local load exceeds available local generation) in any time step based on local conditions for loads, production, and storage. This operational status governs which neighbors the microgrid is compatible with for trading. The equation set used to model and determine an agent's status based on its locally available generation and storage can be found in Johnson and Janko (2018).

Following status determination, each agent sends its status to neighboring agents and receives their statuses in turn. A subset n_i of all agents neighboring agent i ($n_i \subseteq N_i$) is identified as compatible trading partners based on their opposing statuses. The agents in n_i and their net loads are saved to the local database for use in pricing negotiation.

4.2.4. Negotiating Pricing

Pricing negotiation is structured as a series of communications between agents with the option to accept, reject, or make a counter offer upon receipt of an offer from another agent. The decision to accept, reject, or counter offer is based on the agent's unique valuation of energy, which is a function of current grid purchase and sellback rates, the relative net load and electrical load of both agents, the maximum number of allowable negotiation steps, and past experience with that agent.

4.2.4.1. Reputation Between Agents

To account for past experiences in modeling negotiation behaviors between agent *i* and another generic agent *j*, this paper uses terminology and equation structure from Haque (2010) in their biologically inspired model of alliance formation between dolphins. The literature expresses amity between dolphins as the sum of coefficients representing the

familiarity of agent *i* with agent *j* and past rejections experienced by agent *i* from agent *j*. This paper formulates similar coefficients as ratios based on past interactions with other microgrid agents and introduces a new parameter, the value coefficient, that expressed the historical value of this relationship compared to main grid interaction. This value is different for a producer versus a consumer. Additionally, the rejection coefficient was modified to become the acceptance coefficient and represents successful trades between agent *i* from agent *j*. Three weight values ($\omega_1, \omega_2, \omega_3$) are applied to enable agents to set unique priorities for the coefficients. Summed together, these coefficients multiplied by their weights become the reputation coefficient $\Gamma_{i,j}(t)$. This indicates agent *i*'s desire to trade with agent *j* (Eq. 4.1).

Eq. 4.2 defines the familiarity coefficient $\phi_{i,j}(t)$ as the ratio of time steps that agent *i* found agent *j* to be a compatible trading partner to the total time steps in the lifetime of agent i. A value of $\phi_{i,j}(t)$ closer to 1 indicates two agents that have spent a larger percentage of their time together in negotiations. The acceptance coefficient $\mu_{i,j}(t)$ is shown in Eq. 4.3 as the ratio of successful negotiations followed by successful committed trades between agent *i* and agent *j* to the total possible negotiations agent *i* could have had with agent *j*. The closer $\mu_{i,j}(t)$ is to 1, the more likely agent *i* believes trading with agent *j* will be successful. The value coefficient $\zeta_{i,j}(t)$ is defined in Eq. 4.4a and 4.4b by comparing the average agreed upon price between agents *i* and *j* to the maximum possible value (Δ) that can be achieved by each agent. Since each agent seeks to find a lower price than interacting with the grid, the maximum value of Δ between two agents is the difference between the grid purchase price and grid sellback price at time *t*. An epsilon ε of 0.0001

$/kWh is the smallest increment in energy price across which transactions are made and thus the grid rates the agent compares value to are adjusted by this amount. A trading fee F is also included to account for the grid access or interconnection fee associated with trading between microgrids.

$$\Gamma_{i,j}(t) = \omega_1 \phi_{i,j}(t) + \omega_2 \mu_{i,j}(t) + \omega_3 \zeta_{i,j}(t) \tag{4.1}$$

Where:

$$0 > \phi_{i,j}(t), \rho_{i,j}(t), \zeta_{i,j}(t), \Gamma_{i,j}(t), \omega_1, \omega_2, \omega_3 \geq 1$$

$$\phi_{i,j}(t) = \frac{|\tau_{i,j}|}{|\tau_{total,i}|} \tag{4.2}$$

$$\mu_{i,j}(t) = \frac{|\tau_{committed,i,j}|}{|\tau_{i,j}|} \tag{4.3}$$

For consumer agent *i* to producer agent *j*:

$$\zeta_{c,i,j}(t) = \frac{1}{|\tau_{successful,i,j}|} \sum_{z}^{|\tau_{successful,i,j}|} \frac{\Delta(z) - (R_{i,j}(z) - (R_{g,sellback}(z) + \varepsilon + F))}{\Delta(z)} \tag{4.4a}$$

For a producer agent *j* to consumer agent *i*:

$$\zeta_{p,j,i}(t) = \frac{1}{|\tau_{successful,j,i}|} \sum_{z}^{|\tau_{successful,j,i}|} \frac{\Delta(z) - ((R_{g,buy}(z) - \epsilon - F) - R_{j,i}(z))}{\Delta(z)} \tag{4.4b}$$

Where:

$$\Delta(z) = (R_{g,buy}(z) - \varepsilon - F) - (R_{g,sellback}(z) + \varepsilon + F)$$

$$z \in \tau_{successful}$$

$$\varepsilon = 0.0001$$

The values of $\Gamma_{i,j}(t)$ and each of its addends are time step dependent and can change value between two agents after each time step is complete. The values of $\phi_{i,j}(t)$ and $\mu_{i,j}(t)$ are always equivalent to each agent in a trading pair, $\phi_{i,j}(t) = \phi_{j,i}(t)$ and $\mu_{i,j}(t) = \mu_{j,i}(t)$, but $\zeta_{i,j}(t)$ will vary. Each coefficient has an initial value of 1 during the first time

step, indicating that the first set of negotiations are not based on historical interactions and all agents are equally interested in trading with each other.

4.2.4.2. Agent Valuation of Energy

Consumer agent valuation is modeled as a time-dependent positive exponential curve (Faratin, Sierra, and Jennings 1998) that is bounded between the purchase price and sellback rate with the grid (Eq. 4.5a). These boundaries ensure pricing between agents is competitive to the grid. Producer agents are modeled with the same boundaries, but with a negative exponential curve (Eq. 4.6a). The exponential relationship between energy valuation and negotiation session of the current time step is expressed through parameter α (Eq. 4.5b and 4.6b). The convexity of the exponential curve is determined by parameter β, which demonstrates trading behaviors based on situational parameters. For consumer agents, β_c is defined as the ratio between the agent's net load during the current time step and its electrical load in that time step (Eq. 4.5c). This creates the behavior that consumer agents are quicker to accept higher energy rates when they can serve less of their own load locally. The consumer is more willing to buy power at a higher cost, as long as it is less than the price of the main grid. For producer agents, β_p is the ratio of maximum amount of power that can be sold to the other agent and the electrical load of the producer in that time step. This demonstrates the behavior that producer agents are quicker to sell energy at lower rates and to consumers that can buy the most power (Eq. 4.6c).

These situational parameters vary between time steps and thus the valuation curves are also dynamic, allowing a single agent to exhibit any range of the behavioral curves described. Valuations at or after the negotiation step in which the two valuation curves cross will be the accepted price of energy between the two agents. The trading fee F is split

between the producer and consumer involved in the trade and is incorporated into the minimum and maximum prices that a consumer or producer will accept in a given time step (Eq. 4.5d, 4.5e, 4.6d, and 4.6e). The effect of $\Gamma_{i,j}(t)$ on energy valuation curves while all other equation parameters are held constant without trading fees is shown in Fig. 4.4a. The inclusion of a nonzero trading fee and its effect on $\Gamma_{i,j}(t)$ is shown in Fig. 4.4b. The negotiation steps *k* shown in these figures occur within one time step *t*.

For consumer agent *i* to producer agent *j*:

$$V_{i\to j}(t,k) = R_{min,i} + \alpha_i(k)\Gamma_{i,j}(t)\left(R_{max,i} - R_{min,i}\right) \tag{4.5a}$$

$$\alpha_i(k) = e^{\left(1-\frac{\min\left(k,\, k_{max,i}\right)}{k_{max,i}}\right)^{\beta_{c,i}} \ln(\lambda_i)} \tag{4.5b}$$

$$\beta_{c,i} = \frac{L_{N,i}}{L_i} \tag{4.5c}$$

$$R_{min,i} = R_{g,sellback} + \varepsilon + F \tag{4.5d}$$

$$R_{max,i} = R_{g,buy} - \varepsilon - F \tag{4.5e}$$

For producer agent *j* to consumer agent *i*:

$$V_{j\to i}(t,k) = R_{max,j} - \alpha_j(k)\Gamma_{j,i}(t)\left(R_{max,j} - R_{min,j}\right) \tag{4.6a}$$

$$\alpha_j(k) = e^{\left(1-\frac{\min\left(k,\, k_{max,j}\right)}{k_{max,\,j}}\right)^{\beta_{p,j}} \ln(\lambda_j)} \tag{4.6b}$$

$$\beta_{p,j} = \frac{\min\left(L_{N,i},\ L_{N,j}\right)}{L_j} \tag{4.6c}$$

$$R_{min,j} = R_{g,sellback} + \varepsilon + F \tag{4.6d}$$

$$R_{max,j} = R_{g,buy} - \varepsilon - \tag{4.6e}$$

Where:

$$0 \leq \alpha(k) \leq 1$$

$$\alpha(k_{max}) = 1$$

$$\alpha(0) = \lambda$$

$$\varepsilon = 0.0001$$

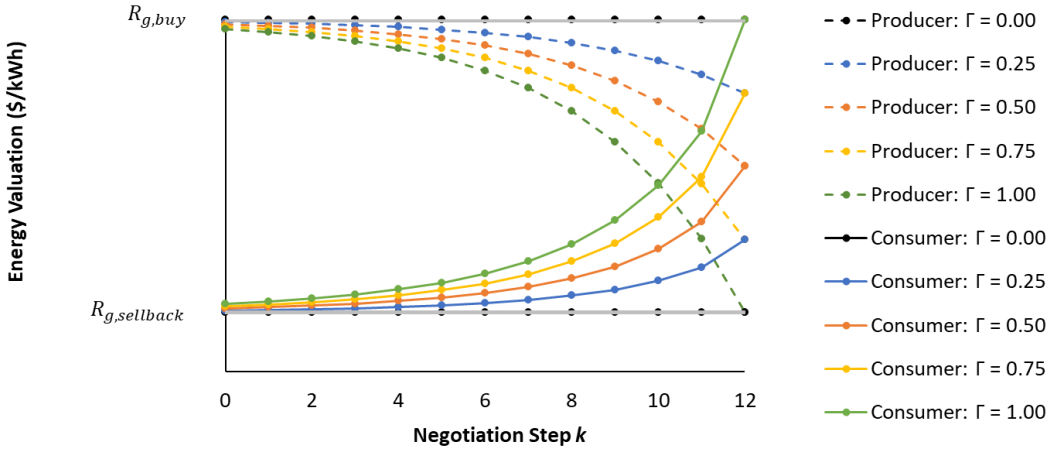

Figure 4.4a: Effect of reputation coefficient on producer and consumer agent valuation curves without trading fee included.

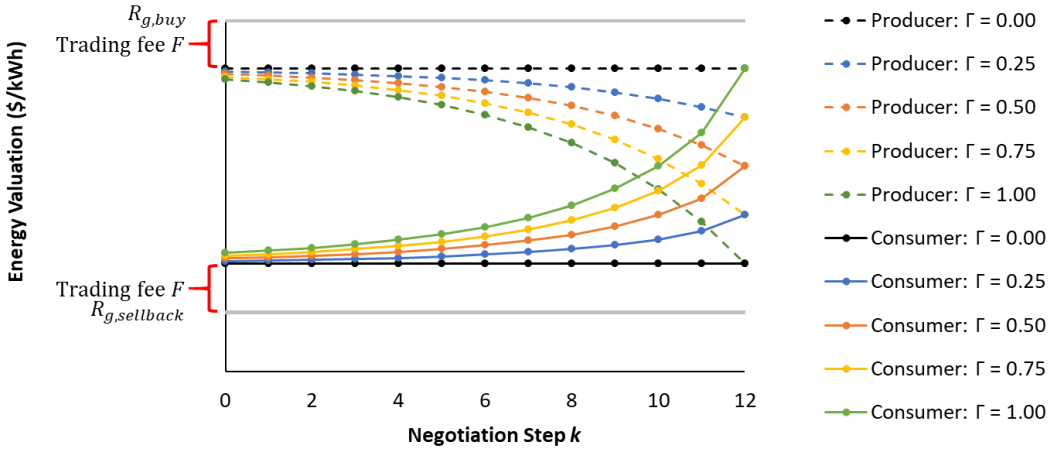

Figure 4.4b: Effect of reputation coefficient on producer and consumer agent valuation curves with trading fee included.

4.2.5. Committing to Trade and Interacting with Main Grid

Agents with successful pricing negotiations accept trading prices with agent *i* creating a subset $\bar{n}_i$ of the compatible agents n_i ($\bar{n}_i \subseteq n_i$). If $\bar{n}_i \neq \emptyset$, the agent then prioritizes its net load to its trading partners in a way that maximizes profit. Initial offers are sent by the trading leaders (either consumers or producers, which can be selected at the beginning of the simulation) and consist of the maximum amount of power that can be offered to each agent. This is calculated as shown in Eq. 4.7 for consumer leaders and Eq. 4.8 for producer leaders as the minimum between the sending agent net load and the receiving agent net load.

For consumer leader agent *i* to producer agent *j*:

$$P_{offer,i,j} = \min\left(L_{N,i}, -L_{N,j}\right) \tag{4.7}$$

For producer leader agent *j* to consumer agent *i*:

$$P_{offer,j,i} = \min\left(-L_{N,j}, L_{N,i}\right) \tag{4.8}$$

Non-leader agents wait until they have received initial offers from each of their compatible partners, then perform an optimization analysis to determine which offers to accept, which to reject, and which to modify. Eq. 4.9a, Eq. 4.9b, and Eq. 4.9c describes the objective function, constraints, and bounds a consumer uses to maximize profit from the offers provided by its compatible agents, and Eq. 4.10a, Eq. 4.10b, and Eq. 4.10c describe the same for a producer. If any results from the optimization function are equivalent to the offered values, the agent commits to the offer and both sending and receiving agents remove that power from the net load they are seeking to meet (Eq. 4.9d and 4.10d). This process repeats until either all agents have a net load of zero or no further trading is

possible. All leftover net load not met after this process is purchased or sold to the grid at the price dictated by the utility rate structure.

For consumer agent *i* to producer agent *j* after initial offer sent:

$$\text{minimize} \quad \sum_{j\in\bar{n}} P_{i,j}R_{accept,i,j} + P_{i,utility}R_{g,buy} \tag{4.9a}$$

$$\sum_{j\in\bar{n}} P_{i,j} + P_{i,utility} = L_{N,i} \tag{4.9b}$$

$$0P_{i,j} \geq \min\left(L'_{N,i}, L_{N,j}\right) \tag{4.9c}$$

$$L'_{N,i} = L_{N,i} - P_{commit,i} \tag{4.9d}$$

For producer agent *j* to consumer agent *i* after initial offer sent:

$$\text{minimize} \quad -\sum_{i\in\bar{n}} P_{j,i}R_{accept,j,i} + P_{j,utility}R_{g,sellback} \tag{4.10a}$$

$$\sum_{i\in\bar{n}} P_{j,i} + P_{j,utility}R_{g,sellback} = -L'_{N,j} \tag{4.10b}$$

$$0 \geq P_{i,j} \geq \min\left(-L'_{N,j}, L_{N,i}\right) \tag{4.10c}$$

$$L'_{N,j} = L_{N,j} + P_{commit,j} \tag{4.10d}$$

Agents that committed power to trade with agent *i* form a subset $\bar{\bar{n}}_i$ of the agents that had successful negotiations with agent i, ($\bar{\bar{n}}_i \subseteq \bar{n}_i$).

4.3. Case Study Data

A 9-node network is used as a case study including a school, three neighborhoods, three commercial buildings, an industrial building, and a hospital. Simulations were completed with hourly load and solar generation data, gathered from existing physical systems or simulated data sources (Janko and Johnson 2018). A summary of these data is provided in Table 4.1.

Table 4.1: 9-Node Network Summary

Parameter	Microgrid Node									
	1	2	3	4	5	6	7	8	9	Network
Average Load (kW)	1109	885	268	310	873	820	209	1156	373	6003
Peak Load (kW)	1577	2637	1852	501	1688	1863	403	1576	1244	10079
Solar Production (kWh/day)	13714	16433	2519	1935	8849	29911	2260	0	2789	78410
Load Factor (-)	0.703	0.336	0.145	0.619	0.517	0.440	0.518	0.734	0.300	0.596
Renewables Fraction (-)	0.515	0.774	0.392	0.260	0.422	1.520	0.451	0.000	0.311	0.544

The effect of network architecture on negotiations and power trading was examined. First, year-long simulations were completed with a fully connected network to determine node-to-node compatibility for trading, quantified by the number of opportunities each connection had for trading throughout the year. Next, connections were ranked by number of compatible time steps. Finally, simulations were run with no connections, and additional simulations were run with an increasing amount of connections that followed increased compatibility until reaching the fully connected network. Each microgrid and the percentage of its yearly time steps spent compatible with each other microgrid is shown in Table 4.2. Selected configurations for simulation are shown in Figure 4.5. All nodes have a grid connection and all connections established between nodes contain a point of common coupling, a disconnect switch, and a communication line. To simplify network diagrams, a single-line was used to represent these components.

Table 4.2: Node Compatibility Percentage Over One Year

Connection \ Node	1	2	3	4	5	6	7	8	9
1		10.8%	14.6%	15.3%	16.2%	14.5%	12.3%	23.3%	14.0%
2	10.8%		20.3%	21.8%	21.2%	8.0%	16.2%	29.9%	15.8%
3	14.6%	20.3%		16.6%	17.4%	20.6%	19.7%	19.3%	21.8%
4	15.3%	21.8%	16.6%		9.9%	29.7%	10.7%	8.2%	13.1%
5	16.2%	21.2%	17.4%	9.9%		27.6%	10.2%	10.2%	13.2%
6	14.5%	8.0%	20.6%	29.7%	27.6%		24.1%	37.8%	23.8%
7	12.3%	16.2%	19.7%	10.7%	10.2%	24.1%		13.7%	4.9%
8	23.3%	29.9%	19.3%	8.2%	10.2%	37.8%	13.7%		14.0%
9	14.0%	15.8%	21.8%	13.1%	13.2%	23.8%	4.9%	14.0%	
Key	0.0%	5.0%	15.0%	20.0%	25.0%	30.0%	35.0%	40.0%	

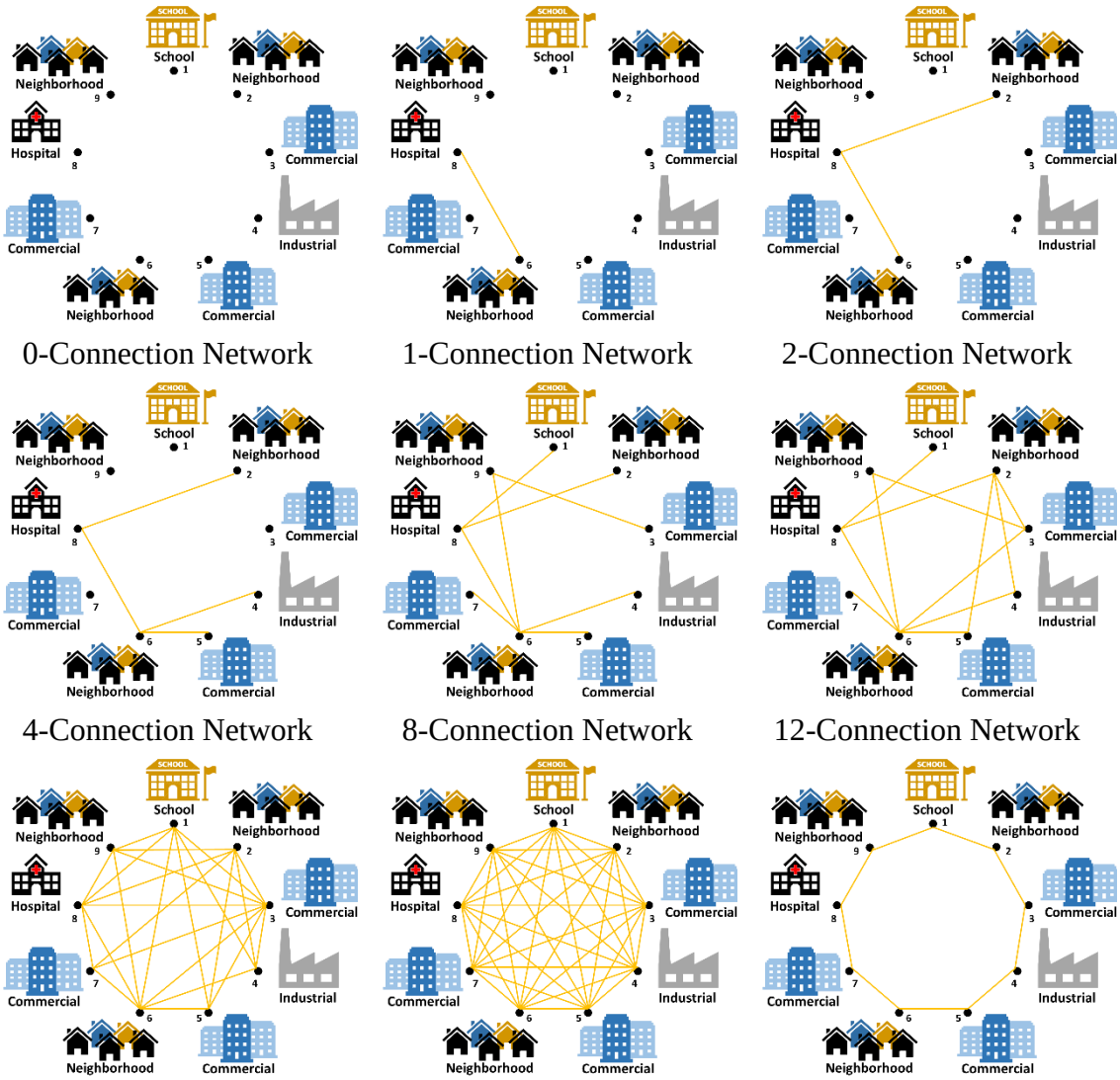

Figure 4.5: Selected network configurations for case studies.

Figure 4.5 shows that the first connection added to the network was between node 8 and node 6 because they had the most compatible time steps throughout the year (37.8%), and the next connection added was between node 8 and node 2 because they had the next-most compatible timesteps (29.9%). This process was continued until all 36 connections were in place. Additionally, a ring network was simulated since it is a standard circuit

configuration in secondary power distribution networks (Naval Facilities Engineering Command 1990).

A time-of-use (TOU) utility rate structure was used for each configuration, as described in Table 4.3. The sellback rate is representative of the wholesale price of electricity to the grid (United States Energy Information Administration 2018), which is a common value to resell power back to the utility when net metering or a higher feed-in tariff s not present. This rate structure was kept consistent to previous work (Janko and Johnson 2018) to permit direct comparison. A trading fee of $0.01/kWh for each participant in a trade was selected for simulation.

Table 4.3: Grid Rate Structure

Price Structure	**Rate ($/kWh)**
Off-peak	0.09
On-peak (1PM-8PM daily)	0.18
Sellback Rate	0.03

4.4. Metrics

Levelized cost of energy (LCOE) for each node and the entire network was used as a comparison metric. The annual LCOE was evaluated over all 8760 hours in the year as described in Eq. 4.11. The network LCOE was calculated as the average cost of all power transactions on the network for the year.

$$LCOE = \frac{\sum_{t=1}^{t=8760} C_n}{\sum_{t=1}^{t=8760} L_n} \tag{4.11}$$

Trading results for each node in each time step were categorized as Utility Only, Nodes Only, and Utility and Nodes. If a node purchased or sold power exclusively to the utility or other nodes, they were counted as Utility Only or Nodes Only time steps, respectively. If a node had to interact with the main grid at the end of a time step after

purchasing or selling to other nodes, that was counted as a Utility and Nodes time step. Time steps in which the amount of production equaled the amount of load were categorized as Self-sufficient, though this was a rare occurrence and not reflected in the results.

At the network level, the grid load factor was utilized to determine the effect of network trading on the utility. This was calculated as a ratio of the average load supplied by the grid over the year (kW) to the peak load of the year (kW). The amount of renewables traded to other nodes instead of sold to the grid was also evaluated to understand differences in local use of renewable generation across the network configurations examined. Relationships between nodes are further described utilizing the reputation coefficient.

4.5. Results

The 0-Connection network shown in Figure 4.5 was simulated and used as a baseline to compare to the other cases where trading was enabled between various nodes. An analysis was conducted on each of the networks described in Figure 4.5 with evenly weighted familiarity, acceptance, and value coefficients to obtain generalized observations about nodal behavior.

A high-level overview of how excess production was sold over the simulated year in each network configuration case is shown in Figure 4.6. Though the 12-Connection network had a slightly higher percentage of renewables sold to other nodes than any other case, the difference between the non-ring connection cases were within ± 10% of each another. This suggests that after the first connection was placed between two highly compatible nodes (nodes 6 and 8), increasing connections within the network had little effect on how much production remained within the network. This finding is further

supported by comparing the Ring and 8-Connection networks. Though they both had 8 total connections, the Ring network did not contain as many highly compatible node parings and ended up with less than half the percentage of renewables sold to nodes when compared to the 8-Connection network.

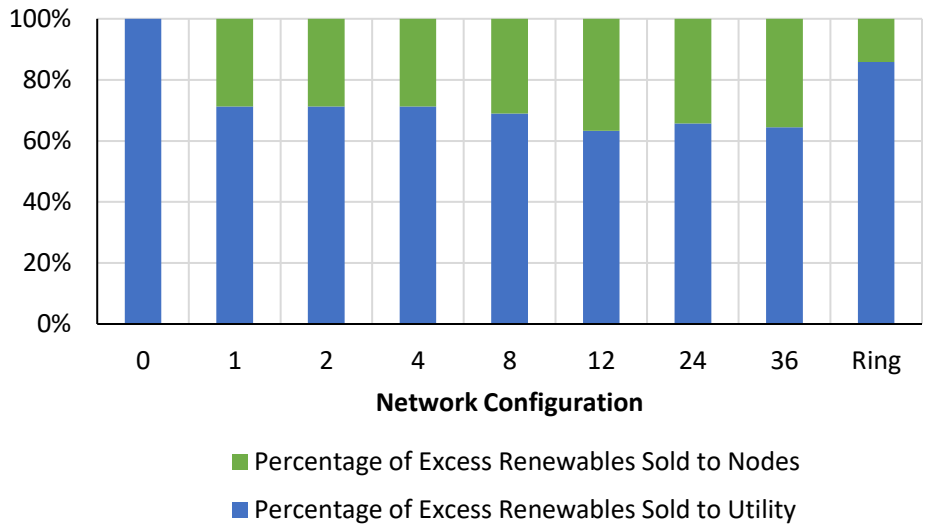

Figure 4.6: Percentage of excess renewables sold to nodes and the utility over the year for each network configuration.

Figure 4.7 displays the grid load factor decreasing as the number of connections increased. Network configurations with the lowest grid load factors correlate with configurations having a higher number of successful trades between nodes. This is logical since more trades completed between nodes means less load must be taken care of by the grid in any given time step. This reduces the average load supplied by the grid.

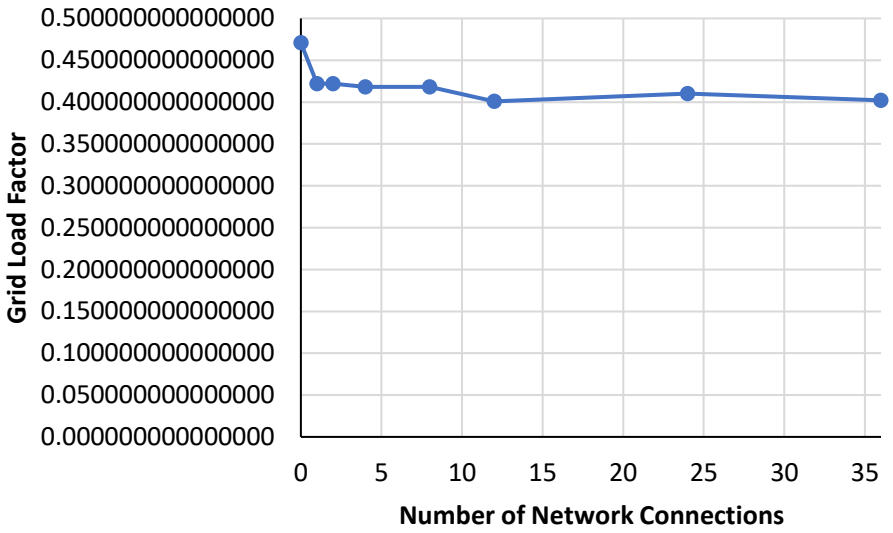

Figure 4.7: Grid load factor as connections are added to the network.

A summary of the LCOE for each node and the network is shown in Figure 4.8 for the 1, 2, 4, 8, 12, 24, and 36 connection cases. All network configurations resulted in a lower LCOE for the network compared to the 0-Connection network. Generally, the LCOE remained steady for nodes and the network as the number of connections was increased from 8 to 36. As nodes were added to the network in decreasing order of compatibility, nodes tended to stick with the same trading partner due to their familiarity coefficient being higher, and hence, the reputation coefficient was also higher between those nodes. This creates network behavior that shows only modest reduction in LCOE as connectivity is increased because the same trades were made between the same nodes even as additional nodes are added. There is no single configuration maximizing economic benefit for all nodes, though the network LCOE was minimized in the 12-Connection network due to this being the configuration with the most successful transactions between nodes overall. However, the network LCOE of all cases with at least one connection were within ± 4% of one another, a negligible difference for the network.

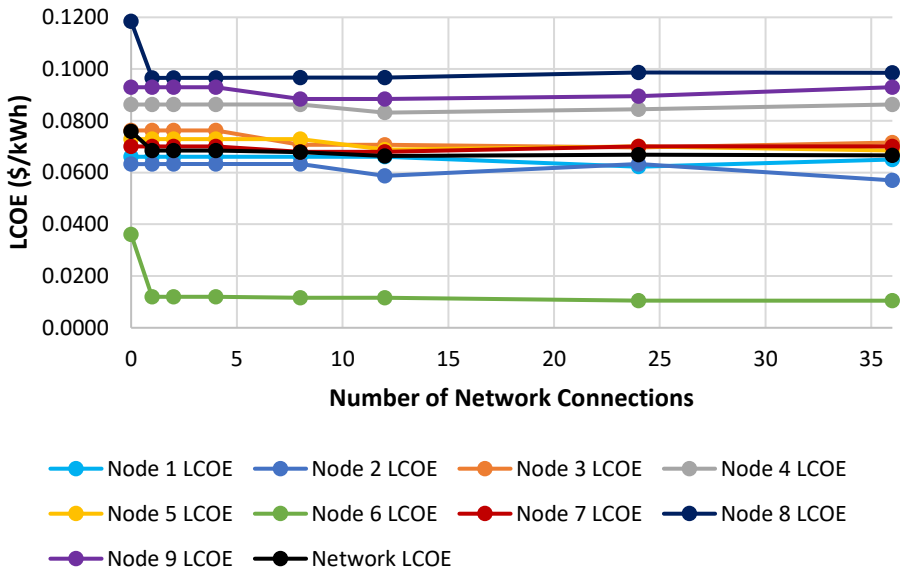

Figure 4.8: Node and network LCOE as connections are added to the network.

An interesting behavior can be observed between the 0-, 1-, and 2-Connection networks for nodes 6, 2 and 8 as their connections were added. As mentioned previously, node 8 is an important player in the network, and when the connection between 6 and 8 was first introduced the benefits of the relationship were immediately apparent. The LCOE for node 8 decreased by 18% and node 6 by 67% when compared to the 0-Connection network. When node 2 is introduced in the 2-Connection case, node 8 has an additional option for purchasing power and node 6 has a direct competitor though is unaware of it. Due to the convexity of the valuation curves, this first interaction between nodes 2, 6, and 8 resulted in node 6 providing the lowest price. When power trade offers are sent by node 6 and node 2 at these prices, node 8 selects node 6 and forms a relationship with that node that continues for the rest of the simulation. No trades are completed between node 8 and node 2 in any other network configuration due to the very strong reputation node 6 holds with node 8.

Competition has a significant effect on benefit experienced by each node in each configuration. This is illustrated by Figure 4.9 that shows a detailed view of the number of time steps each node spent in each trading type for a select number of cases. Node 7 was able to successfully trade in the 8-Connection network where it was connected to node 6. Though node 6 still prioritized trades with node 8, it had sufficient capacity to trade with two nodes and thus maintained a relationship with both. This was also true for the 12-Connection network. However, when node 6 was connected to node 1 in the 24-Connection network, it began to choose node 1 over node 7. Node 7 was not able to compete with other options available to node 6, and its new connections to nodes 8, 2, and 3 were also ineffective. This resulted in node 7 being able to successfully trade in only a handful of time steps. Similar situations can be seen for other nodes such as node 4. Node 4 was unable to be competitive to trade with node 6 in the 8-Connection network, but was able to be competitive with node 2 when they were connected in the 12-Connection network. This continued in the 24-Connection network, but when node 2 was connected to node 1 in the 36-Connection network, node 4 was unable to compete.

Comparing the transaction types for the 8-Connection network and Ring network in Figure 4.9 also shows that although the number of connections were the same the benefit achieved by each node was significantly different. This was due to the lack of connection to preferred partners with high compatibility for some nodes in the Ring network, particularly those that are surrounding node 6 and node 2. This was particularly beneficial for nodes 5 and 7 who were able to be competitive when node 6 had less options of trading partners than the 8-Connection network case. Node 4 experienced no difference due to its location in the network. It had few opportunities to trade with nodes 3 and 5 due to low

compatibility, and when it did attempt to trade it was not competitive compared to nodes 2 and 6 on the opposite sides of nodes 3 and 5. Node 9 experienced some disadvantages in the Ring network due to not being connected to node 6 and node 3 as it was in the 8-Connection network where it traded successfully.

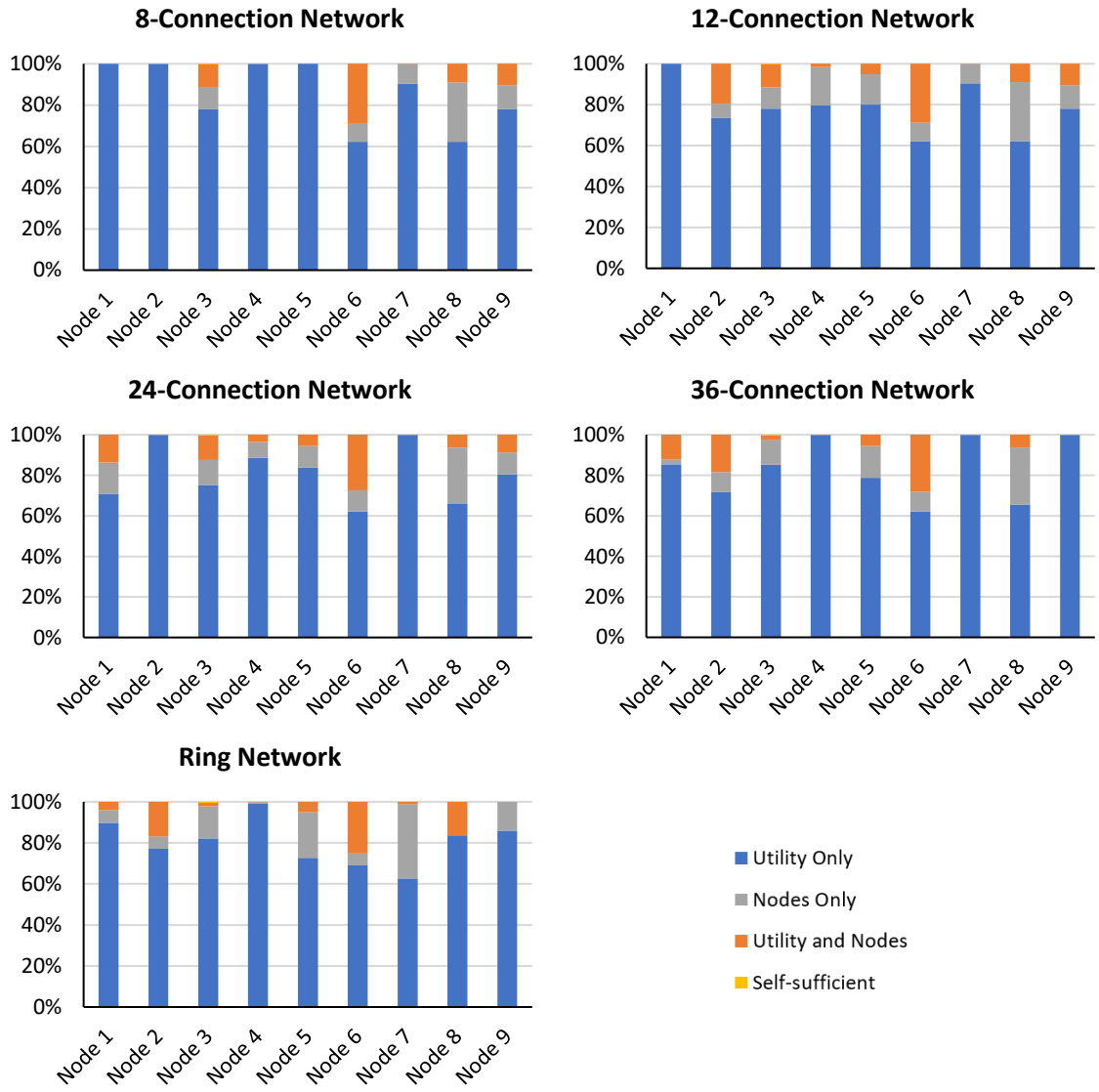

Figure 4.9: Transaction types by percentage of yearly time steps across network connectivity cases.

A detailed view of the relationships between nodes in relation to the reputation coefficient is shown in Figure 4.10. The average reputation coefficient from each node to

each other node in the specified network configuration is shown by the length of the line-dot segments. By referencing Figures 4.4a and 4.4b, it can be seen that reputation coefficients below 0.25 have a low likelihood of valuation curves crossing and result in unsuccessful price negotiation with no possible trade. There are some situations when a node will continue to have a moderate reputation coefficient for another node even if no transactions are made. An example of this is node 7 in the 36-Connection network, which holds a reputation of 0.43 for node 6 and 0.45 for node 3. Node 6 and Node 3 also had relatively favorable reputation coefficients for node 7 at 0.41 and 0.45 respectively. However, both node 6 and node 3 had other prospects with higher reputation coefficients that made them more competitive.

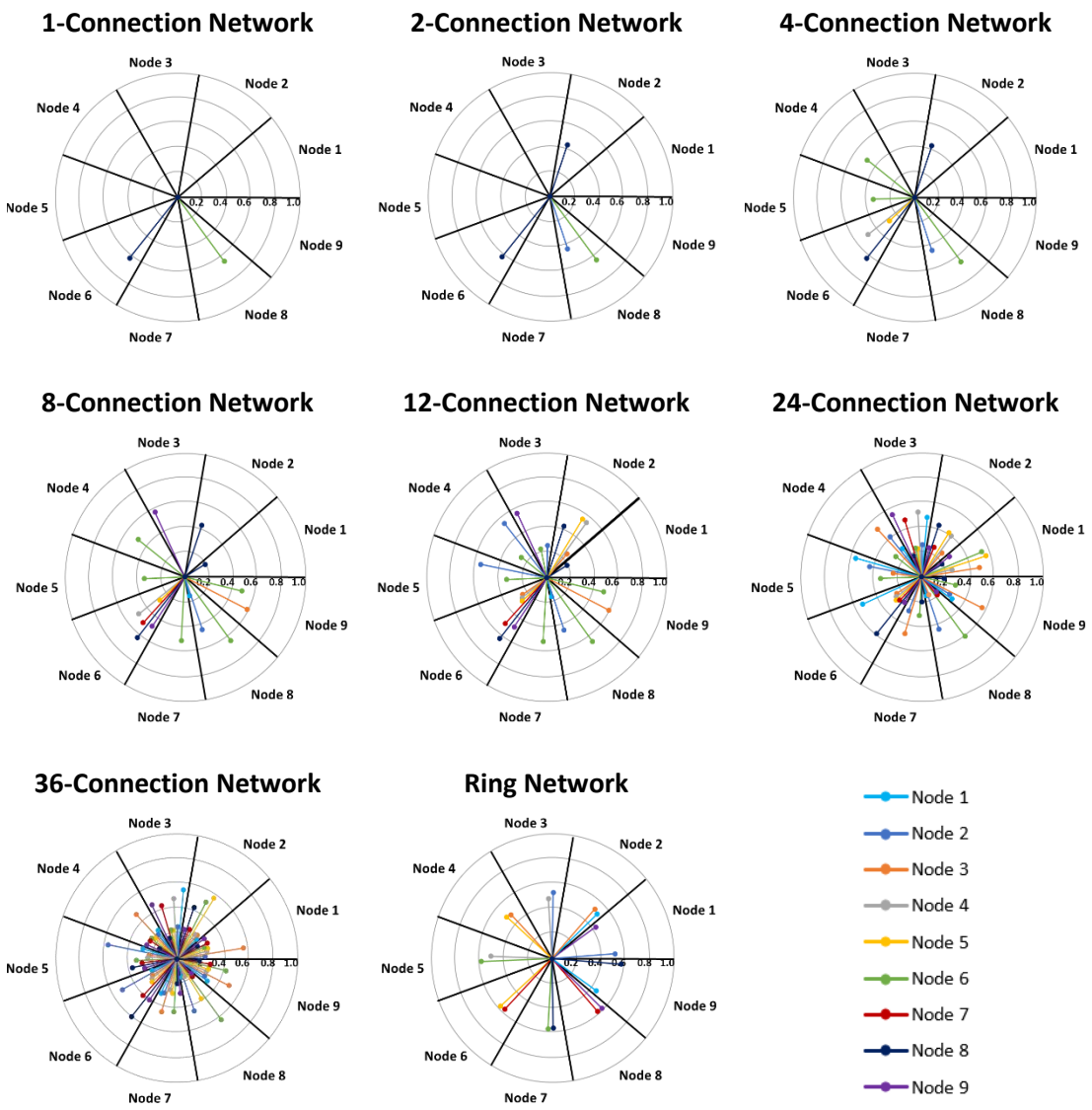

Figure 4.10: Reputation coefficient for each node pair.

Table 4.4 provides a comparison of revenue loss for the utility from trading for each scenario and the required trading fee to recover the full amount. Approximately 22-29% of total annual utility revenue was lost from allowing neighboring microgrids to trade. In several scenarios the trading fee needed to recover that lost revenue exceeded the difference between the grid buy and sell prices making the valuation curves impossible to evaluate. It is also important to note that the highest trading fees needed to recover lost revenue

correlate with the scenarios with the lowest number of successful trades (Ring connection). This is due to the utility needing a larger portion of each trade to recover its revenue when there were less trades made.

Table 4.4: Utility Revenue and Trading Fee Needed to Recover Lost Revenue

Scenario	**Utility Revenue**	**Lost Revenue [% Relative to 0-Connection]**	**Trading Fee Value to Recover Lost Revenue**
0-Connection	$4,890,130	-	-
1-Connection	$3,600,192	$1,289,938 (26.38%)	0.1650
2-Connection	$3,600,175	$1,289,955 (26.38%)	0.1650
4-Connection	$3,600,127	$1,290,003 (26.38%)	0.1650
8-Connection	$3,566,503	$1,323,627 (27.07%)	0.1571
12-Connection	$3,492,385	$1,397,745 (28.58%)	0.1403
24-Connection	$3,520,301	$1,369,829 (28.01%)	0.1470
36-Connection	$3,505,033	$1,385,097 (28.32%)	0.1434
Ring	$3,801,585	$1,088,545 (22.26%)	0.2825

4.6. Conclusion

This chapter outlined a generalizable and scalable approach to manage energy transactions between neighboring nodes of a grid-connected network of microgrids by quantifying familiarity, acceptance, and value between nodes. These characteristics were integrated through several coefficients that altered the convexity of valuation curves observed by each node. Larger coefficients indicated an increased willingness to trade, whereas lower coefficients resulted in less willingness and often resulted in unsuccessful trades. Considered together in a single formulation, these concepts effectively described the reputation between nodes.

The generic mathematical framework was demonstrated on a network of 9 nodes configured with varying levels of connectivity (trading capability). The effects of network

connectivity on nodal trading behavior and economic benefit were analyzed through annual simulations. Configurations that included node pairs with high compatibility (based on number of time steps where they matched to trade) resulted in a larger amount of excess renewables sold between nodes when compared to configurations without. Configurations with the largest number of successful trades between nodes also resulted in the lowest grid load factors due to reduced average load served by the grid. No single network configuration resulted in maximizing economic benefit for all nodes, but the lowest network-level LCOE was achieved in the configuration with the largest number of successful transactions.

Relationships between nodes were structured based on their compatibility and if the network contained connections that created competition between nodes. Since no node had knowledge its trading partners' other connections, each series of negotiations was conducted independently without direct influence of competing entities. The lack of global knowledge of negotiations resulted in some network configurations where a node had few successful trades and the ones that were successful had little value. This resulted in a lower reputation coefficient and an inability to compete with other nodes later in the simulation.

The utility experienced a loss of 22-29% of its revenue when trading was enabled depending on the number of connections in the network. If a trading fee was included for the energy traded ($/kWh), the fee would need to be $0.14/kWh – $0.28/kWh for the utility to recover lost revenue. This almost always exceeds the difference between the grid purchase and grid sell rates, and therefore imposing such a fee would making trading too expensive. This suggests that recovering the full retail value of each kWh not sold will hinder competition and increase network-level LCOE. A utility could instead seek to

recover a smaller value than full retail, such as the costs associated to using the distribution network for trading. The true cost of trading could become more detailed and accurate if considering locational marginal pricing, transmission and distribution losses, or congestion charges. It was also found that the utility needed a larger portion of each trade to recover its revenue when there were less trades made. This suggests that permitting even more trading and competition would decrease the amount of revenue sharing with the utility per trade.

This work built on previous work to include abstract comparison between network topologies. Additional work can explore the effect of coefficients weights on agent behaviors and network-level outcomes. This may also suggest that coefficient weights be adjusted over time to allow nodes to update their strategies to become more competitive and adapt as their net load profiles change shape over a year. Research in differing rate structures between node types (residential, commercial, industrial) would also be beneficial to provide insight into nodal compatibility when the nodes have heterogeneous economic goals.

References

Akter, M. N., Mahmud, M. A., & Oo, A. M. T. (2016). A hierarchical transactive energy management system for energy sharing in residential microgrids. In *IEEE Power and Energy Society General Meeting*, 1–5.

Akter, M. N., Mahmud, M. A., & Oo, A. M. T. (2017). A hierarchical transactive energy management system for energy sharing in residential microgrids. *Energies*, *10*(12).

Aung, H. N., Khambadkone, A. M., Srinivasan, D., & Logenthiran, T. (2010). Agent-based intelligent control for real-time operation of a microgrid. *2010 Joint International Conference on Power Electronics, Drives and Energy Systems, PEDES 2010 and 2010 Power India*.

Chakraborty, S., Nakamura, S., & Okabe, T. (2014). Scalable and optimal coalition formation of microgrids in a distribution system. *IEEE PES Innovative Smart Grid Technologies Conference Europe*, 1–6.

Chen, D., Yanhui, X., Dan, S., Yifeng, O., Yu, Z. & Qiangqiang, W. (2017). Chinese Patent No. CN 107844055. Retrieved from https://worldwide.espacenet.com/publicationDetails/biblio?FT=D&date=20180327&DB=EPODOC&locale=&CC=CN&NR=107844055A

Cintuglu, M. H., Martin, H., & Mohammed, O. A. (2015). Real-time implementation of multiagent-based game theory reverse auction model for microgrid market operation. *IEEE Transactions on Smart Grid*, *6*(2), 1064–1072.

Colman, A. (2014). *Game Theory and Experimental Games The Study of Strategic Interaction*. International Series in Experimental Social Psychology. Burlington: Elsevier Science.

Cominesi, S. R., Farina, M., Giulioni, L., Picasso, B., & Scattolini, R. (2018). A Two-Layer Stochastic Model Predictive Control Scheme for Microgrids. *IEEE Transactions on Control Systems Technology*, *26*(1), 1–13.

Cossentino, M., Lodato, C., Lopez, S., Pucci, M., Vitale, G., & Cirrincione, M. (2011). A multi-agent architecture for simulating and managing microgrids. *Proceedings of the Federated Conference on Computer Science and Information Systems*, 619–622.

Daneshvar, M., Pesaran, M., & Mohammadi-ivatloo, B. (2018). Transactive energy integration in future smart rural network electrification. *Journal of Cleaner Production*, *190*, 645–654.

Eddy, Y. S. F., Gooi, H. B., & Chen, S. X. (2015). Multi-agent system for distributed management of microgrids. *IEEE Transactions on Power Systems*, *30*(1), 24–34.

Esfahani, M. M., Hariri, A., Member, S., & Mohammed, O. A. (2019). A Multiagent-Based Game-Theoretic and Optimization Approach for Market Operation of Multimicrogrid Systems. *IEEE Transactions on Industrial Informatics*, *15*(1), 280–292.

Faratin, P., Sierra, C., & Jennings, N. R. (1998). Negotiation decision functions for autonomous agents. *Robotics and Autonomous Systems*, *24*(3–4), 159–182.

Ghanbarian, M. M., Nayeripour, M., Rajaei, A. H., Jamshidi, F., & Waffenschmidt, E. (2017). Model predictive control of distributed generation micro-grids in island and grid connected operation under balanced and unbalanced conditions. *Journal of Renewable and Sustainable Energy*, *9*(4).

Hammad, E. M., Farraj, A. K., & Kundur, D. (2015a). Grid-independent cooperative microgrid networks with high renewable penetration. *2015 IEEE Power and Energy Society Innovative Smart Grid Technologies Conference, ISGT 2015*, 0–4.

Hammad, E., Farraj, A., & Kundur, D. (2015b). Cooperative Microgrid Networks for Remote and Rural Areas. *Canadian Conference on Electrical and Computer Engineering*, 1572–1577.

Haque, M. A. (2010). *Biologically Inspired Heterogeneous Multi-Agent Systems*. Georgia Institute of Technology, Atlanta, GA.

Harmouch, F. Z., Krami, N., & Hmina, N. (2018). A multiagent based decentralized energy management system for power exchange minimization in microgrid cluster. *Sustainable Cities and Society*, *40*, 416–427.

Harmouch, F. Z., Krami, N., & Hmina, N. (2018). A multiagent based decentralized energy management system for power exchange minimization in microgrid cluster. *Sustainable Cities and Society*, *40*, 416–427.

Hirsch, A., Parag, Y., & Guerrero, J. (2018). Microgrids: A review of technologies, key drivers, and outstanding issues. *Renewable and Sustainable Energy Reviews*, *90*, 402–411.

Holjevac, N., Capuder, T., Zhang, N., Kuzle, I., & Kang, C. (2017). Corrective receding horizon scheduling of flexible distributed multi-energy microgrids. *Applied Energy*, *207*, 176–194.

Janko, S. A., & Johnson, N. G. (2018). Scalable multi-agent microgrid negotiations for a transactive energy market. *Applied Energy*, *229*, 715–727.

Ji, M., Zhang, P., & Cheng, Y. (2018). Distributed microgrid energy optimization using transactive control and heuristic strategy. *IEEE Power and Energy Society General Meeting*, 1–5.

Jiang, G., Ma, F., Shang, J., & Chau, P. Y. K. (2014). Evolution of knowledge sharing behavior in social commerce: An agent-based computational approach. *Information Sciences*, *278*, 250–266.

Johnstone, N., & I. Haščič. (2012). Increasing the penetration of intermittent renewable energy: Innovation in energy storage and grid management In *Energy and Climate Policy: Bending the Technological Trajectory*, OECD Publishing, Paris.

Kantamneni, A., Brown, L. E., Parker, G., & Weaver, W. W. (2015). Survey of multi-agent systems for microgrid control. *Engineering Applications of Artificial Intelligence*, *45*, 192–203.

Kouluri, M. K., & Pandey, R. K. (2011). Intelligent Agent Based Micro grid Control. *2011 2nd International Conference on Intelligent Agent and Multi-Agent Systems (IAMA)*, 62–66.

Kumrai, T., Ota, K., Dong, M., Sato, K., & Kishigami, J. (2017). Optimising operation management for multi-micro-grids control. *IET Cyber-Physical Systems: Theory & Applications*, *3*(1), 24–33.

Li, Q., Chen, F., Chen, M., Guerrero, J. M., & Abbott, D. (2016). Agent-Based Decentralized Control Method for Islanded Microgrids. *IEEE Transactions on Smart Grid*, *7*(2), 637–649.

Li, Q., Chen, F., Chen, M., Guerrero, J. M., & Abbott, D. (2016). Agent-Based Decentralized Control Method for Islanded Microgrids. *IEEE Transactions on Smart Grid*, *7*(2), 637–649.

Liu, W., Gu, W., Wang, J., Yu, W., & Xi, X. (2018). Game theoretic non-cooperative distributed coordination control for multi-microgrids. *IEEE Transactions on Smart Grid*, *9*(6), 6986–6997.

Liu, Y., Zuo, K., Liu, X. (Amy), Liu, J., & Kennedy, J. M. (2018). Dynamic pricing for decentralized energy trading in micro-grids. *Applied Energy*, *228*, 689–699.

Luo, F., Chen, Y., Xu, Z., Liang, G., Zheng, Y., & Qiu, J. (2017). Multiagent-Based Cooperative Control Framework for Microgrids' Energy Imbalance. *IEEE Transactions on Industrial Informatics*, *13*(3), 1046–1056.

Ma, J., Li, P., Lin, X., Zhu, W., & Yuan, X. (2015). Game theory method for multi-objective optimizing operation in microgrid. *IEEE 12th International Conference on Networking, Sensing and Control*, 421–425.

Maknouninejad, A., Lin, W., Harno, H. G., Qu, Z., & Simaan, M. A. (2012). Cooperative control for self-organizing microgrids and game strategies for optimal dispatch of distributed renewable generations. *Energy Systems*, *3*(1), 23–60.

Mei, J., & Kirtley, J. L. (2018). A Non-Cooperative Game Theory Based Controller Tuning Method for Microgrid DC-DC Converters. *IEEE Power and Energy Society General Meeting*, 1–5.

Mei, J., Chen, C., Wang, J., & Kirtley, J. L. (2019). Coalitional game theory based local power exchange algorithm for networked microgrids. *Applied Energy*, *239*, 133–141.

Mihailescu, R., Vasirani, M., & Ossowski, S. (2011). Dynamic Coalition Adaptation for Efficient Agent-Based Virtual Power Plants In R. Goebel, Y. Tanaka, & W. Wahlster (Eds.), *Lecture Notes in Artificial Intelligence 6973 Subseries of Lecture Notes in Computer Science (pp. 101-112).* Berlin Heidelberg: Springer.

Mitchell, S., Kean, A., Mason, A, O'Sullivan, M., & Phillips, A. PuLP 1.6.0 documentation. Retrieved from: https://pythonhosted.org/PuLP/

MITei. (2011). *Managing Large-Scale Penetration of Intermittent Renewables.* Retrieved from: https://energy.mit.edu/wp-content/uploads/2012/03/MITEI-RP-2011-001.pdf

Naval Facilities Engineering Command. (1990). Electric Power Distribution Systems Operations. NAVFAC MO-201.

Nikmehr, N., Najafi-Ravadanegh, S., & Khodaei, A. (2017). Probabilistic optimal scheduling of networked microgrids considering time-based demand response programs under uncertainty. *Applied Energy*, *198*, 267–279.

Noroozi, N., Trip, S., & Geiselhart, R. (2018). Model predictive control of DC microgrids: current sharing and voltage regulation. *IFAC-PapersOnLine*, *51*(23), 124–129.

osBrain. (n.d.). About osBrain. Retrieved from: https://osbrain.readthedocs.io/en/stable/about.html

Pashajavid, E., Shahnia, F., & Ghosh, A. (2017). Provisional internal and external power exchange to support remote sustainable microgrids in the course of power deficiency. *Iet Generation Transmission & Distribution*, *11*(1), 246–260.

Prabaharan, N., Jerin, A. R. A., Najafi, E., & Palanisamy, K. (2018). An overview of control techniques and technical challenge for inverters in micro grid In A. H. Fathima, N. Prabaharan, K. Palanisamy, A. Kalam, S. Mekhilef, J.J. Justo (Eds). *Hybrid-renewable Energy Systems in Microgrids: Integration, Developments and Control* (pp. 97-107). Elsevier Ltd.

Prinsloo, G., Mammoli, A., & Dobson, R. (2017). Customer domain supply and load coordination: A case for smart villages and transactive control in rural off-grid microgrids. *Energy*, *135*, 430–441.

Ren21. (2019). *Renewables 2019 Global Status Report*. Retrieved from: http://www.ren21.net/wp-content/uploads/2018/06/17-8652_GSR2018_FullReport_web_-1.pdf

Rivera, S., Farid, A. M., & Youcef-Toumi, K. (2014). A Multi-Agent System Coordination Approach For Resilient Self-Healing Operations in Multiple Microgrids. In *Industrial Agents: Emerging Applications of Software Agents in Industry* (pp. 269–285). Elsevier.

Saad, W., Han, Z., & Poor, H. V. (2011). Coalitional game theory for cooperative micro-grid distribution networks. *IEEE International Conference on Communications*, 1–5.

Sanjari, M. J., & Gharehpetian, G. B. (2014). Game-theoretic approach to cooperative control of distributed energy resources in islanded microgrid considering voltage and frequency stability. *Neural Computing and Applications*, *25*(2), 343–351.

Shahnia, F., Bourbour, S., & Ghosh, A. (2017). Coupling Neighboring Microgrids for Overload Management Based on Dynamic Multicriteria Decision-Making. *IEEE Transactions on Smart Grid*, *8*(2), 969–983.

Solomon, A. A., Kammen, D. M., & Callaway, D. (2014). The role of large-scale energy storage design and dispatch in the power grid: A study of very high grid penetration of variable renewable resources. Applied Energy, *134*, 75–89.

SQLite. (n.d.). About SQLite. Retrieved from: https://www.sqlite.org/about.html

United States Energy Information Administration. (2018). Wholesale Electricity and Natural Gas Market Data.

Vaahedi, E., Nodehi, K., Heim, D., Rahimi, F., & Ipakchi, A. (2017). The Emerging Transactive Microgrid Controller: Illustrating Its Concept, Functionality, and Business Case. *IEEE Power and Energy Magazine*, *15*(4), 80–87.

Van den Bergh, K. & Delarue, E. (2015). Cycling of conventional power plants: technical limits and actual costs. TME Working Paper – Energy and Environment. Retrieved from: https://core.ac.uk/download/pdf/34627483.pdf

Wang, H., & Huang, J. (2016). Incentivizing Energy Trading for Interconnected Microgrids. *IEEE Transactions on Smart Grid*, *3053*, 1–11.

Wang, X., Wang, C., Xu, T., Guo, L., Li, P., Yu, L., & Meng, H. (2018). Optimal voltage regulation for distribution networks with multi-microgrids. *Applied Energy*, *210*, 1027–1036.

Wei, C., Fadlullah, Z. M., Kato, N., & Takeuchi, A. (2014). GT-CFS: A game theoretic coalition formulation strategy for reducing power loss in micro grids. *IEEE Transactions on Parallel and Distributed Systems*, *25*(9), 2307–2317.

Wu, P., Huang, W., Tai, N., & Liang, S. (2018). A novel design of architecture and control for multiple microgrids with hybrid AC/DC connection. *Applied Energy*, *210*, 1002–1016.

Wu, P., Huang, W., Tai, N., & Liang, S. (2018). A novel design of architecture and control for multiple microgrids with hybrid AC/DC connection. *Applied Energy*, *210*, 1002–1016.

Yu, C. K., Van Der Schaar, M., & Sayed, A. H. (2015). Information-Sharing over Adaptive Networks with Self-Interested Agents. *IEEE Transactions on Signal and Information Processing over Networks*, *1*(1), 2–19.

Zerrahn, A., Schill, W. P., & Kemfert, C. (2018). On the economics of electrical storage for variable renewable energy sources. *European Economic Review*, *108*, 259–279.

Zhang, X., Bao, J., Wang, R., Zheng, C., & Skyllas-Kazacos, M. (2017). Dissipativity based distributed economic model predictive control for residential microgrids with renewable energy generation and battery energy storage. *Renewable Energy*, *100*, 18–34.

CHAPTER 5

DISCUSSION

The following provides a comparative discussion of findings from Chapters 2, 3, and 4 and suggests opportunities for future research.

5.1. Scientific Implications for the Research Community

Chapter 2 examined the implications of high-penetration residential solar photovoltaic (PV) systems with case studies for three locations in the United States. Site-specific and generalizable findings provided insight into how economic and technical metrics are affected by environmental forcings, solar PV system size, electric loads, total system-wide penetration of homes with solar PV, and utility rate structure. Analyses were completed from the perspective of both the utility and the ratepayer, providing a detailed picture of how ratepayers may experience financial changes as utilities attempt to alter their business models to recoup lost revenue from lower electricity sales. Each home in the study contained solar PV, a grid connection, and the option of energy storage. Storage was found to be cost-inefficient when net metering was in effect because, under net metering, the grid acted as a zero-cost lossless battery. Batteries were only cost effective without net metering and with a cost reduction of at least 55%. However, this study only considered a rate structure with energy charges and not demand charges. The comparative financials for batteries may have improved if demand charges were implemented and batteries could be dispatched for peak shaving.

Chapter 2 uncovered a critical finding that utilities will need more generation resources to accommodate higher ramp rate requirements as more residential PV is placed on the grid. The highest ramp rates for each location analyzed in the study occurred in the

late afternoon as solar insolation decreased and occupancy loads increased, however, the maximum annual ramp rate was observed in different months of the year for each city due to differences in load and solar profiles. Dispatchable generation and/or storage will need to meet capacity and reserve requirements during times of high solar insolation and be available to dispatch in the afternoon as solar PV declines and load increases. Ramp rate requirements increased as solar PV penetration increased, which in turn would require utilities to have more dispatchable reserves providing spinning and non-spinning reserve. Some of that reserve will be provided by generation units operating at partial load, which means at lower efficiency and higher emissions factors. This assumes residential solar PV is uncontrolled and utilities are forced to take-on all generation. Advanced controls and coordination of distributed energy resources (DERs) can help mitigate this system-wide problem by allowing local resources to support nearby loads.

The case study and analyses of Chapter 2 consisted of only residential loads. In most distribution systems, other load groups such as commercial, industrial, or public works also contribute to the aggregate peak load of the network. Coordination of power use and sharing between these entities can provide a more consistent system-wide net load profile throughout the day. For instance, a system with residential, commercial, and industrial loads may have a more consistent total load over the day and thus a higher load factor. Commercial and industrial buildings often have lower loads at the same time residences are experiencing high occupancy loads because occupants are leaving from work to return home. There is an opportunity to reduce peak net load, ramp rate requirements, and strain on the grid for the utility if residential, commercial, and industrial buildings all have local generation, storage, or controllable loads available. Strategies are

needed for managing these resources throughout the day, especially during times of occupancy transition from one area to another that result in high ramp rates.

Coordination of DERs can be accomplished using several methodologies. Centralized strategies are common and simple to implement, but as the number of assets increase the associated increase in computation power and time needed to reach a solution may be prohibitive if handled completely by the central controller. Decentralized strategies are thus becoming increasingly common and are easily scalable, but they do require investment into complex hardware installation at each DER asset site. Some of these manageability and scalability challenges can be solved by enable a group of DER assets (e.g., a home, neighborhood, commercial building, or group of buildings with local generation and/or storage) to act as independently controllable entities or microgrids. These microgrids can then be connected into a distribution-level transactive energy network with the ability to share power based on their net load requirements. If self-organization strategies are applied to this framework, microgrids can self-manage local requirements as well as coordinate with one another. Self-organization keeps computation requirements minimal with simple rule sets, automates control decisions, and allows plug-and-play connection of additional microgrids for improved scalability.

Chapter 3 described a generalizable method for managing a self-organizing, transactive energy network of microgrids with metrics assessed at the node-level and network-level. Each microgrid was represented by a single agent that participated in an energy marketplace and negotiated with neighboring agents to reach an acceptable energy price for selling power from producers to consumers. Microgrids could be either producers or consumers based on their net load at a time step, allowing a microgrid to be a consumer

or a producer depending on their own unique load profile at that time of day and year. Energy valuation was quantified by exponential functions unique to each producer and consumer pair and represented willingness to negotiate. Scalability of the method was demonstrated with a 3-node network and a 9-node network using data from real buildings. Results showed that trading between microgrids reduced the levelized cost of energy (LCOE) for all parties with respect to a baseline grid-only case that didn't permit trading. Trading patterns emerged between certain agents that allowed some microgrids to operate at a lower cost than others. These patterns suggest that the combination of local loads and DERs in a microgrid have a certain level of compatibility with other microgrids that is exhibited by their frequency of trading, and upon closer inspection, can be inferred through characteristics such as renewables fraction, load factor, and amount of on-site battery storage. Increasing the amount of storage in each microgrid made trading less effective at lowering energy cost because the microgrids became more energy independent and traded less when batteries were included.

Chapter 3 identified that certain agent pairs can create a lower node-level and network-level cost of energy, suggesting that the connectivity between nodes is important to overall network-level dynamics. Work in Chapter 3 used only ring network configurations, and produced a limited set of possible trading behaviors between agents because each agent was only connected to two adjacent neighbors. Chapter 4 expanded on this concept to permit additional network configurations, and allowed nodes to negotiate with more than their physically adjacent neighboring nodes. A competitive marketplace was developed to manage negotiations between n-many nodes in Chapter 4 to advance the

simpler trading formulation in Chapter 3. Additional methods and metrics were needed to improve understanding of compatibility and relationship formation between microgrids.

Chapter 4 introduced concepts that describe the familiarity, acceptance, and value of relationships between agents to generate a quantitative representation of the "reputation" of one node to another node using data on the history of their interactions. The familiarity coefficient considered direct compatibility between nodes based on net load, the acceptance coefficient considered what percentage of all past interactions with an agent resulted in a successful trade, and the value coefficient represented how the node valued the results of agreed upon prices with an agent compared to grid prices. The reputation coefficient, ranging from 0 to 1, was integrated into the valuation equations from Chapter 3 to adjust an agent's strategy of negotiating with other microgrids. The reputation each node held with its trading partners affected whether they would reach an agreed-upon price and at what value. The resulting value directly affected whether the trade would be completed, since the microgrids were rational agents that tried to sell or purchase their power in order of which agents would maximize their revenue. A trading fee was included to account for the grid access or interconnection fee associated with trading between microgrids. Including this extra fee resulted in agents being less lenient in negotiations, since they needed to have cost savings equal to at least the amount of the fee compared to grid prices for a trade to be beneficial. The same agent-based framework, 9-node network, and rate structure as Chapter 3 were used with the exception of the trading fee.

Chapter 4 presented results showing the effects of network configuration and connectivity on trading. No single network configuration resulted in maximum economic benefit for all nodes, but the configuration with the lowest network LCOE was also the

configuration with the largest number of successful transactions. As suggested by trading patterns identified in Chapter 3, connections between nodes of high compatibility had a significant effect on the amount of successful trades in the network and enabled certain nodes to operate at a lower cost. Increasing network connectivity had decreased marginal benefit for the entire network, though did result in LCOE reduction for certain nodes. A node's ability to operate at a lower cost was dependent on the number of connections its trading partners had and the competitiveness of its prices. Each node had knowledge only of its own connections, and therefore did not know how competitive its prices were. This resulted in certain network configurations in which the node had few successful transactions due to inability to adjust its strategy. Relationships were formed based on each node's ability to be competitive in past interactions and were indicated by the node's reputation coefficient value.

Energy storage was not included in Chapter 4 simulations. When compared to results with no energy storage from Chapter 3 for the same network configuration, the addition of the reputation coefficient in Chapter 4 resulted in decreased LCOE for some nodes and increased LCOE for others. This was due to changes in convexity of the valuation curves between nodes, which resulted in agreements at higher or lower prices depending on reputation coefficient values. Modification of reputation coefficient weights based on the network configuration may be able to improve the economic benefit for each node more evenly and distribute benefit across the entire network. Additionally, including different rate structures for various node types (residential, commercial, and industrial) may incentivize trading at certain times of day and result in more successful trades between

nodes that were not highly competitive in the cases studied where all nodes had the same rate structure.

5.2. Policy and Regulation of Transactive Energy

The control techniques introduced in Chapters 3 and 4 focused on distribution networks. The trading between microgrids would not affect voltages above the substation level and nodes were limited to trading with other microgrids only within their same substation control area. Thus, any revenue recouped by the utility through trading fees would likely be allocated to the distribution service category for infrastructure operations and maintenance and administrative costs. Distribution service costs comprise approximately one-third of the average electricity price in the United States (about $0.0285/kWh for the year 2018) and are expected to increase by 24% by 2050 as infrastructure is upgraded and renewables are integrated (United States Energy Information Administration 2019). The trading fee included in Chapter 4 simulations was equal to a $0.01/kWh for each participant in a trade while still resulting in financial benefit for nodes. This could be increased to ensure the utility recovered the cost of distribution service.

Energy policy and business models must change to permit full implementation of transactive energy markets and peer-to-peer trading. Regulated energy markets have a rigid service territory where independent power producers are not permitted to sell and trade power with each other. Since real-time pricing is a key operational parameter for transactive energy, transactive energy and energy trading fits better into deregulated energy markets with competitive retail markets in place. Within these competitive marketplaces, methods must be in place to allow prices to vary at each customer connection point. One suggested method involves the use of locational marginal pricing (Ghamkhari 2019; Orsini

et al. 2019). Presently used for transmission systems, locational marginal pricing determines the marginal cost of supplying power to a specific point on the grid system. A transactive energy market could transmit these cost signals at the distribution level so that each consumer uses the marginal value of electricity at their connection point to make purchasing choices in real-time (Orsini et al. 2019). This would allow consumption to be naturally encouraged and discouraged based on pricing signals. Building onto the concept of facilitate trading between distribution-level nodes as described in Chapters 3 and 4, these marginal values could be used as the upper bounds of the valuation curves to ensure trading is competitive with grid pricing.

One intermediate step that can be taken towards implementing transactive energy markets involves testing strategies in regulatory sandboxes. This would enable demonstration of transactive energy technologies at manageable scales without affecting larger systems. Another intermediate step that can be taken towards implementation of these techniques involves developing technology to enable participation in distribution-level markets for consumers and owners of DERs and microgrids. This is already being accomplished via development of software platforms but has not reached wide-spread adoption.

5.3. Turning Research into Physical Deployment

A number of commercial products exist for centralized and decentralized microgrid asset coordination. General Electric (GE) offers a line of centralized microgrid control platforms with simple controllers at each asset for taking measurements and sending statuses to the central controller (GE 2019). GE identifies a variety of microgrid applications and case studies including military, campuses, industrial, smart city, islands,

and utility-scale systems. Contrasting with GE's product line, ABB's MGC600 renewable microgrid controller takes a decentralized approach with a specific controller for each type of asset that controls, monitors, and interfaces with that asset (ABB 2013). ABB provides controllers for diesel/gas generators, distribution feeders, solar PV, hydro generators, energy storage systems, wind turbines, single/multiple loads, and network connection. These assets communicate with a local area network and can be added easily to the network. Each asset controller has various functions for supervision of the asset including automatic reconnection, setpoint controls based on incoming information, and spinning reserve management. There are also several existing projects that demonstrate transactive energy and peer-to-peer energy trading in physical setups (Kok and Widergren 2016; Zhang et al. 2017) as detailed in Chapter 1. However, these projects require a centralized system for handling market balancing, which can be difficult to implement and scale.

A completely decentralized control technique with microgrid nodes acting and coordinating as independent entities in a network has not been demonstrated with physical power system assets. For these scalable distribution-level microgrid networks to be feasible, microgrids must have a way to seamlessly integrate with one another and the existing main distribution grid. Plug-and-play primary and secondary controls can be used to automatically synchronize or desynchronize the microgrid with surrounding infrastructure, but physical constraints related to grid interconnection and coordination of each hierarchical control level must be considered.

5.4. Interconnection and Connectivity

IEEE Standard 1547-2018 (IEEE 2018a) provides guidelines for interconnecting and interfacing DERs with electric power systems through the point of common coupling.

According to this standard, all connected assets must meet requirements for voltage and frequency (based on the voltage level at the point of common coupling) and measurement accuracy for various parameters including active and reactive power. They must also have the control capability to reach cease-to-energize state in 2 seconds or less, limit active power, and execute mode or parameter changes with transitions in 30 seconds or less. Various requirements are also included for intentional and unintentional islanding, power quality, and response to abnormal conditions in the area around the electric power system. This standard states that performance requirements can be applied to multiple DER units within a single electric power system based on the aggregate rating of all DER units, and thus has applicability to microgrids and internal asset management.

Recently, the 2030.7-2017 IEEE Standard for the Specification of Microgrid Controllers was created (IEEE 2018b) to describe control functions for a microgrid to seamlessly connect to and disconnect from the main distribution grid for exchanging power and supplying ancillary services. Standard 2030.7-2017 states that interconnection agreements between the grid-system operator and the microgrid owner/operator should be established to describe energy consumption/production of the microgrid and the power quality requirements to be met before connection. Internal determination of system state and dispatch of assets within the microgrid are executed according to a set of rules, with emergency dispatch orders outlined in the event of unplanned islanding. Similar interconnection agreements could be possible for interconnection between multiple microgrids and, if completed, would provide the framework for internal control actions to safely handle both planned and unplanned connections and disconnections. The microgrid

must meet the negotiated power amount and quality prior to closing the switch to enable power flow between the microgrids.

5.5. Coordinating Control and Communication Strategies

Coordination and negotiation of power trading between microgrids and external entities is an advanced form of tertiary control that can be paired with lower-level secondary and primary control for executing trading decisions. Figure 5.1 is a modified version of a figure in IEEE 2030.7-2017, and is adapted here to illustrate how the proposed tertiary coordinating control functions in this dissertation could be paired with conventional secondary control. Secondary control actions such as supply-demand balance, state determination, and dispatch order formation operate in time steps of 5-30 min with information input from lower-level, primary functions (asset controls, instrumentation), higher-level, tertiary functions (optimization, forecasting, operator interface), and external interconnection functions (interchange, transactive energy markets). Primary internal controls at the asset-level such as load frequency control operate in time steps of 30 sec-5 min, while tertiary functions such as dispatch optimization, forecasting, and asset scheduling operate in time steps of 30-60 min.

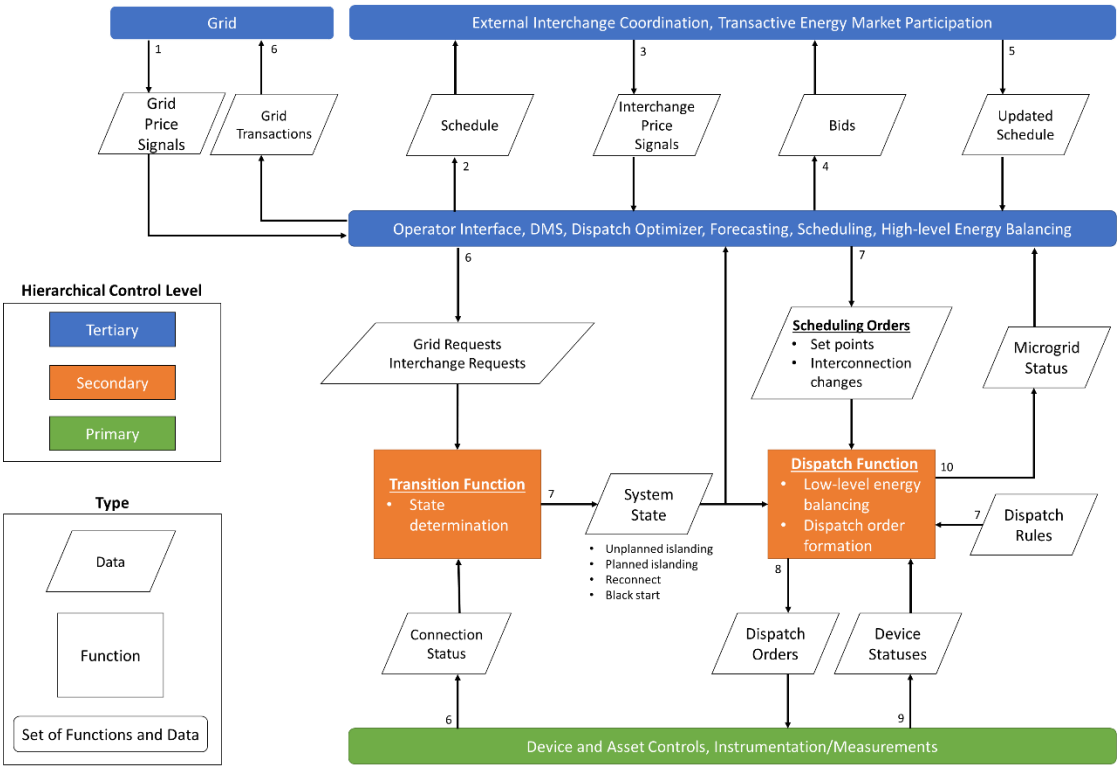

Figure 5.1: Connection of proposed tertiary control to primary and secondary control functions (adapted from IEEE 2018b).

The proposed self-organizing control with external coordination to other microgrids operates on a similar timescale as other tertiary control functions. When connecting a new microgrid to the network, the microgrid must wait until the start of the next time period to ensure proper synchronization. This allows the network to complete all committed trades prior to engaging with the new microgrid. At the primary and secondary control level, the microgrid must prepare to sync with the microgrid network by ensuring that the voltage requirements are met at each point of common coupling as specified by IEEE 1547-2018 (IEEE 2018a). The microgrid must also ensure all nodes that will be directly connected to it are notified of the incoming connection. After being properly synched, each microgrid connected to the new node updates its functions to include the extra node and can engage in negotiation and power trading. This synchronization requires

the network operate on a common communication protocol or a data translator between assets using different protocols. Communication, monitoring, and control guidelines such as those defined by IEEE 2030.5-2018 (IEEE 2018d), IEEE 1815 (IEEE 2016), and IEC 61850 (IEC 2009; IEC 2015; IEC 2018) can be utilized to ensure standardized mechanisms are in place for messaging, interfacing with SCADA systems, and exchanging data with web protocols.

Proper testing of the new microgrid according to IEEE 2030.8 standards (IEEE 2018c) prior to commercialization and commissioning would verify the microgrid controller meets expected performance metrics of other microgrids.

5.6. Future Work

The studies in Chapters 2, 3, and 4 provided foundational scientific thought to the field of transactive energy and demonstrated areas for applied research leading to physical implementation. Results primarily focused on economic metrics to demonstrate the financial potential of microgrid networks that permit trading, utilize agents to manage trading, and implement a self-organizing framework that allows agents to dynamically reconfigure and exhibit different behaviors to optimize trading schemes. Physical constraints from power engineering were not included and left as future work, with examples including capacity constraints in distribution infrastructure, additional physical limitations of assets, and power flow modeling to determine feasibility in physical applications.

Additional studies considering alternative rate agreements such as demand charges or tiered rate structures would expand understanding of system behavior under different regulatory strategies. Similarly, experimenting with different rate structures for each

microgrid customer and scale (residential, commercial, industrial) would help evaluate if microgrid capacity and ratepayer type affects trading and cost reduction. Residential rate structures tend to be either tiered or time-of-use, whereas commercial and industrial rate structures tend to include demand charges. Incorporating demand charges in the proposed methodology will require modification of the valuation curve boundaries and result in different trading behavior. For instance, seasonal effects on trading might become more apparent due to higher electrical loads for HVAC. Buying down the peak demand seen by the utility would result in a larger cost savings over the course of the month for entities with demand charges, making those entities more willing to accept a higher price for trading.

Other areas for consideration are the amount and frequency of information shared between nodes. The cases studied in Chapters 3 and 4 only required sharing the net load with neighboring nodes, but inclusion of other parameters such as forecasted renewables capacity and various durations of asset scheduling plans may result in better coordination given that more information is known between nodes. In addition, the order in which nodes receive that information can affect their strategy and how they interact with them. However, information privacy and security can be a concern for transactive energy markets. Evaluation of performance of these algorithms with varying amounts of information shared would provide valuable insight into what is the least amount of information that can be shared to still obtain desired economic and technical benefits. Examples of how this might be evaluated are shown in Table 5.1 with additional comparisons between centralized and decentralized architectures.

Table 5.1: Proposed Approaches of Information Sharing Between Nodes

Approach	Description	Diagram	Variant	Inputs/Outputs
1	**Centralized economic dispatch** Information is shared directly with central entity, no inter-microgrid communication. *Comparison case with no requests and offering strategy.*	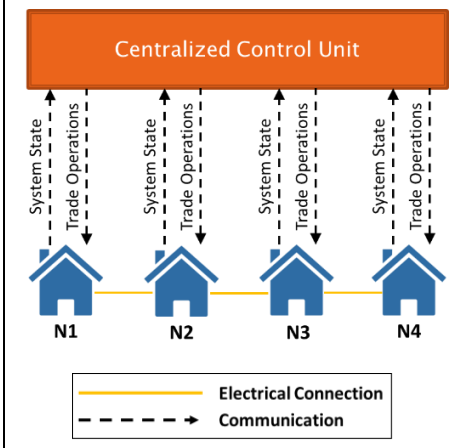	**a**	**Input:** Optimal trade operations (from central command unit) **Output:** System state (to central command unit)
2	**Decentralized architecture** Information related to local unit dispatch is shared between neighboring microgrids at the beginning of each time step to initiate trading. *Requests are made based on knowledge of neighbor states.*	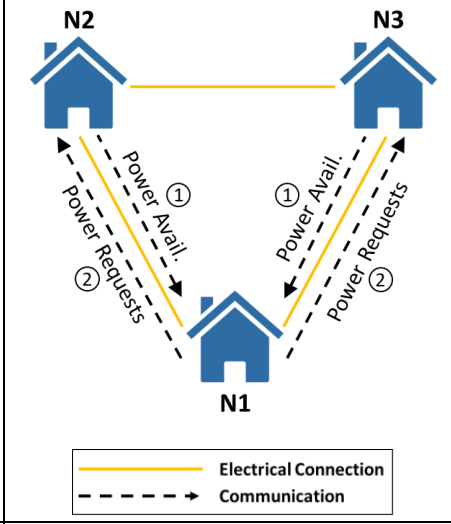	**a**	**Input:** Max/min power levels **Output:** Power requests
			b	**Input:** Unit dispatch lookup table **Output:** Power requests
3	**Decentralized architecture** Information related to requests for power sources/sinks initiates trading between microgrids. *Requests are made without knowledge of neighbor states.*	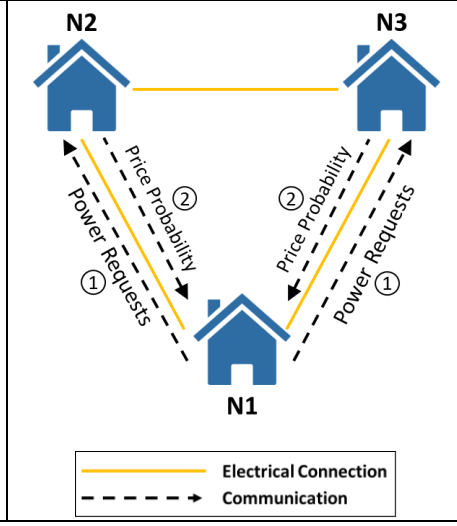	**a**	**Input:** Single point power request **Output:** Power price probabilities
			b	**Input:** Multiple point power request **Output:** Power price probabilities

Approach #1 uses traditional centralized economic dispatch as a baseline comparison case. In this technique, information is shared directly (and privately) with a central control entity through a Supervisory Control and Data Acquisition (SCADA) system. Optimal trading operations between nodes are calculated inside the centralized control entity and sent back out to subsidiary microgrids and other assets. Dedicated fiberoptic lines or secure wireless communications (e.g., radio, satellite) transfer information between nodes and the centralized controller. This approach limits threat vectors from hackers by reducing the functionality of distributed assets, however, the centralized server contains all information and controls placing a single point of failure in the network if attacked.

Approaches #2 and #3 implement a decentralized architecture in which each microgrid node has an independent agent that advocates for the microgrid in the energy trading marketplace. This creates a scalable network that can easily connect new microgrids on the fly. In Approach #2, information on local unit dispatch is shared with neighboring microgrids which then respond with an offer to buy or sell power. Thus, these offers are made with knowledge of neighboring microgrid states. Two variants of Approach #2 could be analyzed. Variant #2a shares less information (maximum and minimum net power levels only) and Variant #2b shares more information (a complete schedule of unit dispatch options in the microgrid). Comparison between these two variants could assess the extent to which information completeness affects optimum trading strategies. In Approach #3, microgrids first send requests for power generation or purchase and then neighboring microgrids respond with the probability of being able to provide power at the requested time and what it will cost. Requests from each microgrid are based on the internal

needs of the microgrid only and not on neighboring microgrid states, which is a departure from Approach #2 in which power requests were completed after knowing the status of neighboring microgrid states. Two variants of Approach #3 are introduced to explore how the number of power requests allowed for each microgrid may affect trading strategies. Variant #3a sends a single point power request (next time step) while Variant #3b allows for multiple point power requests (multiple time steps into the future).

5.7. Concluding Remarks

Self-organizing strategies that enable plug-and-play capability between microgrids in a transactive energy network have numerous applications for islands, campuses, military bases, rural electrification, and residential communities with a common distribution network. As the number of DERs and microgrid systems installed globally continues to grow, solutions that consider energy as a system containing many technical, economic, and political/regulatory components are necessary to facilitate the transition from centralized grid infrastructure to a modern, bidirectional, and decentralized energy network. As these systems grow in complexity, it is increasingly important to consider how coordination and automation of energy assets be accomplished to ensure reliable energy and efficient use of renewable resources. Continued expansion and attention to this research space is critical for successful integration of DERs and microgrids that enable a future with more renewable, resilient, reliable, and cost-effective electricity.

REFERENCES

Abass, Y. A., Al-Awami, A. T., & Jamal, T. (2016). Integrating automatic generation control and economic dispatch for microgrid real-time optimization. *IEEE Power and Energy Society General Meeting*.

ABB. (2013). Renewable Microgrid Controller MGC600. Retrieved from: https://new.abb.com/docs/default-source/ewea-doc/microgrid-controller-600_en_lr(dic2013).pdf

ABB. (2016). Solar inverters - power converters and inverters | ABB. Retrieved from http://new.abb.com/power-converters-inverters/solar

Abramson, D. S., Turiel, I., & Heydari, A. (1990). Analysis of refrigerator-freezer design and energy efficiency by computer modeling: DOE perspective. *ASHRAE Transactions*, *96*(Part I), 1354–1358.

Akter, M. N., Mahmud, M. A., & Oo, A. M. T. (2016). A hierarchical transactive energy management system for energy sharing in residential microgrids. In *IEEE Power and Energy Society General Meeting*, 1–5.

Akter, M. N., Mahmud, M. A., & Oo, A. M. T. (2017). A hierarchical transactive energy management system for energy sharing in residential microgrids. *Energies*, *10*(12).

Al-Mulla, A., & Elsherbini, A. (2014). Demand management through centralized control system using power line communication for existing buildings. *Energy Conversion and Management*, *79*, 477–486.

Al-Saedi, W., Lachowicz, S. W., Habibi, D., & Bass, O. (2013). Power flow control in grid-connected microgrid operation using Particle Swarm Optimization under variable load conditions. *International Journal of Electrical Power and Energy Systems*, *49*(1), 76–85.

Ambia, M. N., Al-Durra, A., & Muyeen, S. M. (2011). Centralized power control strategy for AC-DC hybrid micro-grid system using multi-converter scheme. Industrial *Electronics Conference Proceedings*, *2*(1), 843–848.

Anaya, K. L. & Pollitt, M. G. (2014). Integrated distributed generation: Regulation and trends in three leading countries (EPRG Working Paper No. 1423). Retrieved from University of Cambridge Energy Policy Research Group website: http://www.eprg.group.cam.ac.uk/wp-content/uploads/2015/01/EPRG-WP-1423.pdf

Anderson, R., Christensen, C., & Horowitz, S. (2006). Program design analysis using BEopt (Building Energy Optimization) software: Defining a technology pathway leading to new homes with zero peak cooling demand. *ACEEE Summer Study on Energy Efficiency in Buildings. Panel 2*, 23–35.

Ardani, K. (2014). Benchmarking non-hardware balance-of-system (soft) costs for US photovoltaic systems using a bottom-up approach and installer survey. National Renewable Energy Laboratory, USA.

Arizona State University Campus Metabolism. (2018). Retrieved from: https://cm.asu.edu/

Arnette, A. (2013). Integrating rooftop solar into a multi-source energy planning optimization model. *Applied Energy, 111*, 456-467.

Arteconi, A., Hewitt, N. J., & Polonara, F. (2012). State of the art of thermal storage for demand-side management. *Applied Energy, 93*, 371–389.

Aung, H. N., Khambadkone, A. M., Srinivasan, D., & Logenthiran, T. (2010). Agent-based intelligent control for real-time operation of a microgrid. *2010 Joint International Conference on Power Electronics, Drives and Energy Systems, PEDES 2010 and 2010 Power India*.

Babar, M., Grela, J., Ozadowicz, A. Nguyen, P.H., Hanzelka, Z., & Kamphuis, I.G. (2018). Energy flexometer: Transactive energy-based internet of things technology. *Energies, 11*(3), 568.

Baker, T., Gee, D., Millican, C., & Pearson, L. (2016). Rewiring Utilities for the Power Market of the Future. *The Boston Consulting Group*.

Baker, T., Maciel, J., Dean, J., Seshadri, P., & Gee, D. (2014). Distributed Energy a Distruptive Force. *The Boston Consulting Group*.

Bank, J., Mather, B., Keller, J., & Coddington, M. (2013). High Penetration Photovoltaic Case Study Report. National Renewable Energy Laboratory, Golden, CO. NREL/TP-5500-54742.

Baran, Paul. (1962). On Distributed Communications Networks. Santa Monica, CA: The RAND Corporation. Retrieved from: http://pages.cs.wisc.edu/~akella/CS740/F08/740-Papers/Bar64.pdf

Barkholtz, H.M., Fresquez, A., Chalamala, B.R., & Ferreira, S.R. (2017). A Database for Comparative Electrochemical Performance of Commercial 18650-Format Lithium-Ion Cells. *Journal of the Electrochemical Society, 164*(12), A2697-A2706.

Battelle Memorial Institute. (2015) Pacific Northwest Smart Grid Demonstration Project Technology Performance Report Volume 1: Technology Performance. Retrieved from: https://www.smartgrid.gov/document/Pacific_Northwest_Smart_Grid_Technology_Performance.html

Behboodi, S., Chassin, D.P., Djilali, N., & Crawford, C. (2018). Transactive control of fast-acting demand response based on thermostatic loads in real-time retail electricity markets. *Applied Energy, 210,* 1310-1320.

Bendib, A., Kherbachi, A., Kara, K., & Chouder, A. (2017). Droop controller based primary control scheme for parallel-connected single-phase inverters in islanded AC microgrid. *2017 5th International Conference on Electrical Engineering,* 1–22.

Bhat, R., Begovic, M., Kim, I., & Crittenden, J. (2014). Effects of PV on conventional generation. *2014 47th Hawaii International Conference on System Sciences (HICSS)*, 2380–2387.

Bidram, A., & Davoudi, A. (2012). Hierarchical structure of microgrids control system. *IEEE Transactions on Smart Grid*, *3*(4), 1963–1976.

Bouzid, A. M., Guerrero, J. M., Cheriti, A., Bouhamida, M., Sicard, P., & Benghanem, M. (2015). A survey on control of electric power distributed generation systems for microgrid applications. *Renewable and Sustainable Energy Reviews*, *44*, 751–766.

Brooklyn Microgrid. (2018). Home Page. Retrieved from: https://www.brooklyn.energy/

Brouwer, A. S., van den Broek, M., Zappa, W., & Turkenburg, W. C. (2016). Least-cost options for integrating intermittent renewables in low-carbon power systems. *Applied Energy*, *161*, 48–74.

Browne, D., O'Regan, B., & Moles, R. (2010). Use of multi-criteria decision analysis to explore alternative domestic energy and electricity policy scenarios in an Irish city-region. *Energy*, *35*(2), 518–528.

Bui, V. H., Hussain, A., Nguyen, T. T., & Kim, H. M. (2017). Real-Time optimization for microgrid operation based on auto-configuration in grid-connected mode. *IEEE International Conference on Sustainable Energy Technologies*, 142–146.

Cai, D. W., Adlakha, S., Low, S. H., De Martini, P., & Mani Chandy, K. (2013). Impact of residential PV adoption on retail electricity rates. *Energy Policy*, *62*, 830–843.

Caldognetto, T., & Tenti, P. (2014). Microgrids Operation Based on Master–Slave Cooperative Control. *IEEE Journal of Emerging and Selected Topics in Power Electronics*, *2*(4), 1081–1088.

California Energy Commission. (2018). Energy Commission Adopts Standards Requiring Solar Systems for New Homes, First in Nation. Retrieved from: http://www.energy.ca.gov/releases/2018_releases/2018-05-09_building_standards_adopted_nr.html

California ISO. (2013). Demand response and energy efficiency roadmap: Maximizing preferred resources. California ISO, USA.

Carrasco, J. M., Franquelo, L. G., Bialasiewicz, J. T., Galván, E., Guisado, R. P., Prats, M. A. & Moreno-Alfonso, N. (2006). Power-electronic systems for the grid integration of renewable energy sources: A survey. *IEEE Transactions on Industrial Electronics, 53*(4), 1002–1016.

Chakraborty, S., Nakamura, S., & Okabe, T. (2014). Scalable and optimal coalition formation of microgrids in a distribution system. *IEEE PES Innovative Smart Grid Technologies Conference Europe*.

Chaouachi, A., Kamel, R. M., Andoulsi, R., & Nagasaka, K. (2013). Multiobjective Intelligent Energy Management for a Microgrid. *IEEE Transactions on Industrial Electronics*, *60*(4), 1688–1699.

Chassin, D., Behboodi, S., Shi, Y., & Djilali, N. (2017). H2 -optimal transactive control of electric power regulation from fast-acting demand response in the presence of high renewables. *Applied Energy*, *205*, 304-315.

Chen, D., Yanhui, X., Dan, S., Yifeng, O., Yu, Z. & Qiangqiang, W. (2017). Chinese Patent No. CN 107844055. Retrieved from https://worldwide.espacenet.com/publicationDetails/biblio?FT=D&date=20180327&DB=EPODOC&locale=&CC=CN&NR=107844055A

Chen, W. (1971). *Applied Graph Theory*. Amsterdam; London: North-Holland Publishing.

Chen, Y. & Hu, M. (2016). Balancing collective and individual interests in transactive energy management of interconnected micro-grid clusters. *Energy*, *109*, 1075-1085.

Christensen, C., Anderson, R., Horowitz, S., Courtney, A., & Spencer, J. (2006). BEopt software for building energy optimization: Features and capabilities. National Renewable Energy Laboratory, USA.

Cintuglu, M. H., Martin, H., & Mohammed, O. A. (2015). Real-time implementation of multiagent-based game theory reverse auction model for microgrid market operation. *IEEE Transactions on Smart Grid*, *6*(2), 1064–1072.

Climate Nexus. (2017). China's Climate and Energy Policy. Retrieved from: https://climatenexus.org/international/international-cooperation/chinas-climate-and-energy-policy/

Colman, A. (2014). *Game Theory and Experimental Games The Study of Strategic Interaction*. International Series in Experimental Social Psychology. Burlington: Elsevier Science.

Cominesi, S. R., Farina, M., Giulioni, L., Picasso, B., & Scattolini, R. (2018). A Two-Layer Stochastic Model Predictive Control Scheme for Microgrids. *IEEE Transactions on Control Systems Technology*, *26*(1), 1–13.

Cossentino, M., Lodato, C., Lopez, S., Pucci, M., Vitale, G., & Cirrincione, M. (2011). A multi-agent architecture for simulating and managing microgrids. *Proceedings of the Federated Conference on Computer Science and Information Systems*, 619–622.

Couture, T. & Gagnon, Y. (2010). An analysis of feed-in tariff remuneration models: Implications for renewable energy investment. *Energy Policy*, *38*(2), 955–965.

Crawley, D. B., Lawrie, L. K., Winkelmann, F. C., Buhl, W. F., Huang, Y. J., Pedersen, C. O., Strand, R. K., Liesen, R. J., Fisher, D.E., Witte, M. J., & Glazer, J. (2001). EnergyPlus: Creating a new-generation building energy simulation program. *Energy and Buildings*, *33*(4), 319–331.

Damiani, D., Litynski, J. T., McIlvried, H. G., Vikara, D. M., & Srivastava, R. D. (2012). The US Department of Energy's R&D program to reduce greenhouse gas emissions through beneficial uses of carbon dioxide, *Greenhouse Gases Science and Technology*, *2*(1), 9–19.

Daneshvar, M., Pesaran, M., & Mohammadi-ivatloo, B. (2018). Transactive energy integration in future smart rural network electrification. *Journal of Cleaner Production*, *190*, 645–654.

Darghouth, N. R., Barbose, G., & Wiser, R. (2011). The impact of rate design and net metering on the bill savings from distributed PV for residential customers in California. *Energy Policy*, *39*(9), 5243–5253.

Database of State Incentives for Renewables & Efficiency® - DSIRE. (2015). Retrieved from: http://www.dsireusa.org

Deline, C., Marion, B., Granata, J., Gonzalez, S. (2011). A performance and economic analysis of distributed power electronics in photovoltaic systems. National Renewable Energy Laboratory, USA.

Denholm, P. & Margolis, R. M. (2007). Evaluating the limits of solar photovoltaics (PV) in electric power systems utilizing energy storage and other enabling technologies. *Energy Policy*, *35*(9), 4424–4433.

Denholm, P., Clark, K., & O'Connell, M. (2016). Emerging Issues and Challenges in Integrating High Levels of Solar into the Electrical Generation and Transmission System. National Renewable Energy Laboratory, Golden, CO. NREL/TP-6A20-65800.

Diesendruck, C. E., Sottos, N. R., Moore, J. S., & White, S. R. (2015). *Biomimetic Self-Healing. Angewandte Chemie - International Edition*, *54*(36), 10428–10447.

Dimeas, A.L. and Hatziargyriou, N.D. (2005). Operation of a multiagent system for microgrid control. *IEEE Transactions on Power Systems*, *20*(3), 1447–1455.

Divshali, P. H., Choi, B. J., & Liang, H. (2017). Multi-agent transactive energy management system considering high levels of renewable energy source and electric vehicles. *IET Generation, Transmission & Distribution*, *11*(15), 3713–3721.

D-maps (2016). United States of America. Retrieved from: http://d-maps.com/carte.php?num_car=1682&lang=en

Dressler, Falko. (2008). *Self-Organization in Sensor and Actor Networks*. Hoboken, GB: Wiley.

Du, Y., Li, F., Kou, X., & Pei, W. (2018). Coordinating multi-microgrid operation within distribution system: A cooperative game approach. *IEEE Power and Energy Society General Meeting*.

Eber, K. & Corbus, D. (2013). Hawaii Solar Integration Study: Executive Summary. National Renewable Energy Laboratory, Golden, CO. NREL/TP-5500-57215.

Eddy, Y. S. F., Gooi, H. B., & Chen, S. X. (2015). Multi-agent system for distributed management of microgrids. *IEEE Transactions on Power Systems*, *30*(1), 24–34.

Energy Monitor Worldwide; Amman. (2016). Arizona regulators vote to stop net metering for solar. *SyndiGate Media Inc.*

Esfahani, M. M., Hariri, A., Member, S., & Mohammed, O. A. (2019). A Multiagent-Based Game-Theoretic and Optimization Approach for Market Operation of Multimicrogrid Systems. *IEEE Transactions on Industrial Informatics*, *15*(1), 280–292.

Eto, J., Undrill, J., Roberts, C., Mackin, P., & Ellis, J. (2018). Frequency Control Requirements for Reliable Interconnection Frequency Response (LBNL-2001103). *Lawrence Berkeley National Laboratory*. Retrieved from: http://eta-publications.lbl.gov/sites/default/files/frequency_control_requirements_lbnl-2001103.pdf

Evans, A., Strezov, V., & Evans, T. J. (2016). Assessment of utility energy storage options for increased renewable energy penetration. *Renewable & Sustainable Energy Reviews*, *16*(6), 4141–4147.

Faratin, P., Sierra, C., & Jennings, N. R. (1998). Negotiation decision functions for autonomous agents. *Robotics and Autonomous Systems*, *24*(3–4), 159–182.

Finn, P., O'Connell, M., & Fitzpatrick, C. (2013). Demand side management of a domestic dishwasher: Wind energy gains, financial savings and peak-time load reduction. *Applied Energy*, *101*, 678–685.

Floreano, D., Zufferey, J.C., Srinivasan, M., & Ellington, C. (2010). *Flying Insects and Robots*. Springer Berlin Heidelberg.

Fossati, J. P., Galarza, A., Martín-Villate, A., Echeverría, J. M., & Fontán, L. (2015). Optimal scheduling of a microgrid with a fuzzy logic controlled storage system. *International Journal of Electrical Power and Energy Systems, 68*, 61–70.

Friedman, B., Ardani, K., Feldman, D., Citron, R., & Margolis, R. (2013). Benchmarking Non-Hardware Balance-of-System (Soft) Costs for U.S. Photovoltaic Systems, Using a Bottom-Up Approach and Installer Survey – Second Edition. NREL. (Report No. NREL/TP-6A20-60412)

Fronius USA LLC. (2016). Fronius USA LLC - products - grid-connected PV inverters. Retrieved from https://www.fronius.com/en-us/usa#.Vxu8tWPWzzI

Fulzele, J. B. & Dutt, S. (2011). Optimum planning of hybrid renewable energy system using HOMER. *International Journal of Electrical and Computer Engineering (IJECE), 2*(1), 68–74.

General Electric (GE). (2019). Microgrid Explorer. Retrieved from: https://www.GEGridSolutions.com/microgrid

Ghamkhari, M. (2019). Transactive Energy Pricing in Power Distribution Systems. *2019 IEEE Green Technologies Conference (GreenTech)*, 1–5.

Ghanbarian, M. M., Nayeripour, M., Rajaei, A. H., Jamshidi, F., & Waffenschmidt, E. (2017). Model predictive control of distributed generation micro-grids in island and grid connected operation under balanced and unbalanced conditions. *Journal of Renewable and Sustainable Energy*, *9*(4).

Ghorbani, S., Rahmani, R., & Unland, R. (2017). Multi-agent autonomous decision making in smart micro-grids' energy management: A decentralized approach. Lecture Notes in Computer Science (including Subseries Lecture Notes in Artificial Intelligence and Lecture Notes in Bioinformatics), 10413, 223-237.

Glover, J., Sarma, M., & Overbye, T. (2012). Power system analysis and design (5th ed.). Cengage Learning, Stamford, CT.

Golumbic, M.C. (1980). Algorithmic Graph Theory and Perfect Graphs. *Annals of Discrete Mathematics*, *57*, 1-314. Elsevier Science.

Goop, J., Odenberger, M., & Johnsson, F. (2017). The effect of high levels of solar generation on congestion in the European electricity transmission grid. *Applied Energy*, *205*, 1128-1140.

Gregoratti, D., & Matamoros, J. (2015). Distributed Energy Trading: The Multiple-Microgrid Case. *IEEE Transactions on Industrial Electronics*, *62*(4), 2551–2559.

GridWise Architecture Council. (2015). GridWise Transactive Energy Framework Version 1.0. Pacific Northwest National Laboratory, Richland, WA. PNNL-22946 Ver1.0.

Hafez, O. & Bhattacharya, K. (2012). Optimal planning and design of a renewable energy based supply system for microgrids. *Renewable Energy*, *45*, 7–15.

Hajimiragha, A. H., & Zadeh, M. R. D. (2013). Research and development of a microgrid control and monitoring system for the remote community of Bella Coola: Challenges, solutions, achievements and lessons learned. *IEEE International Conference on Smart Energy Grid Engineering, SEGE 2013*.

Hammad, E. M., Farraj, A. K., & Kundur, D. (2015a). Grid-independent cooperative microgrid networks with high renewable penetration. *2015 IEEE Power and Energy Society Innovative Smart Grid Technologies Conference.*

Hammad, E., Farraj, A., & Kundur, D. (2015b). Cooperative Microgrid Networks for Remote and Rural Areas. *Canadian Conference on Electrical and Computer Engineering*, 1572–1577.

Hammerstrom, D. J. (2007). Pacific Northwest GridWise Testbed Demonstration Projects, Part I Olympic Peninsula Project. *Olympic Peninsula Project, National Technical Information Service*, 1–157.

Han, H., Hou, X., Yang, J., Wu, J., Su, M., & Guerrero, J. M. (2016). Review of power sharing control strategies for islanding operation of AC microgrids. *IEEE Transactions on Smart Grid*, *7*(1), 200–215.

Haque, M. A. (2010). *Biologically Inspired Heterogeneous Multi-Agent Systems*. Georgia Institute of Technology, Atlanta, GA.

Harmouch, F. Z., Krami, N., & Hmina, N. (2018). A multiagent based decentralized energy management system for power exchange minimization in microgrid cluster. *Sustainable Cities and Society*, *40*, 416–427.

Hatziargyriou, N. (2013). *Microgrid Architectures and Control*. S.l. : Wiley.

Hawaii Clean Energy Initiative. (2018). Hawaii State Government. Retrieved from: http://www.hawaiicleanenergyinitiative.org/

He, J., Wang, C., Pan, Y., & Liang, B. (2017). A Simple Decentralized Islanding Microgrid Power Sharing Method without Using Droop Control. *IEEE Transactions on Smart Grid*, *9*(6), 6128–6139.

He, Y., & Wei, J. (2016). A Game-Theoretic Model for Energy Trading of Privacy-Preserving Microgrid Social Networks. *2016 IEEE International Conference on Smart Grid Communications*, 388–394.

Hendron, R. & Engebrecht, C. (2010). Building America House Simulation Protocols. National Renewable Energy Laboratory, USA.

Herbes, C., Brummer, V., Rognli, J., Blazejewski, S., & Gericke, N. (2017). Responding to policy change: New business models for renewable energy cooperatives – Barriers perceived by cooperatives' members. *Energy Policy*, *109*, 82-95.

Hernández-Moro, J. & Martínez-Duart, J. M. (2013). Analytical model for solar PV and CSP electricity costs: Present LCOE values and their future evolution. *Renewable and Sustainable Energy Reviews*, *20*, 119–132.

Hirsch, A., Parag, Y., & Guerrero, J. (2018). Microgrids: A review of technologies, key drivers, and outstanding issues. *Renewable and Sustainable Energy Reviews*, *90*, 402–411.

Hobbs, B. (1995). Optimization methods for electric utility resource planning. European *Journal of Operational Research*, *83*(1), 1-20.

Holjevac, N., Capuder, T., Zhang, N., Kuzle, I., & Kang, C. (2017). Corrective receding horizon scheduling of flexible distributed multi-energy microgrids. *Applied Energy*, *207*, 176–194.

Holmberg, D., Hardin, D., Cunningham, R., Melton, R., & Widergren, S. (2016). Transactive Energy Application Landscape Scenarios. *Smart Electric Power Alliance*.

Horhoianu, A. (2018). Microgrid Primary Control And Continuous-Time Operation. *2018 International Conference on Development and Application Systems*, 38–42.

Hug, G., Kar, S., & Wu, C. (2015). Consensus + innovations approach for distributed multiagent coordination in a microgrid. *IEEE Transactions on Smart Grid*, *6*(4), 1893-1903.

IEC. (2009). Communication networks and systems for power utility automation - Part 7-420: Basic communication structure - Distributed energy resources logical nodes. Retrieved from: https://webstore.iec.ch/publication/6019

IEC. (2015). Communication networks and systems for power utility automation - Part 80-3: Mapping to web protocols - Requirements and technical choices. Retrieved from: https://webstore.iec.ch/publication/23695

IEC. (2018). Communication networks and systems for power utility automation - Part 8-2: Specific communication service mapping (SCSM) - Mapping to Extensible Messaging Presence Protocol (XMPP). Retrieved from: https://webstore.iec.ch/publication/34345

IEEE. (2016). IEEE Standard for Exchanging Information Between Networks Implementing IEC 61850 and IEEE Std 1815(TM) [Distributed Network Protocol (DNP3)]. https://doi.org/10.1109/IEEESTD.2016.7786998

IEEE. (2018a). IEEE Standard for Interconnection and Interoperability of Distributed Energy Resources with Associated Electric Power Systems Interfaces. https://doi.org/10.1109/IEEESTD.2018.8332112

IEEE. (2018b). IEEE Standard for the Specification of Microgrid Controllers. https://doi.org/10.1109/IEEESTD.2018.8340204

IEEE. (2018c). IEEE Standard for the Testing of Microgrid Controllers. https://doi.org/10.1109/IEEESTD.2018.8444947

IEEE. (2018d). IEEE Standard for Smart Energy Profile Application Protocol. https://doi.org/10.1109/IEEESTD.2018.8608044

Institute for Energy Research. (2014). Electricity Transmission.

International Energy Agency (IEA). (2014). Technology Roadmap Solar Photovoltaic Energy. OECD/IEA, France.

International Energy Agency (IEA). (2015). Energy Prices & Taxes: Quarterly Statistics; 2015 IIS 2380-P2; ISSN 0256–2332. OECD/IEA, France.

International Energy Agency. (2017). 2017 Amendment of the Renewable Energy Sources Act (EEG 2017). IEA/IRENA Joint Policies and Measures Database.

Ito, H. (2008). Computational geometry and graph theory: International conference, Kyoto CGGT 2007: Revised selected papers. *Japan Conference on Discrete and Computational Geometry*. Berlin: Springer.

Jadhav, A. M., Patne, N. R., & Guerrero, J. M. (2019). A Novel Approach to Neighborhood Fair Energy Trading in a Distribution Network of Multiple Microgrid Clusters. *IEEE Transactions on Industrial Electronics*, *66*(2), 1520–1531.

Jaiswal, S., & Ghose, T. (2017). Optimal real power dispatch of centralized micro-grid control operation. *Proceedings of IEEE International Conference on Circuit, Power and Computing Technologies*.

Jang, Y., & Kim, M. (2017). A Dynamic Economic Dispatch Model for Uncertain Power Demands in an Interconnected Microgrid. *Energies*, *10*(3), 300. https://doi.org/10.3390/en10030300

Janko, S. A., & Johnson, N. G. (2018). Scalable multi-agent microgrid negotiations for a transactive energy market. *Applied Energy*, *229*, 715–727.

Janko, S.A., Arnold, M.R., & Johnson, N.G. (2016). Implications of high-penetration renewables for ratepayers and utilities in the residential solar photovoltaic (PV) market. *Applied Energy, 180*, 37-51.

Ji, M., Zhang, P., & Cheng, Y. (2018). Distributed microgrid energy optimization using transactive control and heuristic strategy. *IEEE Power and Energy Society General Meeting*, 1–5.

Jiang, G., Ma, F., Shang, J., & Chau, P. Y. K. (2014). Evolution of knowledge sharing behavior in social commerce: An agent-based computational approach. *Information Sciences*, *278*, 250–266.

Jiang, Z. (2006). Agent-Based Control Framework for Distributed Energy Resources Microgrids. *2006 IEEE/WIC/ACM International Conference on Intelligent Agent Technology*, 646–652.

Johnson, N., Lilienthal, P., & Schoechle, T. (2011). Modeling distributed premises-based renewables integration using HOMER. *2011 Grid-Interop Conference, Phoenix, AZ.*

Johnstone, N., & I. Haščič. (2012). Increasing the penetration of intermittent renewable energy: Innovation in energy storage and grid management In *Energy and Climate Policy: Bending the Technological Trajectory*, OECD Publishing, Paris.

Jun, Z., Junfeng, L., Jie, W., & Ngan, H.W. (2011). A multi-agent solution to energy management in hybrid renewable energy generation system. *Renewable Energy*, *36*(5), 1352-1363.

Kahrobaeian, A., & Mohamed, Y. A. R. I. (2015). Networked-based hybrid distributed power sharing and control for islanded microgrid systems. *IEEE Transactions on Power Electronics*, *30*(2), 603–617.

Kantamneni, A., Brown, L. E., Parker, G., & Weaver, W. W. (2015). Survey of multi-agent systems for microgrid control. *Engineering Applications of Artificial Intelligence*, *45*, 192–203.

Kar, S. & Hug, G. (2012). Distributed robust economic dispatch in power systems: A consensus + innovations approach. *2012 IEEE Power Energy and Society General Meeting*.

Kar, S., Moura, J.M.F., & Ramanan, K. (2012). Distributed parameter estimation in sensor networks: Nonlinear observation models and imperfect communication. *IEEE Transactions on Information Theory*, *58*(4), 3575–3605.

Katiraei, F. & Aguero, J. R. (2011). Solar PV integration challenges. *Power and Energy Magazine, IEEE*, *9*(3), 62–71.

Kempton, W. & Tomić, J. (2005). Vehicle-to-grid power implementation: From stabilizing the grid to supporting large-scale renewable energy. *Journal of Power Sources*, *144*(1), 280–294.

Kern, E. C., Gulachenski, E. M., & Kern, G. A. (1989). Cloud effects on distributed photovoltaic generation: Slow transients at the Gardner, Massachusetts, photovoltaic experiment. *IEEE Transactions on Energy Conversion, 4*(2), 184–190.

Khodaei, A. (2015). Provisional microgrids. *IEEE Transactions on Smart Grid*, *6*(3), 1107–1115.

Kim, B., Bae, S., & Kim, H. (2017). Optimal energy scheduling and transaction mechanism for multiple microgrids. *Energies*, *10*(4).

Kirchner, M. (2012). Providing reliable data center backup power. Consulting - Specifying Engineer, N/a.

Kok, K. (2013). The PowerMatcher: Smart Coordination for the Smart Electricity Grid. Retrieved from: www.tinyurl.com/PowerMatcherBook

Kok, K., & Widergren, S. (2016). A Society of Devices: Integrating Intelligent Distributed Resources with Transactive Energy. *IEEE Power and Energy Magazine*, *14*(3), 34–45.

Kou, P., Liang, D., & Gao, L. (2017). Distributed EMPC of multiple microgrids for coordinated stochastic energy management. *Applied Energy*, *185*, 939–952.

Kouluri, M. K., & Pandey, R. K. (2011). Intelligent Agent Based Micro grid Control. *2011 2nd International Conference on Intelligent Agent and Multi-Agent Systems (IAMA)*, 62–66.

Kumar Nunna, H. S. V. S., & Doolla, S. (2013). Multiagent-based distributed-energy-resource management for intelligent microgrids. *IEEE Transactions on Industrial Electronics*, *60*(4), 1678–1687.

Kumrai, T., Ota, K., Dong, M., Sato, K., & Kishigami, J. (2017). Optimising operation management for multi-micro-grids control. *IET Cyber-Physical Systems: Theory & Applications*, *3*(1), 24–33.

Lacey, S. (2014). This Is What the Utility Death Spiral Looks Like. Green Tech Media.

Lagorse, J., Simoes, M. G., & Miraoui, A. (2009). A Multiagent Fuzzy-Logic-Based Energy Management of Hybrid Systems. *IEEE Transactions on Industry Applications*, *45*(6), 2123–2129.

Lahon, R., Gupta, C. P., & Fernandez, E. (2019). Coalition formation strategies for cooperative operation of multiple microgrids. *IET Generation, Transmission & Distribution*, *13*, 3661–3672.

Laird, F. N. (2013). Against transitions? Uncovering conflicts in changing energy systems. *Science as Culture*. *22*(2), 149–156.

Lakhtakia, A. & Martin-Palma, R.J. (2013). Engineered Biomimicry. Elsevier.

Lam, R. K. & Yeh, H. G. (2014). PV ramp limiting controls with adaptive smoothing filter through a battery energy storage system. *2014 IEEE Green Energy and Systems Conference*, 55-60.

Lambert, T., Gilman, P., & Lilienthal, P. (2006). Micropower system modeling with HOMER. *Integration of Alternative Sources of Energy*, *1*(15), 379–418.

Leepa, C. & Unfried, M. (2013). Effects of a cut-off in feed-in tariffs on photovoltaic capacity: Evidence from Germany. *Energy Policy, 56*, 536-542.

Leeuwen, J.V. (1990). Handbook of theoretical computer science. Amsterdam; Oxford: Elsevier.

Leng, D and Polmai, P. (n.d.). Control of a Microgrid Based on Distributed Cooperative Control of Multi-Agent System.

Lewis, F. L., Qu, Z., Davoudi, A., & Bidram, A. (2013). Secondary control of microgrids based on distributed cooperative control of multi-agent systems. *IET Generation, Transmission & Distribution*, *7*, 822–831.

LG Chem ESS Battery Division. (n.d.). Introducing Our RESU. Retrieved from: http://www.lgesspartner.com/front/normal/en/main/main.dev

Li, J., Xiong, R., Yang, Q., Liang, F., Zhang, M., & Yuan, W. (2017). Design/test of a hybrid energy storage system for primary frequency control using a dynamic droop method in an isolated microgrid power system. *Applied Energy*, *201*, 257–269.

Li, J., Yang, Q., Yao, P., Sun, Q., Zhang, Z., Zhang, M., & Yuan, W. (2016). A Novel use of the Hybrid Energy Storage System for Primary Frequency Control in a Microgrid. *Energy Procedia*, *103*, 82–87.

Li, Q., Chen, F., Chen, M., Guerrero, J. M., & Abbott, D. (2016). Agent-Based Decentralized Control Method for Islanded Microgrids. *IEEE Transactions on Smart Grid*, *7*(2), 637–649.

Li, S., Fu, X., Jaithwa, I., Alonso, E., Fairbank, M., & Wunsch, D. C. (2015). Control of Three-Phase Grid-Connected Microgrids using Artificial Neural Networks. *2015 7th International Joint Conference on Computational Intelligence (IJCCI)*.

Li, Y., Liu, N., & Zhang, J. (2016). Jointly optimization and distributed control for interconnected operation of autonomous microgrids. *Proceedings of the 2015 IEEE Innovative Smart Grid Technologies - Asia, ISGT ASIA 2015*.

Lilic, J. (2015). Peer-to-Peer Transaction and Control: Microgrid Intelligence System for Energy built on Ethereum. TransactiveGrid. Retrieved from: https://www.slideshare.net/JohnLilic/transactive-grid

Liu, W., Gu, W., Wang, J., Yu, W., & Xi, X. (2018). Game theoretic non-cooperative distributed coordination control for multi-microgrids. *IEEE Transactions on Smart Grid*, *9*(6), 6986–6997.

Liu, X., O'Rear, E. G., Tyner, W. E., & Pekny, J. F. (2014). Purchasing vs. leasing: A benefit-cost analysis of residential solar PV panel use in California. *Renewable Energy*, *66*, 770–774.

Liu, Y., Zuo, K., Liu, X. (Amy), Liu, J., & Kennedy, J. M. (2018). Dynamic pricing for decentralized energy trading in micro-grids. *Applied Energy*, *228*, 689–699.

Liu, Z., Wu, Q., Huang, S., & Zhao, H. (2017). Transactive energy: A review of state of the art and implementation. *2017 IEEE Manchester PowerTech, Manchester*.

Logenthiran, T., Srinivasan, D., & Khambadkone, A. M. (2011). Multi-agent system for energy resource scheduling of integrated microgrids in a distributed system. *Electric Power Systems Research*, *81*(1), 138–148.

Logenthiran, T., Srinivasan, D., Khambadkone, A., and Aung, H. (2010). Multi- agent system (MAS) for short-term generation scheduling of a micro- grid. *IEEE International Conference on Sustainable Energy Technology.*

Løken, E. (2007). Use of multicriteria decision analysis methods for energy planning problems. *Renewable and Sustainable Energy Reviews*, *11*(7), 1584–1595.

Lou, G., Gu, W., Wang, L., Xu, B., Wu, M., & Sheng, W. (2017). Decentralised secondary voltage and frequency control scheme for islanded microgrid based on adaptive state estimator. *IET Generation, Transmission & Distribution*, *11*(15), 3683–3693.

Lovins, A. (2013). Reinventing fire: Bold business solutions for the new energy era. Chelsea Green Publishing.

Lund, H. & Münster, E. (2003). Management of surplus electricity-production from a fluctuating renewable-energy source. *Applied Energy*, *76*(1), 65–74.

Lund, H. (2005). Large-scale integration of wind power into different energy systems. *Energy*, *30*(13), 2402–2412.

Luo, F., Chen, Y., Xu, Z., Liang, G., Zheng, Y., & Qiu, J. (2017). Multiagent-Based Cooperative Control Framework for Microgrids' Energy Imbalance. *IEEE Transactions on Industrial Informatics*, *13*(3), 1046–1056.

Luo, X., Wang, J., Dooner, M., & Clarke, J. (2015). Overview of current development in electrical energy storage technologies and the application potential in power system operation. *Applied Energy*, *137*, 511-536.

Lynch, M.A.., Shortt, A., Tol, R.S.J., & Malley, M.J. (2013). Risk–return incentives in liberalised electricity markets. *Energy Economics*, *40*, 598-608.

Ma, J., Li, P., Lin, X., Zhu, W., & Yuan, X. (2015). Game theory method for multi-objective optimizing operation in microgrid. *IEEE 12th International Conference on Networking, Sensing and Control*, 421–425.

Madkour, S. A. (2016). Transactive Energy Control of Electric Energy Storage to Mitigate the Impact of Transportation Electrification in Distribution Systems. University of Ontario Institute of Technology.

Mahmoud, M. S., & Hussain, S. A. (2015). Adaptive PI secondary control for smart autonomous microgrid systems. *International Journal of Adaptive Control and Signal Processing*, *29*, 1442–1458.

Maknouninejad, A., Lin, W., Harno, H. G., Qu, Z., & Simaan, M. A. (2012). Cooperative control for self-organizing microgrids and game strategies for optimal dispatch of distributed renewable generations. *Energy Systems*, *3*(1), 23–60.

Martínez Ceseña, E.A., Good, N., Syrri, A.L.A., & Mancarella, P. (2018). Techno-economic and business case assessment of multi-energy microgrids with co-optimization of energy, reserve and reliability services. *Applied Energy*, *210*, 896-913.

Marzband, M., Azarinejadian, F., Savaghebi, M., Pouresmaeil, E., Guerrero, J. M., & Lightbody, G. (2018). Smart transactive energy framework in grid-connected multiple home microgrids under independent and coalition operations. *Renewable Energy*, *126*, 95–106.

McLaren, J., Gagnon, P., Anderson, K., Elgqvist, E., Fu, R., & Remo, T. (2016). Battery Energy Storage Market: Commercial Scale, Lithium-ion Projects in the U.S. National Renewable Energy Laboratory, Golden, CO. NREL/PR-6A20-67235.

Mei, J., & Kirtley, J. L. (2018). A Non-Cooperative Game Theory Based Controller Tuning Method for Microgrid DC-DC Converters. *IEEE Power and Energy Society General Meeting*, 1–5.

Mei, J., Chen, C., Wang, J., & Kirtley, J. L. (2019). Coalitional game theory based local power exchange algorithm for networked microgrids. *Applied Energy*, *239*, 133–141.

Mihailescu, R., Vasirani, M., & Ossowski, S. (2011). Dynamic Coalition Adaptation for Efficient Agent-Based Virtual Power Plants In R. Goebel, Y. Tanaka, & W. Wahlster (Eds.), *Lecture Notes in Artificial Intelligence 6973 Subseries of Lecture Notes in Computer Science (pp. 101-112).* Berlin Heidelberg: Springer.

Miller, C. A. & Richter, J. (2014). Social planning for energy transitions. *Current Sustainable/Renewable Energy Reports, 1*(3), 77–84.

Mills, A. D. & Wiser, R. H. (2015). Strategies to mitigate declines in the economic value of wind and solar at high penetration in California. *Applied Energy, 147,* 269–278.

Minciardi, R. & Robba, M. (2017). A bilevel approach for the stochastic optimal operation of interconnected microgrids. *IEEE Transactions on Automation Science and Engineering*, *14*(2), 482–493.

Minciardi, R. & Sacile, R. (2012). Optimal control in a cooperative network of smart power grids. *IEEE Systems Journal*, *6*(1), 126–133.

Mitchell, S., Kean, A., Mason, A, O'Sullivan, M., & Phillips, A. PuLP 1.6.0 documentation. Retrieved from: https://pythonhosted.org/PuLP/

MITei. (2011). *Managing Large-Scale Penetration of Intermittent Renewables.* Retrieved from: https://energy.mit.edu/wp-content/uploads/2012/03/MITEI-RP-2011-001.pdf

Moayedi, S., & Davoudi, A. (2016). Distributed tertiary control of DC microgrid clusters. *IEEE Transactions on Power Electronics*, *31*(2), 1717–1733.

Mohamed, A. A., Elsayed, A. T., Youssef, T. A., & Mohammed, O. A. (2017). Hierarchical control for DC microgrid clusters with high penetration of distributed energy resources. *Electric Power Systems Research*, *148*, 210–219.

Mohammadi, A., Mehrtash, M., and Kargarian, A. (2018). Diagonal quadratic approximation for decentralized collaborative TSO+ DSO optimal power flow. *IEEE Transactions on Smart Grid*, *10*(3), 2358-2370.

Mondol, J. D., Yohanis, Y. G., & Norton, B. (2009). Optimising the economic viability of grid-connected photovoltaic systems. *Applied Energy*, *86*(7), 985–999.

Mongkoltanatas, J., Riu, D., & Lepivert, X. (2013). H infinity controller design for primary frequency control of energy storage in islanding MicroGrid. *2013 15th European Conference on Power Electronics and Applications, EPE 2013*.

Mulder, G., Six, D., Claessens, B., & Broes, T. (2013). The dimensioning of PV-battery systems depending on the incentive and selling price conditions. *Applied Energy*, *111*, 1126–1135.

National Renewable Energy Laboratory (NREL). (2016). Microgrid Testing. Retrieved from https://www.nrel.gov/docs/fy16osti/65839.pdf

National Renewable Energy Laboratory. (2016a). PVWatts calculator. Retrieved from http://pvwatts.nrel.gov

National Renewable Energy Laboratory. (2016b). NREL: Energy analysis - distributed generation energy technology operations and maintenance costs. Retrieved from http://www.nrel.gov/analysis/tech_cost_om_dg.html

Naval Facilities Engineering Command. (1990). Electric Power Distribution Systems Operations. NAVFAC MO-201.

Naval Facilities Engineering Command. (1990). Electric Power Distribution Systems Operations. NAVFAC MO-201.

Navigant. (2017). Global DER Deployment Forecast Database.

Negrão, C. O. & Hermes, C. J. (2011). Energy and cost savings in household refrigerating appliances: A simulation-based design approach. *Applied Energy*, *88*(9), 3051–3060.

Nemet, A., Klemeš, J. J., Varbanov, P. S., & Kravanja, Z. (2012). Methodology for maximising the use of renewables with variable availability. *Energy*, *44*(1), 29–37.

Nguyen, A. T., Reiter, S., & Rigo, P. (2014). A review on simulation-based optimization methods applied to building performance analysis. *Applied Energy*, *113*, 1043–1058.

Nikmehr, N., Najafi-Ravadanegh, S., & Khodaei, A. (2017). Probabilistic optimal scheduling of networked microgrids considering time-based demand response programs under uncertainty. *Applied Energy*, *198*, 267–279.

Noroozi, N., Trip, S., & Geiselhart, R. (2018). Model predictive control of DC microgrids: current sharing and voltage regulation. *IFAC-PapersOnLine*, *51*(23), 124–129.

North American Electric Reliability Corporation (NERC). (2011). Balancing and Frequency Control. Retrieved from: https://www.nerc.com/docs/oc/rs/NERC%20Balancing%20and%20Frequency%20Control%20040520111.pdf

Nunna, H. & Doolla, S. (2012). Demand response in smart distribution system with multiple microgrids. *IEEE Transactions on Smart Grid*, *3*(4), 1641–1649.

Olivares, D. E., Canizares, C. A., & Kazerani, M. (2014). A centralized energy management system for isolated microgrids. *IEEE Transactions on Smart Grid*, *5*(4), 1864–1875.

Olivares, D. E., Mehrizi-Sani, A., Etemadi, A. H., Cañizares, C. A., Iravani, R., Kazerani, M., Hajimiragha, A., Gomis-Bellmunt, O., Saeedifard, M., Palma-Behnke, R., Jiménez-Estévez, G.A., & Hatziargyriou, N. D. (2014). Trends in microgrid control. IEEE *Transactions on Smart Grid*, *5*(4), 1905–1919.

OpenEI.org. (2011). NREL RSF Measured Data 2011. Retrieved from: https://openei.org/datasets/dataset/nrel-rsf-measured-data-2011

OpenEI.org. (n.d.). Retrieved from: https://openei.org/datasets/files/961/pub/

Orsini, L., Kemenade, C., Webb, M., & Heitmann, P. (2019). Transactive Energy A New Approach for Future Power Systems. LO3 Energy. Retrieved from: https://exergy.energy/wp-content/uploads/2019/03/TransactiveEnergy-PolicyPaper-v2-2.pdf

osBrain. (n.d.). About osBrain. Retrieved from: https://osbrain.readthedocs.io/en/stable/about.html

Østergaard, P. A. (2009). Reviewing optimisation criteria for energy systems analyses of renewable energy integration. *Energy*, *34*(9), 1236–1245.

Oyarzabal, J., Jimeno, J., Ruela, J., Engler, A., & Hardt, C. (2005). Agent based micro grid management system. *International Conference on Future Power Systems*.

Parhizi, S., Lotfi, H., Khodaei, A., & Bahramirad, S. (2015). State of the art in research on microgrids: A review. *IEEE Access*, *3*, 890–925.

Pashajavid, E., Shahnia, F., & Ghosh, A. (2017). Provisional internal and external power exchange to support remote sustainable microgrids in the course of power deficiency. *Iet Generation Transmission & Distribution*, *11*(1), 246–260.

Pashajavid, E., Shahnia, F., & Ghosh, A. (2017a). Development of a Self-Healing Strategy to Enhance the Overloading Resilience of Islanded Microgrids. *IEEE Transactions on Smart Grid*, *8*(2), 868–880.

Pashajavid, E., Shahnia, F., & Ghosh, A. (2017b). Provisional internal and external power exchange to support remote sustainable microgrids in the course of power deficiency. *IET Generation Transmission & Distribution*, *11*(1), 246–260.

Patsalides, M., Evagorou, D., Makrides, G., Achillides, Z., Georghiou, G. E., Stavrou, A., Efthymiou, V., Zinsser, B., Schmitt, W. and Werner, J. H. (2007). The effect of solar irradiance on the power quality behaviour of grid connected photovoltaic systems. *International Conference on Renewable Energies and Power Quality, ICREPQ, La Coruña, ES, 25 - 27 Mar 2007.*

Piclo. (2018). Home Page. Retrieved from: https://piclo.energy/

Pillai, G. G., Putrus, G. A., Georgitsioti, T., Pearsall, N. M. (2014). Near-term economic benefits from grid-connected residential PV (photovoltaic) systems. *Energy*, *68*, 832–843.

PowerMatcherSuite Transactive Smart Energy. (2017). In Operation. Retrieved from: http://flexiblepower.github.io/cases/in-operation/

Prabaharan, N., Jerin, A. R. A., Najafi, E., & Palanisamy, K. (2018). An overview of control techniques and technical challenge for inverters in micro grid In A. H. Fathima, N. Prabaharan, K. Palanisamy, A. Kalam, S. Mekhilef, J.J. Justo (Eds). *Hybrid-renewable Energy Systems in Microgrids: Integration, Developments and Control* (pp. 97-107). Elsevier Ltd.

Prinsloo, G., Mammoli, A., & Dobson, R. (2017). Customer domain supply and load coordination: A case for smart villages and transactive control in rural off-grid microgrids. *Energy*, *135*, 430–441.

Professional Services Close-up. (2012). Chicago's Rush University Medical Center Leverages GE's Emergency Power System. Business Insights: Global.

Purohit, I. & Purohit, P. (2010). Techno-economic evaluation of concentrating solar power generation in India. *Energy Policy*, *38*(6), 3015–3029.

Quesada, J., Sebastián, R., Castro, M., & Sainz, J. A. (2014). Control of inverters in a low voltage microgrid with distributed battery energy storage. Part I: Primary control. *Electric Power Systems Research*, *114*, 126–135.

Raghami, A., Ameli, M. T., & Hamzeh, M. (2013). Primary and secondary frequency control in an autonomous microgrid supported by a load-shedding strategy. *PEDSTC 2013 - 4th Annual International Power Electronics, Drive Systems and Technologies Conferenc*e, 282–287.

Rahmani-Andebili, M. (2017). Scheduling deferrable appliances and energy resources of a smart home applying multi-time scale stochastic model predictive control. *Sustainable Cities and Society*, *32*, 338-347.

Rahmani-Andebili, M. (2018). Cooperative Distributed Energy Scheduling in Microgrids. *Electric Distribution Network Management and Control*, 235-254. Springer Nature Singapore.

Reichelstein, S. & Yorston, M. (2013). The prospects for cost competitive solar PV power. *Energy Policy*, *55*, 117–127.

Ren21. (2019). *Renewables 2019 Global Status Report*. Retrieved from: http://www.ren21.net/wp-content/uploads/2018/06/17-8652_GSR2018_FullReport_web_-1.pdf

Rezaei, N., & Kalantar, M. (2014). Economic-environmental hierarchical frequency management of a droop-controlled islanded microgrid. *Energy Conversion and Management*, *88*, 498–515.

Rivera, S., Farid, A. M., & Youcef-Toumi, K. (2014). A Multi-Agent System Coordination Approach For Resilient Self-Healing Operations in Multiple Microgrids. In *Industrial Agents: Emerging Applications of Software Agents in Industry* (pp. 269–285). Elsevier.

Rokrok, E., Shafie-khah, M., & Catalão, J. P. S. (2018). Review of primary voltage and frequency control methods for inverter-based islanded microgrids with distributed generation. *Renewable and Sustainable Energy Reviews*, *82*, 3225–3235.

Roosa, S. A. & Jhaveri, A. G. (2009). Carbon Reduction: Policies, Strategies and Technologies. Lilburn, GA, USA: Fairmont Press, Incorporated.

Rosa de Jesus, D.A. (2018). Modeling and Simulation of Energy Grids Under Transactive Energy Markets. University of Puerto Rico.

Roy, B., Basu, A. K., & Paul, S. (2014). Techno-economic feasibility analysis of a grid connected solar photovoltaic power system for a residential load. *2014 First International Conference on Automation, Control, Energy and Systems (ACES)*, 1–5.

Ruddell, B. L, Salamanca, F., & Mahalov, A. (2014). Reducing a semiarid city's peak electrical demand using distributed cold thermal energy storage. *Applied Energy*, *134*, 34–44.

Sadd, W., Han, Z., & Poor, H. V. (2011). Coalitional Game Theory for Cooperative Micro-Grid Distribution Networks. *IEEE International Conference on Communications*.

Sadineni, S. B., Atallah, F., & Boehm, R. F. (2012). Impact of roof integrated PV orientation on the residential electricity peak demand. *Applied Energy*, *92*, 204–210.

Salpakari, J. & Lund, P. (2016). Optimal and rule-based control strategies for energy flexibility in buildings with PV. *Applied Energy*, *161*, 425–436.

Salt River Project. (2018). SRP – Tesla Agreement. Retrieved from: https://www.srpnet.com/newsroom/releases/030718.aspx

Sanjari, M. J., & Gharehpetian, G. B. (2014). Game-theoretic approach to cooperative control of distributed energy resources in islanded microgrid considering voltage and frequency stability. *Neural Computing and Applications*, *25*(2), 343–351.

Satchwell, A., Mills, A. D., Barbose, G. L., Wiser, R. H., Cappers, P., and Darghouth, N. (2014). Financial Impacts of Net-Metered PV on Utilities and Ratepayers: A Scoping Study of Two Prototypical U.S. Utilities. Lawrence Berkeley National Laboratory, USA.

Schmietendorf, K., Peinke, J., & Kamps, O. (2017). The impact of turbulent renewable energy production on power grid stability and quality. *The European Physical Journal B*, *90*(11), 1-6.

SciPy.org. (2018). Scientific Computing Tools for Python. Retrieved from: https://www.scipy.org/about.html

Shahnia, F., Bourbour, S., & Ghosh, A. (2017). Coupling Neighboring Microgrids for Overload Management Based on Dynamic Multicriteria Decision-Making. *IEEE Transactions on Smart Grid*, *8*(2), 969–983.

Sharma, A., Srinivasan, D., & Kumar, D. S. (2016). A comparative analysis of centralized and decentralized multi-agent architecture for service restoration. *2016 IEEE Congress on Evolutionary Computation*, 311–318.

Shen, J., Jiang, C., & Li, B. (2015). Controllable load management approaches in smart grids. *Energies*, *8*(10), 11187-11202.

Silvente, J., Kopanos, G. M., Pistikopoulos, E. N., & Espuña, A. (2015). A rolling horizon optimization framework for the simultaneous energy supply and demand planning in microgrids. *Applied Energy*, *155*, 485–501.

SMA Solar Technology AG. (2016). Solar Inverters. Retrieved from http://www.sma-america.com/products/solarinverters.html

Solar Energy Industries Association (SEIA). (2014). Solar Market Insight Report 2014 Q3.

SolarCity. (2015). How Much Do Solar Panels Cost? Find the Cost of Solar Energy. Retrieved from: http://www.solarcity.com/residential/how-much-do-solar-panels-cost

Solomon, A. A., Kammen, D. M., & Callaway, D. (2014). The role of large-scale energy storage design and dispatch in the power grid: A study of very high grid penetration of variable renewable resources. Applied Energy, *134*, 75–89.

Song, N. O., Lee, J. H., Kim, H. M., Im, Y., & Lee, J. (2015). Optimal energy management of multi-microgrids with sequentially coordinated operations. *Energies*, *8*(8), 8371–8390.

SonnenCommunity. (2018). Home Page. Retrieved from: https://sonnengroup.com/sonnencommunity/

Sonnenschein, M., Lünsdorf, O., Bremer, J., & Tröschel, M. (2015). Decentralized control of units in smart grids for the support of renewable energy supply. *Environmental Impact Assessment Review*, *52*, 40–52.

SQLite. (n.d.). About SQLite. Retrieved from: https://www.sqlite.org/about.html

State of Green. (2017). Denmark to be Coal-Free by 2030. Retrieved from: https://stateofgreen.com/en/partners/state-of-green/news/denmark-to-be-coal-free-by-2030/

Tesla. (2018). Powerwall. Retrieved from: https://www.tesla.com/powerwall

The GridWise Architecture Council. (2015). GridWise Transactive Energy Framework Version 1.0 (PNNL-22946). Retrieved from: https://www.gridwiseac.org/pdfs/te_framework_report_pnnl-22946.pdf

Tian, P., Xiao, X., Wang, K., & Ding, R. (2016). A Hierarchical Energy Management System Based on Hierarchical Optimization for Microgrid Community Economic Operation. *IEEE Transactions on Smart Grid*, *7*(5), 2230–2241.

Ton, D. & Smith, M. (2012). The U.S. Department of Energy's Microgrid Initiative. *The Electricity Journal*, *25*(8), 84-94.

Ton, D. T., & Smith, M. A. (2012). The U.S. Department of Energy's Microgrid Initiative. *The Electricity Journal*, *25*(8), 84–94.

Tsikalakis, A. G., & Hatziargyriou, N. D. (2008). Centralized control for optimizing microgrids operation. *IEEE Transactions on Energy Conversion*, *23*(1), 241–248.

U.S. Census Bureau. (2010a). Median and Average Square Feet of Floor Area in New Single-Family Houses Completed by Location. Retrieved from http://www.census.gov/const/C25Ann/sftotalmedavgsqft.pdf

U.S. Census Bureau. (2010b). Census data – 2010 Census. Retrieved from http://www.census.gov/2010census/data/

U.S. Department of Energy (DOE) Office of Electricity. (n.d.) Microgrid Portfolio of Activities. Retrieved from https://www.energy.gov/oe/services/technology-development/smart-grid/role-microgrids-helping-advance-nation-s-energy-syst-0

U.S. Department of Energy: Energy Efficiency & Renewable Energy (EERE). (2014). Weather Data for Simulation.

U.S. Energy Information Administration (EIA). (2014). December 2014 Monthly Review. Washington, DC: U.S. Energy Information Administration, DOE/EIA-0035; 2014. P. 1–201.

U.S. Energy Information Administration (EIA). (2015). Wholesale Electricity and Natural Gas Market Data.

U.S. Energy Information Administration (EIA). (2016). Electricity Data Browser – Average Retail Price of Electricity. Retrieved from http://www.eia.gov/electricity/data.cfm

Umeozor, E. C., & Trifkovic, M. (2016). Operational scheduling of microgrids via parametric programming. *Applied Energy*, *180*, 672–681.

Undrill, J. (2018). Primary Frequency Response and Control of Power System Frequency (LBNL-2001105). *Lawrence Berkeley National Laboratory*. Retrieved from: https://www.ferc.gov/industries/electric/indus-act/reliability/frequency-control-requirements/primary-response.pdf

United States Energy Information Administration. (2018). Wholesale Electricity and Natural Gas Market Data.

United States Energy Information Administration. (2019). Annual Energy Outlook 2019.

Vaahedi, E., Nodehi, K., Heim, D., Rahimi, F., & Ipakchi, A. (2017). The Emerging Transactive Microgrid Controller: Illustrating Its Concept, Functionality, and Business Case. *IEEE Power and Energy Magazine*, *15*(4), 80–87.

Van den Bergh, K. & Delarue, E. (2015). Cycling of conventional power plants: technical limits and actual costs. TME Working Paper – Energy and Environment. Retrieved from: https://core.ac.uk/download/pdf/34627483.pdf

Vandebron. (n.d.). Home Page. Retrieved from: https://vandebron.nl/

Vandoorn, T., De Kooning, J., Van de Vyver, J., & Vandevelde, L. (2013). Three-Phase Primary Control for Unbalance Sharing between Distributed Generation Units in a Microgrid. *Energies*, *6*(12), 6586–6607.

Wand, R. & Leuthold, F. (2011). Feed-in tariffs for photovoltaics: Learning by doing in Germany, *Applied Energy*, *88*(12), 4387–4399.

Wang, H., & Huang, J. (2016). Incentivizing Energy Trading for Interconnected Microgrids. *IEEE Transactions on Smart Grid*, *3053*, 1–11.

Wang, J., Zhai, Z. J., Jing, Y., Zhang, X., & Zhang, C. (2011). Sensitivity analysis of optimal model on building cooling heating and power system. *Applied Energy*, *88*(12), 5143–5152.

Wang, K., Yuan, X., Geng, Y., & Wu, X. (2019). A Practical Structure and Control for Reactive Power Sharing in Microgrid. *IEEE Transactions on Smart Grid*, *10*(2), 1880–1888.

Wang, X., Wang, C., Xu, T., Guo, L., Li, P., Yu, L., & Meng, H. (2018). Optimal voltage regulation for distribution networks with multi-microgrids. *Applied Energy*, *210*, 1027–1036.

Wang, Z., Wu, W., & Zhang, B. (2018). Distributed newton method for primary voltage control in Islanded DC microgrid. *IEEE Power and Energy Society General Meeting*.

Wang, Z., Yang, K., & Wang, X. (2012). Privacy constrained energy management in microgrid systems. *2012 IEEE 3rd International Conference on Smart Grid Communications*, 670–674.

Wei, C., Fadlullah, Z. M., Kato, N., & Takeuchi, A. (2014). GT-CFS: A game theoretic coalition formulation strategy for reducing power loss in micro grids. *IEEE Transactions on Parallel and Distributed Systems*, *25*(9), 2307–2317.

Whited, M., Woolf, T., & Napoleon, A. (2015). Utility Performance Incentive Mechanisms. *Synapse Energy Economics, Inc*.

Winoto, P. (2007). Modified Bargaining Protocols for Automated Negotiation in Open Multi-Agent Systems. University of Saskatchewan, Saskatoon.

Wirth, H. (2015). Recent Facts about Photovoltaics in Germany. Fraunhofer Institute for Solar Energy Systems.

Wood, L., Hemphill, R., Howat, J., Cavanagh, R., Borenstein, S., Deason, J., & Schwartz, L. (2016). Recovery of Utility Fixed Costs: Utility, Consumer, Enviornmental, and Economist Perspectives. Lawrence Berkeley National Laboratory. (Report No. 5)

Wu, J. & Guan, X. (2013). Coordinated multi-microgrids optimal control algorithm for smart distribution management system. *IEEE Transactions on Smart Grid*, *4*(4), 2174–2181.

Wu, P., Huang, W., Tai, N., & Liang, S. (2018). A novel design of architecture and control for multiple microgrids with hybrid AC/DC connection. *Applied Energy*, *210*, 1002-1016.

Xiang, J., Wang, Y., Li, Y., & Wei, W. (2016). Stability and steady-state analysis of distributed cooperative droop controlled DC microgrids. *IET Control Theory & Applications*, *10*(18), 2490–2496.

Yan, R., Saha, T. K., Modi, N., & Masood, N. (2015). The combined effects of high penetration of wind and PV on power system frequency response. *Applied Energy*, *145*, 320–330.

Yang, X., Cui, Z., & Xiao, R. (2013). *Swarm Intelligence and Bio-Inspired Computation*. Elsevier.

Yang, X., Du, Y., Su, J., Chang, L., Member, S., Shi, Y., & Lai, J. (2016). An Optimal Secondary Voltage Control Strategy for an Islanded Multibus Microgrid. *IEEE Journal of Emerging and Selected Topics in Power Electronics*, *4*(4), 1236–1246.

Yu, C. K., Van Der Schaar, M., & Sayed, A. H. (2015). Information-Sharing over Adaptive Networks with Self-Interested Agents. *IEEE Transactions on Signal and Information Processing over Networks*, *1*(1), 2–19.

Yu, Z., Ai, Q., Gong, J., & Piao, L. (2016). A novel secondary control for microgrid based on synergetic control of multi-agent system. *Energies*, *9*(4), 1–14.

Yun, G. Y. & Steemers, K. (2011). Behavioural, physical and socio-economic factors in household cooling energy consumption. *Applied Energy*, *88*(6), 2191–2200.

Zachel, C. (2013). Generators and transfer switches: Emergency power system solutions. *Consulting-Specifying Engineer*, *50*(8).

Zenginis, I., Vardakas, J.S., Echave, C., Morató, M., Abadal, J., & Verikoukis, C.V. (2017). Cooperation in microgrids through power exchange: An optimal sizing and operation approach. *Applied Energy*, *203*, 972-981.

Zenginis, I., Vardakas, J.S., Echave, C., Morató, M., Abadal, J., & Verikoukis, C.V. (2017). Cooperation in microgrids through power exchange: An optimal sizing and operation approach. *Applied Energy*, *203*, 972-981.

Zerrahn, A., Schill, W. P., & Kemfert, C. (2018). On the economics of electrical storage for variable renewable energy sources. *European Economic Review*, *108*, 259–279.

Zhang, B., Li, Q., Wang, L., & Feng, W. (2018). Robust optimization for energy transactions in multi-microgrids under uncertainty. *Applied Energy*, *217*, 346-360.

Zhang, C., Wu, J., Long, C., & Cheng, M. (2017). Review of Existing Peer-to-Peer Energy Trading Projects. *Energy Procedia*, *105*, 2563–2568.

Zhang, D., Li, S., Zeng, P., & Zang, C. (2014). Optimal microgrid control and power-flow study with different bidding policies by using powerworld simulator. *IEEE Transactions on Sustainable Energy*, *5*(1), 282–292.

Zhang, W., & Xu, Y. (2019). Distributed Optimal Control for Multiple Microgrids in a Distribution Network. *IEEE Transactions on Smart Grid*, *10*(4), 3765–3779.

Zhang, X., Bao, J., Wang, R., Zheng, C., & Skyllas-Kazacos, M. (2017). Dissipativity based distributed economic model predictive control for residential microgrids with renewable energy generation and battery energy storage. *Renewable Energy*, *100*, 18–34.

Zheng, W.D. and Cai, J.D. (2010). A multi-agent system for distributed energy resources control in microgrid. *IEEE 5th International Conference on Critical Infrastructure*.

APPENDIX A

SELECTION OF REPRESENTATIVE LITERATURE

Appendix A: Selection of Representative Literature

	Method					Case Study					
Ref #	Objective	Control Techniques	Internal Microgrid Control Modeled	Internal Microgrid Control Topology	Microgrid Network Control Topology	Network Architecture	Time Scale	Grid	Voltage Level	Asset Types	Max Node #
[1]	Self-healing	Agent-based control, logical control, droop control	Yes	Centralized	Centralized/ Decentralized	Arbitrary	≤ 1 sec	Yes	Low/ med	Electrical	2
[2]	Cost reduction, improvement of storage utilization efficiency, operation complexity reduction	Agent-based control, DEC-POMDP, dynamic programming, look-head dual multiplier	No	Centralized	Decentralized	Arbitrary	Hour	Yes	Low/ med	Electrical/ thermal	103
[3]	Cost reduction, carbon emission reduction, energy independence	MILP, Nash bargaining method	Yes	Centralized	Centralized	Modified or Exact Existing Systems	Hour	Yes	Low/ med	Electrical	6
[4]	Cost reduction, energy-not-served reduction	Transactive energy, stochastic programing, latin hyperbolic sampling, fast-forward selection	Yes	Centralized	Centralized	Modified or Exact Existing Systems	Hour	Yes	Low/ med	Electrical/ thermal	9
[5]	Self-healing	Agent-based control, approximate optimization, heuristic methods	Yes	Centralized	Decentralized	Modified or Exact Benchmarking Test Cases (Other)	15 sec	Yes	Low/ med	Electrical	3

[1] Pashajavid, E., Shahnia, F., & Ghosh, A. (2017a). Development of a Self-Healing Strategy to Enhance the Overloading Resilience of Islanded Microgrids. *IEEE Transactions on Smart Grid*, *8*(2), 868–880.
[2] Wu, J., & Guan, X. (2013). Coordinated Multi-Microgrids Optimal Control Algorithm for Smart Distribution Management System. *IEEE Transactions on Smart Grid*, *4*(4), 2174–2181.
[3] Zenginis, I., Vardakas, J.S., Echave, C., Morató, M., Abadal, J., & Verikoukis, C.V. (2017). Cooperation in microgrids through power exchange: An optimal sizing and operation approach. *Applied Energy*, *203*, 972-981.
[4] Daneshvar, M., Pesaran, M., & Mohammadi-ivatloo, B. (2018). Transactive energy integration in future smart rural network electrification. *Journal of Cleaner Production*, *190*, 645–654.
[5] Rivera, S., Farid, A. M., & Youcef-Toumi, K. (2014). A Multi-Agent System Coordination Approach for Resilient Self-Healing Operations in Multiple Microgrids. In *Industrial Agents: Emerging Applications of Software Agents in Industry*, 269–285. Elsevier.

Appendix A: Selection of Representative Literature (continued)

	Method					Case Study					
Ref #	Objective	Control Techniques	Internal Microgrid Control Modeled	Internal Microgrid Control Topology	Microgrid Network Control Topology	Network Architecture	Time Scale	Grid	Voltage Level	Asset Types	Max Node #
[6]	Cost reduction	Agent-based control, dynamic pricing, aggregators, exact optimization	Yes	Decentralized	Decentralized	Modified or Exact Existing Systems	Hour	Yes	Low/ med	Electrical	5
[7]	Optimal coalition formation, reduce grid dependency	Agent-based control, coalitional game theory, approx. optimization, heuristic methods	No	N/A	Decentralized	Synthetically Generated (Random)	Hour	Yes	Med	Electrical	500
[8]	Reduce grid dependency, reduce load shedding	Agent-based control, game-theoretic double-auction, reverse auction models	Yes	Centralized	Centralized	Modified or Exact IEEE Test Cases	5 min	Yes	Med	Electrical	3
[9]	Reliability	Agent-based control, coalitional game theory, distributed merge-swap algorithm	No	N/A	Decentralized	Synthetically Generated (Random)	Hour	No	Not specified	Electrical	200
[10]	Increased utility	Coalitional game theory, second-price sealed-bid auction	No	N/A	Centralized	Synthetically Generated (Random)	5 min	Yes	Med	Electrical	24

[6] Liu, Y., Zuo, K., Liu, X. (Amy), Liu, J., & Kennedy, J. M. (2018). Dynamic pricing for decentralized energy trading in micro-grids. *Applied Energy*, *228*, 689–699.
[7] Chakraborty, S., Nakamura, S., & Okabe, T. (2014). Scalable and optimal coalition formation of microgrids in a distribution system. *IEEE PES Innovative Smart Grid Technologies Conference Europe*.
[8] Esfahani, M. M., Hariri, A., Member, S., & Mohammed, O. A. (2019). A Multiagent-Based Game-Theoretic and Optimization Approach for Market Operation of Multimicrogrid Systems. *IEEE Transactions on Industrial Informatics*, *15*(1), 280–292.
[9] Hammad, E. M., Farraj, A. K., & Kundur, D. (2015). Grid-independent cooperative microgrid networks with high renewable penetration. *2015 IEEE Power and Energy Society Innovative Smart Grid Technologies Conference*.
[10] Mei, J., Chen, C., Wang, J., & Kirtley, J. L. (2019). Coalitional game theory based local power exchange algorithm for networked microgrids. *Applied Energy*, *239*, 133–141.

Appendix A: Selection of Representative Literature (continued)

	Method					Case Study					
Ref #	Objective	Control Techniques	Internal Microgrid Control Modeled	Internal Microgrid Control Topology	Microgrid Network Control Topology	Network Architecture	Time Scale	Grid	Voltage Level	Asset Types	Max Nodes
[11]	Cost reduction	Coalitional game theory, cooperative games, linearized OPF	Yes	Centralized	Decentralized	Modified or Exact IEEE Test Cases	Hour	Yes	Med	Electrical /thermal	10
[12]	Reduce grid dependency, active power support	Agent-based control, logical control	Yes	Centralized	Decentralized	Arbitrary	1 min	Yes	Low/ med	Electrical	3
[13]	Improved control speed, ancillary services	Agent-based control, bi-level game model	No	N/A	Decentralized	Modified or Exact IEEE Test Cases	Not specif ied	Yes	Med	Electrical	3
[14]	Cost reduction	Hierarchical control, bi-level optimization, stochastic model, PSO	Yes	Centralized	Centralized/ Decentralized	Arbitrary	Hour	Yes	Low/ med	Electrical	3
[15]	Overload management	Agent-based control, dynamic multi-criteria decision-making algorithm	No	N/A	Centralized	Arbitrary	Not specif ied	No	Low/ med	Electrical	6
[16]	Improved efficiency, improved voltage stability, ancillary services	Virtual aggregators, virtual power exchange, logical control	Yes	Centralized	Decentralized	Arbitrary	≤ 1 sec	Yes	Low/ med	Electrical	2

[11] Du, Y., Li, F., Kou, X., & Pei, W. (2018). Coordinating multi-microgrid operation within distribution system: A cooperative game approach. *IEEE Power and Energy Society General Meeting*.
[12] Harmouch, F. Z., Krami, N., & Hmina, N. (2018). A multiagent based decentralized energy management system for power exchange minimization in microgrid cluster. *Sustainable Cities and Society*, *40*, 416–427.
[13] Wang, X., Wang, C., Xu, T., Guo, L., Li, P., Yu, L., & Meng, H. (2018). Optimal voltage regulation for distribution networks with multi-microgrids. *Applied Energy*, *210*, 1027–1036.
[14] Nikmehr, N., Najafi-Ravadanegh, S., & Khodaei, A. (2017). Probabilistic optimal scheduling of networked microgrids considering time-based demand response programs under uncertainty. *Applied Energy*, *198*, 267–279.
[15] Shahnia, F., Bourbour, S., & Ghosh, A. (2017). Coupling Neighboring Microgrids for Overload Management Based on Dynamic Multicriteria Decision-Making. *IEEE Transactions on Smart Grid*, *8*(2), 969–983.
[16] Mohamed, A. A., Elsayed, A. T., Youssef, T. A., & Mohammed, O. A. (2017). Hierarchical control for DC microgrid clusters with high penetration of distributed energy resources. *Electric Power Systems Research*, *148*, 210–219.

Appendix A: Selection of Representative Literature (continued)

	Method					Case Study					
Ref #	Objective	Control Techniques	Internal Microgrid Control Modeled	Internal Microgrid Control Topology	Microgrid Network Control Topology	Network Architecture	Time Scale	Grid	Voltage Level	Asset Types	Max Nodes
[17]	Cost reduction, emissions reduction, optimal battery size	Fitness-based modified game, PSO, multi-objective optimization	Yes	Centralized	Centralized	Arbitrary	Not specified	Yes	Low	Electrical	4
[18]	Cost reduction	Two-level hierarchical optimization, MILP	Yes	Centralized	Centralized	Modified or Exact Existing Systems	Hour	Yes	Low	Electrical	5
[19]	Reduced power losses	Coalitional game theory, cooperative games, logical control	No	N/A	Centralized/ Decentralized	Synthetically Generated (Random)	Not specified	Yes	Low/ med	Electrical	30
[20]	Cost reduction	Agent-based control, hierarchical control, naïve auction algorithm	Yes	Centralized	Decentralized	Arbitrary	15 min	Yes	Low/ med	Electrical	4
[21]	Improved control speed, stability	Hierarchical control, ADMM	Yes	Centralized	Decentralized	Arbitrary	≤ 1 Sec	Yes	Med	Electrical	4
[22]	Cost reduction, reduce power losses	Coalitional game theory, cooperative games, heuristic methods, stochastic model	Yes	Centralized	Centralized	Modified or Exact IEEE Test Cases, Modified or Exact Benchmarking Test Cases (Other)	Hour	Yes	Med	Electrical	6

[17] Kumrai, T., Ota, K., Dong, M., Sato, K., & Kishigami, J. (2017). Optimising operation management for multi-micro-grids control. *IET Cyber-Physical Systems: Theory & Applications*, *3*(1), 24–33.
[18] Tian, P., Xiao, X., Wang, K., & Ding, R. (2016). A Hierarchical Energy Management System Based on Hierarchical Optimization for Microgrid Community Economic Operation. *IEEE Transactions on Smart Grid*, *7*(5), 2230–2241.
[19] Sadd, W., Han, Z., & Poor, H. V. (2011). Coalitional Game Theory for Cooperative Micro-Grid Distribution Networks. *IEEE International Conference on Communications*.
[20] Kumar Nunna, H. S. V. S., & Doolla, S. (2013). Multiagent-based distributed-energy-resource management for intelligent microgrids. *IEEE Transactions on Industrial Electronics*, *60*(4), 1678–1687.
[21] Zhang, W., & Xu, Y. (2019). Distributed Optimal Control for Multiple Microgrids in a Distribution Network. *IEEE Transactions on Smart Grid*, *10*(4), 3765–3779.
[22] Lahon, R., Gupta, C. P., & Fernandez, E. (2019). Coalition formation strategies for cooperative operation of multiple microgrids. *IET Generation, Transmission & Distribution*, *13*, 3661–3672.

Appendix A: Selection of Representative Literature (continued)

	Method					Case Study					
Ref #	Objective	Control Techniques	Internal Microgrid Control Modeled	Internal Microgrid Control Topology	Microgrid Network Control Topology	Network Architecture	Time Scale	Grid	Voltage Level	Asset Types	Max Nodes
[22]	Cost reduction, reduce power losses	Coalitional game theory, cooperative games, heuristic methods, stochastic model	Yes	Centralized	Centralized	Modified or Exact IEEE Test Cases , Modified or Exact Benchmarking Test Cases (Other)	Hour	Yes	Med	Electrical	6
[23]	Cost reduction	Distributed convex optimization, subgradient-based cost minimization algorithm	No	N/A	Decentralized	Abstract (Graph theory-based)	Not specified	No	Low/ med	Electrical	4
[24]	Energy balance	Aggregator, game theory, competitive games, logical control	Yes	Centralized	Decentralized	Not specified	15 min	Yes	Low/ med	Electrical	6
[25]	Cost reduction, privacy preservation	Distributed optimization, OPF, naïve auction algorithm	Yes	Centralized	Decentralized	Arbitrary	Hour	Yes	Low/ med	Electrical	2
[26]	Cost reduction, stability, reliability	Distributed model predictive control, stochastic model	Yes	Centralized	Decentralized	Not specified	Hour	Yes	Low/ med	Electrical	10

[23] Gregoratti, D., & Matamoros, J. (2015). Distributed Energy Trading: The Multiple-Microgrid Case. *IEEE Transactions on Industrial Electronics*, *62*(4), 2551–2559.
[24] Jadhav, A. M., Patne, N. R., & Guerrero, J. M. (2019). A Novel Approach to Neighborhood Fair Energy Trading in a Distribution Network of Multiple Microgrid Clusters. *IEEE Transactions on Industrial Electronics*, *66*(2), 1520–1531.
[25] Kim, B., Bae, S., & Kim, H. (2017). Optimal energy scheduling and transaction mechanism for multiple microgrids. *Energies*, *10*(4), 1–17
[26] Kou, P., Liang, D., & Gao, L. (2017). Distributed EMPC of multiple microgrids for coordinated stochastic energy management. *Applied Energy*, *185*, 939–952.

APPENDIX B

CO-AUTHOR APPROVAL OF USE

November 18, 2019

Samantha Janko
The Polytechnic School, Ira A. Fulton Schools of Engineering
7418 East Innovation Way South, Building ISTB-3 Rm 183
Mesa, AZ 85212

RE: Solar PV Publication and Rights to Use in PhD Dissertation

This letter is offered by Michael Arnold to Samantha Janko to approve use of the work "Implications of High-penetration Renewables for Ratepayers and Utilities in the Residential Solar Photovoltaic (PV) Market" in her PhD dissertation entitled "Self-organizing Coordination of Multi-Agent Microgrid Networks".

Sincerely,

Michael Arnold